A Spectroscopic and Photometric Survey of Novae in M31

A. W. Shafter[1], M. J. Darnley[2], K. Hornoch[3], A. V. Filippenko[4], M. F. Bode[2], R. Ciardullo[5], K. A. Misselt[6], R. A. Hounsell[2], R. Chornock[4,7], and T. Matheson[8]

ABSTRACT

We report the results of a multi-year spectroscopic and photometric survey of novae in M31 that resulted in a total of 53 spectra of 48 individual nova candidates. Two of these, M31N 1995-11e and M31N 2007-11g, were revealed to be long-period Mira variables, not novae. These data double the number of spectra extant for novae in M31 through the end of 2009 and bring to 91 the number of M31 novae with known spectroscopic classifications. We find that 75 novae (82%) are confirmed or likely members of the Fe II spectroscopic class, with the remaining 16 novae (18%) belonging to the He/N (and related) classes. These numbers are consistent with those found for Galactic novae. We find no compelling evidence that spectroscopic class depends sensitively on spatial position or population within M31 (i.e., bulge vs. disk), although the distribution for He/N systems appears slightly more extended than that for the Fe II class. We confirm the existence of a correlation between speed class and ejection velocity (based on line width), as in the case of Galactic novae. Follow-up photometry allowed us to determine light-curve parameters for a total of 47 of the 91 novae with known spectroscopic class. We confirm that more luminous novae generally fade the fastest, and that He/N novae are typically faster and brighter than their Fe II counterparts. In addition, we find a weak dependence of nova speed class on position in M31, with the spatial distribution of the fastest novae being slightly more extended than that of slower novae.

[1]Department of Astronomy, San Diego State University, San Diego, CA 92182, USA

[2]Astrophysics Research Institute, Liverpool John Moores University, Birkenhead CH41 1LD, UK

[3]Astronomical Institute, Academy of Sciences, CZ-251 65 Ondřejov, Czech Republic

[4]Department of Astronomy, University of California, Berkeley, CA 94720-3411, USA

[5]Department of Astronomy and Astrophysics, The Pennsylvania State University, 525 Davey Lab, University Park, PA 16802, USA

[6]Steward Observatory, University of Arizona, Tucson, AZ, 85721, USA

[7]Harvard-Smithsonian Center for Astrophysics, 60 Garden Street, Cambridge, MA 02138, USA

[8]National Optical Astronomy Observatory, 950 North Cherry Avenue, Tucson, AZ 85719-4933, USA

Subject headings: galaxies: stellar content — galaxies: individual (M31) — stars: novae, cataclysmic variables

1. Introduction

Classical novae form a subclass of the cataclysmic variable stars. They are semidetached binary star systems where a late-type Roche-lobe-filling star transfers mass to a white dwarf companion (e.g., Warner 1995, 2008). If the mass accretion rate onto the white dwarf is sufficiently low to allow the accreted gas to become degenerate, a thermonuclear runaway (TNR) will eventually ensue in the accreted envelope, leading to a nova eruption. These eruptions can reach an absolute magnitude as bright as $M_V \approx -10$ (e.g., Starrfield et al. 2008), making them among the most luminous explosions in the Universe. Their high luminosities and rates (~ 50 yr^{-1} in a galaxy like M31; Shafter & Irby 2001; Darnley et al. 2006) make novae powerful probes of the properties of close binaries in different (extragalactic) stellar populations. The most thoroughly studied extragalactic system is M31, where more than 800 novae have been discovered over the past century (e.g., see Pietsch et al. 2007e; Shafter 2008, and references therein).

Despite this large number of novae discovered, very few follow-up studies of their photometric, or particularly their spectroscopic, properties have been attempted. Most recent M31 surveys have been undertaken through narrow-band filters in order to take advantage of the fact that novae fade more slowly in Hα than they do in the continuum (e.g., Ciardullo et al. 1987; Shafter & Irby 2001). Such observations are ideal for determining the rate and spatial distribution of novae within a galaxy, but not for characterizing the nova light curves. As shown by Ciardullo et al. (1990b) the Hα light curves are not simply correlated with the peak luminosity as are the broad-band light curves. Moreover, most of the broad-band light-curve data for M31 novae come from the early photographic studies of Arp (1956) and Rosino (1964, 1973), as summarized by Capaccioli et al. (1989), and from observations in Crimea and Latvia during the period between 1977 and 1990 (Sharov & Alksnis 1992).

Similarly, spectroscopic data for M31 novae have, until recently, also been limited. The dearth of available spectra is not surprising given that novae in M31 are by definition transient, and relatively faint, reaching peak brightnesses in the range $m_V \approx 18$ to $m_V \approx 15$ mag before fading back to quiescence. Furthermore, since their eruptions are not predictable in advance, spectroscopic observations require not only timely access to large telescopes, but coordination with a photometric survey dedicated to discovering suitable targets. Humason (1932) was the first to report spectroscopic observations of classical novae in M31, and it was not until more than half a century later that Ciardullo et al. (1983) published the spectra

of four Hα emission-line sources, which they identified as classical novae in eruption. The number of nova spectra has increased dramatically in recent years thanks to greater access to queue scheduling on large telescopes, such as the Hobby-Eberly Telescope (HET).

In order to better understand the spectroscopic properties of novae in M31, and to study any variation with spatial position in the galaxy, we began a multi-year M31 nova survey in the Fall of 2006 using the HET. The program was motivated in large part by the work of Williams (1992), who realized that the spectra of Galactic novae (taken within a few weeks of eruption) can be divided into one of two principal spectroscopic types: Fe II and He/N. These types are believed to be related to fundamental properties of the progenitor binary such as the white dwarf mass. As part of our HET program, we have measured the spectra of 26 M31 novae (representing $\sim 1/3$ of the total for which spectra are available), making it the most significant spectroscopic follow-up study of Local Group novae since the pioneering work of Tomaney & Shafter (1992). To supplement these data, we have included 21 M31 nova spectra obtained over the years with the Lick Observatory 3-m Shane reflector. Finally, in order to characterize the light curves, we have employed a variety of telescopes to acquire broad-band photometric measurements of many of the novae in our spectroscopic sample. Here, we report the results of our survey.

2. Observations

2.1. Spectroscopy

During the early part of our survey, optical spectra were obtained primarily with the Lick 3-m Shane reflector using the Kast double spectrograph (Miller & Stone 1993), although the observation of M31N 1990-10b was taken with the older UV Schmidt spectrograph (Miller & Stone 1987). Most spectra were acquired in one of two basic instrument configurations. One used the D55 dichroic beamsplitter to split the spectrum over ∼5200–5500 Å, with blue light being passed through the 600/4310 grism and red light being reflected off a 300/7500 (or 600/5000) grating. The resulting combined spectra cover the range ∼3300–10000 Å (∼3300–7900 Å), with the 2.0″-wide slit giving a spectral resolution of ∼6 Å in the blue and ∼11 Å (6 Å) in the red. The other setup removed the beamsplitter and all light was sent to a 600/5000 grating on the red side, providing ∼6 Å resolution over the range ∼4300–7000 Å.

The data were reduced using standard techniques (e.g., Foley et al. 2003). Routine CCD processing and spectrum extraction were completed with IRAF[1], and the data were extracted

[1]IRAF is distributed by the National Optical Astronomy Observatory, which is operated by the Associ-

with the optimal algorithm of Horne (1986). We obtained the wavelength scale from low-order polynomial fits to calibration-lamp spectra. Small wavelength shifts were then applied to the data after cross-correlating a template sky to the night-sky lines that were extracted with the nova. Using our own IDL routines, we fit spectrophotometric standard-star spectra to the data in order to flux calibrate our spectra and to remove telluric lines (Wade & Horne 1988; Matheson et al. 2000). A summary of the Lick observations is given in Table 1.

Most of the spectra in this survey, and all of the ones obtained in the past few years, were acquired with the Marcario Low-Resolution Spectrograph (LRS; Hill et al. 1998) on the HET. Initially, we employed the $g2$ grating with a $2.0''$ slit and the GG385 order-blocking filter, covering 4275–7250 Å at a resolution of $R \approx 650$. Later, to obtain more coverage at longer wavelengths, we opted to use the lower resolution $g1$ grating with a $1.0''$ slit and the GG385 filter. This choice increased our wavelength coverage to 4150–11000 Å while yielding a resolution of $R \approx 600$. In practice, the useful spectral range of the $g1$ grating is limited to $\lambda \lesssim 9000$ Å where the effects of order overlap are minimal. All HET spectra were reduced using standard IRAF routines to flat-field the data and to optimally extract the spectra. These were placed on relative flux scales through comparison with observations of spectrophotometric standards routinely used at the HET. The data were not corrected for absorption by the Earth's atmosphere, and telluric absorption features are visible in some of the spectra. A summary of the HET observations is given in Table 2.

Between the Lick and HET observations, we obtained a total of 53 spectra of M31 nova candidates (21 with the Shane and 32 with the HET). These data, shown in Figures 1–12, include 46 M31 novae (5 with two spectra each), and two long-period Mira variables originally thought to be novae. Because the observations were made under a variety of atmospheric conditions with the stellar image typically overfilling the spectrograph slit, our data can not be considered spectrophotometric. Thus, all spectra have been displayed on a relative flux scale. In the caption for each figure we have indicated the time elapsed between discovery of the nova and the date of our spectroscopy. Although the date of discovery does not necessarily reflect the time of maximum light, M31 has been monitored much more frequently over the past decade, and we estimate that the discovery date is likely within a few days of peak brightness in the majority of recent cases.

---

ation for Research in Astronomy, Inc. under cooperative agreement with the National Science Foundation.

2.2. Photometry

To complement our spectroscopic survey, we were able to amass sufficient photometric observations to produce light curves for many of the novae in our survey. Our primary motivation was to measure nova fade rates (t_2) that could then be correlated with other properties, such as spectroscopic class. The photometric data consist both of targeted (mostly B and V-band) observations, which were obtained primarily with the Liverpool Telescope (LT; Steele et al. 2004) and the Faulkes Telescope North (FTN; Burgdorf et al. 2007), and survey images (mainly R band), taken over the years with a variety of telescopes. The LT and FTN data were reduced using a combination of IRAF and Starlink software, calibrated using standard stars from Landolt (1992), and checked against secondary standards from Magnier et al. (1992), Haiman et al. (1994), and Massey et al. (2006).

Our extensive R-band observations were taken largely from the photometric database compiled by one of us (K.H.) as part of an ongoing program to monitor nova light curves in M31. These data include both survey and targeted images taken with various telescopes with diameters of 0.26–6 m. Most of the images come from the 0.65-m telescope of the Ondřejov Observatory (operated partly by the Charles University, Prague) and the 0.35-m telescope in the private observatory of K.H. at Lelekovice. Standard reduction procedures for raw CCD images were applied (bias and dark-frame subtraction and flat-field correction) using the SIMS[2] and Munipack[3] programs. Reduced images of the same series were coadded to improve the signal-to-noise ratio; the total exposure time of these series varied from a few minutes up to about one hour. To facilitate nova detection, the gradient of the galaxy background was flattened by the spatial median filter using SIMS. Photometric and astrometric measurements of the novae were then performed using "Optimal Photometry" (based on fitting of point-spread function profiles) in GAIA[4] and APHOT (a synthetic aperture photometry and astrometry software package developed by M. Velen and P. Pravec at the Ondřejov Observatory; see Pravec et al. [1994]), respectively. Five to ten comparison stars were used for individual brightness measurements. B, V, and R magnitudes for comparison stars located in the M31 field were taken from Massey et al. (2006). Finally, in the case of images taken using the Sloan Digital Sky Survey (SDSS) g' and r' filters, we computed g' and r' magnitudes for comparison stars from $BVRI$ magnitudes taken from Massey et al. (2006) using empirical color transformations between the SDSS $ugriz$ system and the Johnson-Cousins $UBVRI$ system published by Jordi et al. (2006). A summary of all of our

[2]http://ccd.mii.cz/

[3]http://munipack.astronomy.cz/

[4]http://www.starlink.rl.ac.uk/gaia

photometric observations is presented in Table 3.

Between our targeted and archival observations, we were able to produce light curves for a total of 47 of the 91 M31 novae with measured spectra (46 spectra from the present survey and 45 from the literature). The light curves are presented in Figures 13–20. Before turning to a discussion of this wealth of data, we briefly review our present understanding of nova populations, both in the Galaxy and in M31.

3. Nova Populations

3.1. Background

It has been conjectured, based both on Galactic and extragalactic observations, that there may exist more than one population of novae (e.g., Della Valle et al. 1992; Della Valle & Livio 1998; Shafter 2008; Kasliwal et al. 2011, and references therein). Initially, Galactic observations suggested that novae associated with the disk were on average more luminous and faded more quickly than novae thought to be associated with the bulge (e.g., Duerbeck 1990; Della Valle et al. 1992). However, the interpretation of Galactic nova data is complicated by the need to correct for interstellar extinction, which can be significant and varies widely with the line of sight to a particular nova. Furthermore, extinction hampers the discovery of a significant fraction of objects: although Galactic novae occur at an estimated rate of $\sim$30–35 yr^{-1} (Shafter 1997, 2002), only about one in five of these are discovered and subsequently studied in any detail. Consequently, although much has been learned from the study of Galactic novae, it is clear that these data are not ideal for establishing the population characteristics of novae.

Nova eruptions are luminous enough to be detected as far away as the Virgo cluster. However, despite the considerable data amassed in recent years, evidence for distinct nova populations in extragalactic systems is conflicting. Ciardullo et al. (1990b) argued that a galaxy's nova rate was independent of the galaxy's Hubble type, and therefore independent of the galaxy's dominant stellar population. A few years later, based largely on the same data, but with different assumptions regarding the luminosity normalization, Della Valle et al. (1994) proposed that nova rates and light-curve properties (e.g., rate of decline from maximum light) did in fact vary between galaxies of differing Hubble types, with late-type systems such as M33 and the Magellanic Clouds having generally faster fading novae and higher luminosity-specific nova rates. However, subsequent studies (e.g., Shafter et al. 2000; Ferrarese et al. 2003; Shafter & Williams 2004) have questioned these results, arguing that (given the considerable uncertainties that plague the determination of luminosity-specific

nova rates) the available data are insufficient to establish any significant correlation. Further, the broader implications of the argument by Della Valle & Duerbeck (1993) that novae in the Large Magellanic Cloud (LMC) generally were brighter and faded faster than those seen in the older stellar populations of the Galaxy or M31's bulge, has been called into question by Ferrarese et al. (2003) who showed that novae in M49, the first-ranked Virgo elliptical galaxy, generally faded at least as fast as novae in the LMC.

3.2. The Spatial Distribution of Novae in M31

The nearby Sb spiral, M31, is by far the most thoroughly studied extragalactic system, with observations of novae going back to Hubble (1929). Spanning ~ 4 deg on the sky, M31 is well resolved spatially, and offers a convenient target for the study of nova populations. In a classic nova survey from the mid 1950s, Arp (1956) reported the discovery of 30 M31 novae with the 60-in reflector at the Mount Wilson Observatory. Three principal conclusions of Arp's study [augmented by data from Hubble (1929)] were that (1) the frequency of novae dropped off more sharply than the galaxy's light, (2) the nova density decreased within $\sim 4'$ of the nucleus, and (3) the frequency distribution of nova maximum magnitudes is bimodal, with peaks $m_{pg} \approx 16.0$ and $m_{pg} \approx 17.5$ mag (also see Capaccioli et al. 1989). A subsequent survey by Ciardullo et al. (1987) using Hα imaging confirmed that the nova spatial distribution is more centrally concentrated than the background light; in fact the distribution was consistent with a purely bulge population. The central "hole" in the nova distribution noted by Arp was not seen in the Hα data, and was assumed to be an artifact of the poor contrast against the bright nuclear background in Arp's photographic images.

Several more recent studies of the spatial distribution of M31 novae have confirmed the association with M31's bulge population (e.g., Capaccioli et al. 1989; Shafter & Irby 2001; Darnley et al. 2004, 2006), but a major uncertainty in these studies is whether a significant fraction of disk novae are being missed due to internal extinction within the galaxy (see also Hatano et al. 1997). Taken at face value, the association of novae with M31's bulge population came as a surprise given that Galactic novae have long been recognized to have a significant disk population (e.g., Duerbeck 1984, 1990). To address this discrepancy, Ciardullo et al. (1987) proposed the idea that a significant fraction of the novae in M31's bulge could have been formed in the dense cores of the galaxy's globular clusters and subsequently been ejected into the bulge through three-body interactions within the clusters, through tidal disruption of some clusters, or a combination of both processes.

3.3. The Spectroscopic Classification of Galactic Novae

A promising new approach for studying nova populations is to consider the character of a nova's spectrum within a few weeks after maximum light. When analyzing a large sample of Galactic nova spectra, Williams (1992) realized that the novae could be naturally segregated into two principal spectroscopic classes (Fe II and He/N) based on the emission lines in their spectra. Novae displaying prominent Fe II emission (the Fe II novae) usually show P Cygni absorption profiles, evolve more slowly, have lower expansion velocities, and show lower levels of ionization, compared to novae with strong lines of He and N (the He/N novae). Complicating this division is the fact that a small fraction of novae initially exhibit Fe II emission lines along with broad (full width at half-maximum intensity [FWHM] $\gtrsim$ 2500 km s^{-1}) Balmer emission before going on to develop spectra typical of the He/N novae. Such systems are referred to as either hybrid or Fe IIb novae. Both Fe II and He/N novae (although more often the He/N systems) occasionally go on to develop strong Ne emission in their post-outburst spectra, which suggests that the higher-mass ONe white dwarfs may be found in both classes of novae.

Della Valle & Livio (1998) analyzed the spatial distribution of a sample of 22 Galactic novae with data suitable for determining their spectroscopic class. By restricting their sample to novae with well-determined distances (i.e., from expansion parallax), they were able to use the observed positions to estimate the distance of each nova from the Galactic plane. They discovered that the fastest and brightest novae were primarily associated with the He/N spectroscopic class, and that the progenitors were preferentially located close to the Galactic plane (i.e., $z \lesssim 100$ pc). Fainter and dimmer novae, on the other hand, were more typically members of the Fe II class, and were found at much greater heights (up to $z \gtrsim 1000$ pc). Thus, they concluded that the progenitors of the He/N novae were associated with a younger stellar population that are thought to contain a higher proportion of massive white dwarfs.

The precise mechanism that leads to the formation of two distinct post-eruption spectra is not well understood, but is thought to depend most sensitively on the mass of the white dwarf. Systems with relatively massive white dwarfs reach the critical density and temperature for a TNR after accreting a relatively small amount of hydrogen-rich material from the companion star (Starrfield et al. 2008; Townsley & Bildsten 2005). Once the TNR takes place, some fraction of this small accreted mass is ejected at high velocity in the form of a discrete shell. In systems with lower mass white dwarfs, more material is accreted prior to the TNR, and this larger amount of gas is ejected in a combination of a low-mass shell (early in the outburst), and an optically thick wind (shortly thereafter). It is this optically thick wind which is thought to be responsible for the formation of the P Cyg profiles seen in the lower excitation Fe II nova spectra. Thus, the fact that spectroscopic observations appear

to offer a powerful discriminant between nova systems of varying white dwarf mass from differing stellar populations provided the principal motivation for our spectroscopic survey of novae in M31.

4. The M31 Nova Survey

4.1. Spectroscopic Class

Through the end of 2009, a total of 837 nova candidates have been discovered in M31 since the observations of Hubble (1929) began nearly a century ago.(Pietsch et al. 2007e) [5] Of these, spectra are now available for a total of 91 M31 novae, including the 46 from our present survey. As described above, novae spectra are, in principle, divisible into one of three primary classes: Fe II, He/N, and hybrid (or Fe IIb) novae. In practice, however, it is often difficult to make an unambiguous classification. Spectra are taken at different times after eruption, and the signal-to-noise ratio can vary widely from spectrum to spectrum. In addition, a nova can, on occasion, show characteristics of more than one class. For example, during the course of our spectroscopic survey, we have identified three novae (M31N 2007-10a, 2007-10b, and 2007-11b) that might have been traditionally classified as He/N or hybrid, but which do not share all of the characteristics of those classes. These spectra are dominated by prominent but narrow (FWHM < 2000 km s^{-1}) lines of H, He I, and He II, with weaker N III and Fe II emission features occasionally seen. In the basic scheme of Williams (1992), such novae would be difficult to classify. Henceforth, we will refer to these objects as narrow-line He/N, or He/Nn, novae.

The spectra of all novae included in our survey (see Figs. 1–12) were examined and subsequently classified into one of six groups: Fe II, likely Fe II (Fe II:), He/N, likely He/N (He/N:), He/Nn, and hybrid (also known as broad-lined Fe II or Fe IIb novae). We found a total of 30 Fe II novae (∼65%), 6 likely Fe II novae (∼13%), 3 He/N novae (∼6.5%), 3 likely He/N novae (∼6.5%), 3 He/Nn novae (∼6.5%), and 1 hybrid/Fe IIb nova (∼2%).[6] When all 91 novae with measured spectra are considered (see Table 4), the relative percentages remain similar with ∼74% (67 novae), ∼8% (7 novae), ∼11% (9 novae), ∼7% (6 novae), and ∼1% (one nova) representing the Fe II, Fe II:, He/N, He/N: (including the He/Nn systems),

[5] see also http://www.mpe.mpg.de/∼m31novae/opt/m31/index.php

[6] Most, perhaps all, novae that are classified as He/N appear to display some weak Fe II emission near maximum light, and are therefore technically members of the hybrid class. Rather than referring to all of these novae as hybrid objects, we reserve the hybrid classification for those novae with prominent Fe II emission early on (e.g., M31N 2006-10b).

and hybrid classes, respectively. Thus, when all the data are considered, approximately 4 out of 5 ($\sim 82\%$) of the total are likely Fe II novae, with the remaining systems falling in the He/N and related (He/Nn and hybrid/Fe IIb) classes.

There is some exiguous evidence that the relative percentage of He/N and hybrid/Fe IIb novae may be somewhat higher in the Milky Way. In his original paper, Williams (1992) indicated that $\sim 40\%$ of novae in his Galactic sample belonged to the He/N class. Similarly, Della Valle & Livio (1998) found that as many as 10 out of 27 (37%) in their sample of novae with well-determined distances (from expansion parallax) were He/N or Fe IIb systems. More recently, however, Shafter (2007) has reviewed all available spectroscopic data for Galactic novae, finding that only 20 out of the 94 systems ($\sim 21\%$) with sufficient spectroscopic data available for classification appeared to be He/N or hybrid systems. This is consistent with the fraction found in our M31 survey. The relatively large fraction of He/N and Fe IIb systems included in the Della Valle & Livio (1998) study, in particular, may be the result of their sample selection, which was restricted to novae with distances determined from expansion parallax. Such novae are more likely to be nearby and thus located in the Galactic disk.

4.1.1. The Spatial Distribution of Spectroscopic Class

The apparent concentration of He/N and hybrid/Fe IIb novae toward the disk of the Galaxy (Della Valle & Livio 1998) is an intriguing finding, and it would be of considerable interest if it could be confirmed in M31. While it is not possible to determine the height of a given nova above M31's galactic plane, we can explore differences in the spatial distributions between the different spectroscopic classes. Based on the Galactic results of Della Valle & Livio (1998), one might expect that the He/N and related systems would be preferentially associated with the disk of M31, while the Fe II systems would perhaps display a more centrally concentrated, bulge-like distribution.

In Figure 21 we have plotted the projected positions of the 91 M31 novae with known spectroscopic class. Despite the expectation that the He/N nova distribution might be more extended compared to the Fe II systems, there appears to be no obvious dependence of spectroscopic type with spatial position in the galaxy. This impression can be misleading, however, since the high inclination of M31 to the plane of the sky ($i \approx 77^{\circ}$) makes it difficult to assign an unambiguous position within M31 to a given nova. This is particularly true for novae near the center of M31 where the foreground disk is superimposed on the galactic bulge. On the other hand, novae observed at a large galactocentric radius ($\gtrsim 15'$) are likely to be associated with the disk of the galaxy. In order to approximate the true position of a

nova within M31, we have assigned each nova an isophotal radius, defined as the length of the semimajor axis of an elliptical isophote [computed from the R-band surface photometry of Kent (1987)] that passes through the observed position of the nova.

In Figure 22 we show the cumulative distributions of the Fe II and He/N (and hybrid) novae plotted as a function of their isophotal radius. Although it appears that the He/N-hybrid distribution may be slightly more extended than the Fe II distribution, a Kolmogorov-Smirnov (KS) test reveals that the distributions would be expected to differ by more than that observed 81% of the time if they were drawn from the same parent population. When only a subset of the novae with well-established spectroscopic types are considered, this probability decreases slightly to 73%.

The interpretation of these results is complicated by the fact that our spectroscopic data are drawn from a sample of M31 novae that may not be spatially complete. As mentioned earlier, although the CCD surveys conducted in Hα are essentially complete in the innermost regions of the galaxy, they did not typically cover the full disk of M31. In recent years the situation has improved with the availability of wide-field surveys, such as the ROTSE-IIIb program, which have provided good coverage over most of the galaxy. Given the nature of the M31 surveys, we suspect that our spectroscopic sample may be biased somewhat toward novae at smaller galactocentric radii (where, historically, the galaxy has been more frequently monitored), and thus may favor one spectroscopic class over the other. Nevertheless, such a bias should not affect the distributions of Figure 22 in a differential sense: both Fe II and He/N novae are detectable throughout the galaxy. Another potential source of bias involves the fact that the He/N novae are on average brighter and faster fading than the Fe II systems (see §4.2.1 below). One could argue that the brighter He/N novae might be easier to detect against the bright background of the bulge. However, this advantage would be offset to some degree by the fact that these novae generally fade more quickly, making them more likely to be missed in synoptic surveys. Consequently, we conclude, as did Di Mille et al. (2010) based on a smaller sample of novae, that there is no compelling evidence from the observed spatial positions of the novae in our sample that the Fe II and He/N novae arise from different stellar populations in M31.

4.1.2. Nova Expansion Velocity

One of the defining properties of the He/N spectroscopic class is that the emission-line widths are considerably broader than those seen in the Fe II novae. Specifically, Williams (1992) found that the emission lines of Galactic novae in the He/N class are characterized by a half-width at zero intensity (HWZI) > 2500 km s^{-1}. Empirically, we have found that for

most nova line profiles, the HWZI roughly equals the FWHM; since the latter is the more easily measured quantity, we have adopted it to characterize the spectra in our survey. The values of the FWHM and the equivalent widths of Hα and Hβ in our nova spectra are given in Table 5.

Although the emission-line width is expected to be correlated with the expansion velocity of the nova ejecta, the FWHM does not necessarily yield the expansion velocity directly. In an idealized nova, the broad emission features typically seen in an He/N system are believed to be formed mainly in a discrete, optically thin shell ejected at relatively high velocity from near the white dwarf's surface. In this case, the line profiles are expected to be flat-topped and nearly rectangular in appearance, with the FWHM closely approximating the ejection velocity of the shell. In the Fe II systems, however, the lines are mainly produced in a wind, which originates at a distance above the surface of the white dwarf that varies as the outburst evolves. Thus, the escape velocity for this wind is smaller than that at the white dwarf's surface. As a result, the expansion velocity (and hence line width) may depend on the time elapsed since eruption.

When comparing the emission-line widths of the novae in our sample, it must be kept in mind that our spectroscopic data were obtained at varying times after eruption, and thus do not necessarily reflect the relative expansion velocities accurately. Nevertheless, as Figure 23 illustrates, a clear difference between the ejection velocities of the two principal classes of novae (Fe II and He/N) is apparent. Without exception, the novae belonging to the He/N class are characterized by Hα FWHM > 2500 km s^{-1}, while the Fe II systems all have Hα FWHM less than this value. Interestingly, although He/Nn novae display prominent lines of helium as do the standard He/N novae, they are narrow-line objects that resemble a typical Fe II nova at times (e.g., see M31N 2007-11b in Fig. 8). In addition, they often do not display prominent lines of nitrogen as do the typical He/N systems.

4.2. Photometric Properties

To further explore the properties of the novae in our survey, whenever possible we have augmented our spectroscopic data with available photometric observations. Few light curves are available for the novae in our spectroscopic sample that erupted prior to the start of our HET survey in 2006. Nevertheless, when the entire set of spectroscopic novae is considered, we have sufficient photometric data to estimate decline rates for half of the sample.

A convenient and widely used parameterization of the decline rate is t_2, which represents the time (in days) for a nova to decline 2 mag from maximum light. According to the

criteria of Warner (2008), novae with $t_2 \lesssim 25$ days are considered "fast" or "very fast," with the slowest novae characterized by t_2 values of several months or longer. Rates of decline, and corresponding values of t_2, have been measured (for all novae with sufficient photometric coverage) by performing weighted linear least-squares fits to the declining portion of the light curves that extend up to 3 mag below peak. In an attempt to account for systematic errors in the individual photometric measurements, the weights used in the fits were composed of the sum of the formal errors on the individual photometric measurements plus a constant systematic error estimate of 0.1 mag. The net effect of including the systematic error component was a reduction of the relative weighting of points with small formal errors and a corresponding increase in the formal errors of the best-fit parameters and in the uncertainties in t_2 derived from them.

Because our photometric observations do not always begin immediately after discovery, and the date of discovery does not always represent the date of eruption, we have made two modifications to our photometric data in order to better estimate the light-curve parameters. First, when available, we have augmented our light-curve data with the discovery dates and magnitudes given in the catalog of Pietsch et al. (2007e).[7] Second, for some novae we have modified (brightened) the peak magnitude slightly through an extrapolation of the declining portion of the light curve up to 2.5 days pre-discovery in cases where upper flux limits (within 5 days of discovery) are available. The light-curve parameters resulting from our analysis are given in Table 6.

4.2.1. MMRD Relations

If we adopt a distance modulus for M31 of $\mu_0 = 24.38$ mag (Freedman et al. 2001) and a foreground reddening, $E(B-V) = 0.062$ mag (Schlegel et al. 1998), we can compute the absolute magnitude at maximum light, and thereby produce calibrated maximum-magnitude versus rate-of-decline (MMRD) relations. The MMRD relations (the peak absolute magnitude vs. log t_2) for the B, V, and R light curves are shown in Figures 24, 25, and 26, respectively. These plots illustrate not only that the peak nova luminosity is correlated with the rate of decline (i.e., the brightest novae generally fade the fastest), as was first studied extensively by McLaughlin (1945) for Galactic novae, but that the He/N systems are typically among the brightest and fastest novae. Weighted, linear least-squares fits to our B, V,

[7] see also http://www.mpe.mpg.de/∼m31novae/opt/m31/index.php

and R-band[8] data yield

$$M_B = -9.75 \pm 0.11 + (1.69 \pm 0.085)\ \log\ t_2, \tag{1}$$

$$M_V = -9.78 \pm 0.10 + (1.70 \pm 0.080)\ \log\ t_2, \tag{2}$$

and

$$M_R = -10.89 \pm 0.12 + (2.08 \pm 0.077)\ \log\ t_2, \tag{3}$$

respectively. The peculiar He/Nn object M31N 2007-10b, which has particularly scanty light-curve coverage, has a relatively large uncertainty in the peak magnitude. For comparison, in Figure 24 we show the theoretical M_B vs. log t_2 relation of Livio (1992), while in Figure 25 we include the Galactic M_V relation from Downes & Duerbeck (2000):

$$M_V = -11.32 \pm 0.44 + (2.55 \pm 0.32)\ \log\ t_2. \tag{4}$$

The slope of our M31 V-band MMRD relation is shallower than that for the Galactic data, and the M31 data are also systematically fainter than expected from the best-fitting Galactic relations. The latter discrepancy, in particular, as well as some of the scatter generally seen in the MMRD relations, is likely due to the fact that we have only corrected the M31 data for Galactic foreground extinction, not for extinction internal to M31. Based on these comparisons, it appears that the M31 nova sample perhaps suffers as much as 0.5 mag of extinction from within M31 itself, especially in the disk of the galaxy. This value is consistent with an estimate of $A(r') = 0.5$ mag adopted by Darnley et al. (2006) based on the mean for Sb galaxies (Holwerda et al. 2005). In addition, our estimates of maximum light are based upon the magnitude at discovery, which will underestimate the peak luminosity in some cases. If we divide the novae in our sample into two groups, those with isophotal radii $r \leq 10'$ and those with $r > 10'$, we find that the latter sample is slightly fainter at peak by an average of ~ 0.4 mag (16.6 ± 1.1 vs. 17.2 ± 0.9 mag), although the difference is not statistically significant.

In agreement with the results of the Galactic study by Della Valle & Livio (1998), it appears that the He/N novae are on average "faster" than their Fe II counterparts. Indeed,

[8]The R-band MMRD relation includes r'-band data for novae where R-band observations are not available. When both R and r' observations are available for a given nova, only the more extensive data set is used.

although our sample is dominated by Fe II systems, three of the four fastest novae are He/N or related (He/Nn) systems. On the other hand, with the exception of the He/Nn nova M31N 2007-10b, we do not find strong evidence for a significant population of fast, but relatively faint, novae that apparently do not follow the classic MMRD relation. As discussed by Kasliwal et al. (2011), it is possible that these novae arise from progenitors containing high $\dot{M}$ (hot) and relatively massive white dwarfs, similar to what is expected for recurrent novae. Perhaps such novae are related to the class of He/Nn novae described earlier.

Given that the He/N novae generally fade more quickly than the Fe II systems, and that He/N novae have significantly higher expansion velocities based on their emission-line widths, the expansion velocity should be inversely correlated with the light-curve parameter, t_2. In Figure 27 we have plotted the measured t_2 value (based on the V band when possible) versus the measured Hα FWHM for the 25 novae in our survey where it is possible to measure both parameters. As expected, there is a clear trend of faster novae exhibiting higher expansion velocities. The one exception is the He/Nn nova, M31N 2007-10a, which apparently evolved quite quickly despite its relatively slow expansion velocity. Based on these data (excluding M31N 2007-10a), a weighted linear least-squares fit yields the following:

$$\log\, t_2\ (\mathrm{d}) = 6.84 \pm 0.10 - (1.68 \pm 0.02)\ \log\ [\mathrm{H}\alpha\ \mathrm{FWHM}\ (\mathrm{km/s})]. \qquad (5)$$

This relation can be compared with a similar one for Galactic novae found by McLaughlin (1960). A major factor in the discrepancy between the two may arise because in McLaughlin's relation the expansion velocities are derived from the absorption-line minima (P Cyg profiles) measured near maximum light. Typically, such velocities are only 20% to 50% of those inferred from the emission-line FWHM. The scatter in our data, particularly for the slower novae, is probably due in part to the time dependence of the derived velocities, as referred to in §4.1.2 above.

4.2.2. Spatial Distribution of Nova Speed Class

The question of whether the photometric properties of novae in M31 (e.g., peak brightness, fade rate) vary with spatial position in the galaxy (and possibly with stellar population) has yet to be thoroughly studied. Most recent surveys, which have concentrated primarily on the *discovery* of novae either for the purpose of measuring the spatial distribution, the overall rate, or both, lack the high cadence required to produce useful nova light curves. Light-curve data, when available, often only cover Hα or the R band where the relationship between fade rate and peak luminosity is weak or absent (e.g., Ciardullo et al. 1990b). As

mentioned earlier, available broad-band nova data come largely from the photographic surveys of Arp (1956), Rosino (1964, 1973), and Sharov & Alksnis (1992). As noted above, the observation by Arp (1956) that the apparent magnitude distribution for M31 appeared to be bimodal, with peaks corresponding to $M_B \approx -8.5$ and $M_B \approx -7.0$ mag at the distance of M31, was later taken as evidence for the existence of two nova populations (e.g., Capaccioli et al. 1989).

The available light-curve data from previous surveys can be used to augment the extensive photometry obtained as part of our survey to study the variation of nova speed class with spatial position in M31. In particular, Capaccioli et al. (1989) has summarized the light-curve properties (peak magnitude and rate of decline) for novae in the Hubble (1929), Arp (1956), and Rosino (1964, 1973) surveys. From this compilation, we have selected the "high quality" data from their Table VI to supplement the light curves given in Table 6. Using this combined data set, we have assembled values of t_2 for a total of 74 novae. Of these, 35 (approximately half the total) are characterized by $t_2 \leq 25$ days, and were categorized as either "fast" or "very fast" according to the definition in Warner (2008). For our purposes we simply refer to this group as the "fast" novae. We refer to the remaining 35 novae with $t_2 > 25$ days as "slow" novae. Given the uncertainties involved in accurately measuring t_2, we did not restrict our sample of fade rates to any particular color or bandpass; however, when data were available in multiple colors, we chose the t_2 values based on B-band observations to be as consistent as possible with data from earlier surveys.

In Figure 28 we have plotted separately the spatial distributions of the "fast" and "slow" novae. It appears that the slower novae (red circles) are perhaps more centrally concentrated than the fast sample (blue squares). This impression is confirmed when we consider the cumulative distributions shown in Figure 29. A KS test reveals that the two distributions would be expected to differ by more than they do 23% of the time if they were drawn from the same parent distribution. Thus, our data are consistent with the notion that "faster" novae, both in the Galaxy (Duerbeck 1990; Della Valle et al. 1992) and in M31, are more associated with the disk population than are the slower novae. We caution, however, that selection effects could potentially complicate the interpretation of this result. As was pointed out earlier in our discussion of spectroscopic class, our nova sample is not likely to be spatially complete. It is possible that we may be preferentially missing faster novae in the outer regions of the galaxy where the temporal sampling of the surveys has perhaps been less frequent. If so, our conclusion that the faster novae appear to be more spatially extended would actually be strengthened. Taken at face value, our results suggest that the photometric characteristics of novae are likely affected by changes in the underlying stellar population.

4.3. Discussion of Selected M31 Novae

Below we highlight several individual novae of particular significance. These objects have either have been detected as a super-soft X-ray source (SSS), or have been observed extensively, both photometrically and spectroscopically, or have some peculiarity that warrants further discussion.

4.3.1. M31N 1993-10g and 1993-11c

As part of a program of follow-up spectroscopy of Local Group transients, one of us (A.V.F.) obtained spectra of two novae in the bulge of M31 on 1993 Nov. 8 and 17 (UT dates are used throughout this paper). The positions of the two objects are near that of two novae discovered in the survey by Shafter & Irby (2001), M31N 1993-10g and 1993-11c, which are separated by $\sim 49''$. Unfortunately, the original observing logs are no longer available, so we are unable to make an unambiguous connection between the two spectra and the two novae. Based on approximate coordinate information in the FITS header for the spectrum taken on 1993 Nov. 17, we have made the tentative assignments indicated in Figures 1 and 2. The spectrum we have associated with M31N 1993-11h is clearly that of an Fe II nova, while that of 1993-11c is less certain but consistent with an Fe II classification.

Both novae have been identified as possible recurrent nova candidates by Shafter & Irby (2001). The position of M31N 1993-10g is coincident with 1964-01a to within $9.8''$, while that of 1993-11c is within $3.6''$ and $6.5''$ of 1967-12a and 1923-02a, respectively. Given that the coordinates for novae discovered on photographic plates are not known precisely in many cases, these both appear to be plausible recurrent nova candidates. However, both novae are located only $\sim 2'$ from the nucleus of M31 where the nova density is high, increasing the probability of a chance positional coincidence. For a given observed separation s, we can compute the probability of a chance coincidence, P_C, by considering the nova density in an annulus of area A, centered at the position of each nova. Specifically,

$$P_C = 1 - \exp\Big[\sum_{\rm i=1}^{\rm n-1} \ln(1 - {\rm ix})\Big], \tag{6}$$

where n is the number of novae in the annulus, and $x = \pi s^2/A$. In both cases of interest here, we find that $P_C \gtrsim 0.95$, making it highly likely that the two outbursts were a chance coincidence from separate objects, and therefore not from a recurrent nova.

4.3.2. M31N 1995-11e

M31N 1995-11e was identified during the nova survey of Shafter & Irby (2001), who first recorded the object on 1995 Nov. 28 at $m_{H\alpha} = 18.1$ mag. The object evolved quite slowly, reaching $m_{H\alpha} = 17.9$ mag after approximately a month before slowly fading. Then, on 2008 July 6.8, K. Nishiyama and F. Kabashima (Miyaki-Argenteus Observatory, Japan) found that the object had appeared again at $m \approx 18.6$ mag (unfiltered) before reaching $m \approx 18$ mag on Sep. 09. Our spectrum presented here (see Fig. 12) and originally reported by Shafter et al. (2008) clearly shows that the object is a long-period red variable star (i.e., a Mira variable), and not a nova.

4.3.3. M31N 2001-10a

M31N 2001-10a was discovered as part of the POINT-AGAPE (Darnley et al. 2004) and the Naini Tal microlensing surveys (Joshi et al. 2004). Our spectroscopic data and r'-band photometry show that M31N 2001-10a was a relatively slowly evolving Fe II nova characterized by $t_2 = 73$ days. X-ray observations reported by Henze et al. (2010, 2011) show the nova to be a long-lived SSS that was still detectable more than 7 yr post outburst. The long duration of the SSS phase is indicative of prolonged burning on the surface of the white dwarf. This is expected for the relatively large accreted mass associated with slowly evolving outbursts on a low-mass white dwarf.

4.3.4. M31N 2005-01a

M31N 2005-01a, discovered by Hornoch (2005) on 2005 Jan. 07.89, was a particularly luminous nova that was well covered photometrically near maximum light, reaching $R = 15.04$ mag (see Fig. 14). Our spectrum (see Fig. 4), taken 8 days post discovery when the nova was near $R = 15.3$ mag, shows that the object was clearly an Fe II system. It appears to be one of a small number of luminous Fe II novae ($M \lesssim -9.0$ mag) similar to M31N 2007-11d and 2009-10b (see Figs. 24–26).

4.3.5. M31N 2005-07a

M31N 2005-07a, discovered by K.H. on Jul 2005 27.909 at $R = 18.4$ mag, reached $R = 17.4$ mag on Jul 29.919. Our spectrum (see Fig. 4), taken $\sim$2 days post discovery

when the nova was near maximum, is characterized by narrow Hα emission and a number of extremely weak features that may include He and N emission. We tentatively classify the object as an Fe II: system, but it is possibly related to the He/Nn novae.

4.3.6. M31N 2005-09b

M31N 2005-09b was discovered in the outskirts of M31 by Quimby et al. (2005) on Sep. 1.23 using the 0.45-m ROTSE-IIIb telescope at the McDonald Observatory. The nova reached $m = 16.5$ mag (unfiltered) a day later on Sep. 2.23. Optical spectra by Leonard (2005) and Pietsch et al. (2006) reveal moderately broad Balmer (Hα: FWHM $\approx$ 2000 km s^{-1}, HWZI $\approx$ 2200 km s^{-1}), Fe II, Na D, and He I emission features. The nova is consistent with membership in the Fe II spectroscopic class; however, the emission-line width is at the high end of what is normally seen in Fe II novae, and the nova could be plausibly included in the Fe IIb or hybrid class.

4.3.7. M31N 2006-09c

M31N 2006-09c was discovered independently by Quimby (2006), K. Itagaki, P. Kušnirák, and K.H. on 2006 Sep. 18.[9] It was detected $\sim$ 150 days post discovery by both the IRAC and IRS instruments on the *Spitzer Space Telescope* as part of an infrared survey of selected M31 novae recently conducted by Shafter et al. (2011). No evidence of an infrared excess characteristic of dust formation was apparent at the time of these observations. The nova was also detected as a weak SSS by Henze et al. (2011) and originally classified as a Fe II nova by Shafter et al. (2006). Our R-band photometry shows that $t_2 = 26$ days, indicating a moderate rate of decline typical of the Fe II class.

4.3.8. M31N 2006-10a

M31N 2006-10a was a relatively faint nova discovered at $R = 18.7$ mag on 2006 Oct. 25.8 by K.H.[10] Our observations (see Figs. 5 and 14) reveal the object to be a slowly evolving Fe II nova. It was also observed by Shafter et al. (2011) $\sim$ 110 days post discovery as part of

[9] see http://www.cbat.eps.harvard.edu/CBAT_M31.html#2006-09c, and http://www.mpe.mpg.de/~m31novae/opt/m31/M31_table.html

[10] see http://www.cbat.eps.harvard.edu/CBAT_M31.html#2006-09c

their *Spitzer* survey. M31N 2006-10a showed the clearest evidence of the 10 novae observed by *Spitzer* for a near-infrared excess (in this case peaking at $\lambda \approx 4$ μm), suggestive of dust formation. They went on to estimate the total mass of dust formed to be $\sim 2 \times 10^{-6}$ $M_\odot$ under the assumption that the dust was carbon based. Henze et al. (2011) found no evidence of X-ray emission from this nova during the time of their observations.

4.3.9. M31N 2006-10b

M31N 2006-10b was discovered independently by K. Itagaki on 2006 Oct. 31.583 and by R. Quimby and F. Castro at $m \approx 16.4$ mag on unfiltered CCD images taken 2006 Oct. 31.09.[11] The time of maximum light is well constrained by Itagaki's image from Oct. 30.530 (limiting mag 20.0), which shows no evidence of the nova. Although the light curve is not complete near maximum light, the available evidence suggests that the nova faded quite rapidly, with estimates of $t_2(B) = 21$ days and $t_2(V) = 11$ days.

We obtained two spectra of the nova, the first ~ 1 day post discovery on 2006 Nov. 01, and the other ~ 3 weeks later on 2006 Nov. 23. M31N 2006-10b can be technically considered a "hybrid" nova given that Fe II emission was seen the day after discovery, but by the time of the second observation the spectrum had clearly evolved into that of a classic He/N nova. The object was observed 102 and 110 days post discovery by Shafter et al. (2011) with the *Spitzer* IRS and IRAC, respectively, but not detected with either instrument.

4.3.10. M31N 2006-11a

M31N 2006-11a is a typical Fe II nova (see Fig. 6) that was discovered by K. Itagaki at $m = 17.4$ mag (unfiltered) on 2006 Nov. 25.494.[12] The object was observed by Shafter et al. (2011) as part of their *Spitzer* survey. It was marginally detected by the IRAC, but not with the IRS, 86 and 77 days after discovery, respectively.

---

[11] see http://www.cbat.eps.harvard.edu/CBAT_M31.html#2006-10b

[12] see http://www.cbat.eps.harvard.edu/CBAT_M31.html#2006-11a

4.3.11. M31N 2007-02b

This nova was discovered by one of us (K.H.) on 2007 Feb. 03.[13] It was classified as a likely hybrid nova by Pietsch et al. (2007a) based on possible He and N emission in the spectrum. Our spectrum, taken on 2007 Feb. 10.06, suggests the object is an Fe II system (see Fig. 7), although there appears to be a broader component in the Hα and (possibly) the Hβ emission lines that is often seen in the hybrid systems. The light curve measured in the R band yields $t_2(R) = 35$ days, which is typical of an Fe II nova but would be somewhat slow for a hybrid system. The object was also detected as a SSS by Henze et al. (2011), and was still detectable 2 yr after eruption. Such a long active SSS phase is characteristic of a relatively large accreted mass. We conclude that the object was likely an Fe II nova.

4.3.12. M31N 2007-06b

M31N 2007-06b was discovered by Quimby et al. (2007) as part of the ROTSE IIIb program at McDonald Observatory on 2007 Jun 19.4 at $m = 16.8$ mag (unfiltered) and found to be spatially coincident with the M31 globular cluster Bol 111. The nova faded by at least 1 mag in ~ 9 days, suggesting $t_2 \lesssim 18$ days. Spectroscopic observations by Shafter & Quimby (2007) revealed the nova to be a member of the He/N spectroscopic class. The object was subsequently detected as a SSS by Pietsch et al. (2007b).

4.3.13. M31N 2007-07f

M31N 2007-07f was a slowly evolving nova discovered in the outskirts of M31 as part of the ROTSE-IIIb program by Yuan et al. (2007), and is apparently a member of the Fe II spectroscopic class (Quimby 2007, private communication). The object exhibited a slow rise to maximum light, reaching $m = 17.7 \pm 0.3$ mag on 2007 Jul. 24.02. Approximately 203 days later the object was observed in the *Spitzer* survey of Shafter et al. (2011) and detected by the IRAC. As discussed by Shafter et al. (2011), 2007-07f showed evidence (although more marginal than for M31N 2006-10a) for a weak infrared excess, consistent with that expected from dust grains formed in the ejecta.

---

[13] see http://www.cbat.eps.harvard.edu/CBAT_M31.html#2007-02b

4.3.14. M31N 2007-08d

This object was discovered by Pietsch et al. (2007c) at $R = 18.7$ mag on 2007 Aug. 24.081. Our spectrum (see Fig. 7) and light curve (Fig. 15) reveal the object to be a member of the Fe II class with $t_2 \approx 63$ days. The nova was included in the Shafter et al. (2011) *Spitzer* survey and marginally detected with the IRAC, but not the IRS, about 158 and 183 days post discovery, respectively.

4.3.15. M31N 2007-10a

M31N 2007-10a was discovered K. Itagaki on Oct. 5.606 and independently by Pietsch et al.[14] The spectrum was classified by Gal-Yam & Quimby (2007) as an Fe II nova, but our spectrum (see Fig. 7) reveals narrow Balmer, He I $\lambda\lambda$4921, 5016, 5876, and He II λ4686 emission, with only a trace of Fe II, possibly blended with He I at 5169 Å. M31N 2007-10a is the prototype of our proposed He/Nn spectroscopic class. The nova faded rapidly with $t_2(B) \approx t_2(V) \approx 7$ days, and was not subsequently detected as an SSS by Henze et al. (2011), nor as an infrared source in the *Spitzer* survey of Shafter et al. (2011).

4.3.16. M31N 2007-10b

M31N 2007-10b is the best example from our survey of a faint but fast nova similar to the class of novae discovered by Kasliwal et al. (2011). The nova was discovered by Burwiz et al. (2007) at $R = 17.8$ mag, who were able to constrain the time of maximum to within a day of 2007 Oct. 13.26, and independently by K.H. and P. Kušnirák.[15] The nova faded unusually quickly: our B, V, and R light curves suggest $t_2 \approx 3$–4 days. Rau et al. (2007) classified the object as an He/N nova based on a spectrum obtained ~ 3 days post discovery, and noted that the emission lines were unusually narrow (FWHM H$\alpha = 1450 \pm 100$ km s^{-1}) for this class. Based on the available photometric and spectroscopic data, we suggest that the object is a member of our proposed He/Nn class. Consistent with its rapid evolution, the object was detected by Henze et al. (2011) as a SSS with an X-ray duration of less than 100 days.

---

[14] see http://www.cbat.eps.harvard.edu/CBAT_M31.html#2007-10a

[15] see http://www.cbat.eps.harvard.edu/CBAT_M31.html#2007-10b

4.3.17. M31N 2007-11b

M31N 2007-11b, our third example of an He/Nn nova, was discovered by Pietsch et al. (2007d) and independently by E. Ovcharov and A. Valcheva.[16] Although our spectrum (see Fig. 8) appears to be quite similar to that of an Fe II nova (albeit with weak Fe II emission), subsequent spectra by Rau (2007) and Barsukova et al. (2007b) showed that the object quickly developed prominent, narrow (FWHM H$\alpha = 1430\pm100$ km s^{-1}) Balmer, He I, and He II emission lines. Unlike the other He/Nn systems (M31N 2007-10a and 2007-10b), the light-curve evolution of 2007-11b was not particularly fast, with $t_2(B) = 25$ days and $t_2(V) = 45$ days, respectively.

4.3.18. M31N 2007-11d

M31N 2007-11d was an unusually bright and slowly rising nova discovered by K. Nishiyama and F. Kabashima on Nov. 17.57, and subsequently studied extensively by Shafter et al. (2009). The early spectrum was that of a classic Fe II system: narrow Balmer and Fe II emission lines flanked to the blue by pronounced P-Cyg absorption features. Another spectrum obtained ~ 2 weeks later revealed moderately broad Balmer and Fe II emission lines (FWHM H$\alpha = 2260$ km s^{-1}) with weak He I and O I emission (see Fig. 8). The nova faded moderately rapidly ($t_2[V] = 9.5$ days) for an Fe II nova, and was apparently not detected as an SSS source despite what must have been a relatively large accreted mass. It was also observed, but not detected, with the *Spitzer* IRS (Shafter et al. 2011).

4.3.19. M31N 2007-11g

M31N 2007-11g was discovered by Ovcharov et al. (2007) on 2007 Nov 28.716 at $R \approx 18.7$ mag. Our spectrum, presented in Fig. 12 and originally reported by Shafter et al. (2007), clearly shows that the object is not a nova, but rather a long-period Mira variable in M31.

4.3.20. M31N 2007-12b

M31N 2007-12b was a relatively bright and rapidly evolving He/N nova. It was discovered on 2007 Dec. 9.53 by K. Nishiyama and F. Kabashima1 at $m = 16.1$–16.2 mag

[16] see http://www.cbat.eps.harvard.edu/CBAT_M31.html#2007-11b

(unfiltered), and independently by K.H. on Dec. 10.73 at $R = 17.0$ mag.[17] Subsequent spectroscopic observations revealed the object to be a rapidly declining ($t_2 = 8.7[B], 7.2[V]$ days) He/N system (see Fig. 9 and Table 6). Initially, the object was thought to be a recurrent nova given its close proximity to the position of M31N 1969-08a; however, subsequent astrometry established that the two novae were, in fact, distinct objects.

Archival *Hubble Space Telescope* observations of the pre-outburst location of M31N 2007-12b (Bode et al. 2009) revealed the presence of a coincident stellar source with magnitude and color very similar to those of the Galactic recurrent nova RS Ophiuchi, where the red giant secondary star dominates the light at quiescence. This discovery, coupled with the rapid photometric evolution and the object's detection by the *Swift* satellite (Burrows et al. 2005) as an SSS (Kong & Di Stefano 2008), were interpreted by Bode et al. (2009) as strong evidence that M31N 2007-12b is, nevertheless, a recurrent nova system.

4.3.21. M31N 2007-12d

M31N 2007-12d was discovered independently by Henze et al. (2007) and by K. Nishiyama & F. Kabashima[18] on 2007-Dec. 17.57. Although no detailed light-curve data exist, Henze et al. (2011) estimated a rapid decline with $t_2 \approx 4$ days. Our spectrum (see Fig. 9) reveals the nova to be a classic He/N system with broad emission lines of H, He, and N (FWHM H$\alpha \approx 5000$ km s^{-1}) indicating a high expansion velocity. The nova was detected briefly (< 20 days) as an SSS by Henze et al. (2011).

4.3.22. M31N 2009-10b

M31N 2009-10b was discovered by K.H. and P. Kušnirák on 2009 Oct. 9.986 (Hornoch 2009), and independently by K. Itagaki on Oct. 11.414.[19]. It was an unusually bright nova that reached $R = 14.7$ mag (Hornoch et al. 2009b) before fading relatively rapidly ($t_2 \approx 10$ days in B and V). Spectroscopic observations by Di Mille et al. (2009b) and Barsukova et al. (2009b) show conclusively that the nova belongs to the Fe II spectroscopic class, making it quite similar to M31N 2007-11d.

---

[17] see http://www.cbat.eps.harvard.edu/CBAT_M31.html#2007-12b

[18] see http://www.cbat.eps.harvard.edu/CBAT_M31.html#2007-12d

[19] see http://www.cbat.eps.harvard.edu/CBAT_M31.html#2009-10b

5. Conclusions

Whether there exist two distinct populations of classical novae is an important but unanswered question. In an attempt to gain further insight, we have conducted a major spectroscopic survey of novae in the nearby galaxy M31. These data have allowed us to determine spectroscopic classes for a total of 46 novae, more than doubling the number previously available. Specifically, after combining our data with published spectra, we have now been able to compile a list of spectroscopic classes for a total of 91 novae that erupted prior to 2010. In addition, we have undertaken photometric observations of many of the recent novae in this group in order to measure their light curves (i.e., their peak brightness and rate of decline). Whenever possible, we have augmented our photometric observations with light-curve data from the literature.

Our combined spectroscopic and photometric survey has allowed us to explore the spatial distribution of novae in M31 to a greater extent than has been possible previously. An analysis of these data has enabled us to arrive at the following conclusions.

• As part of this survey we have found that $\sim 80\%$ of the M31 novae with available spectra belong to the Fe II class. The remaining $\sim 20\%$ are composed of novae whose spectra are characterized by H, He, and N emission lines, with Fe II emission features either weak or absent. Usually these latter systems display relatively broad (FWHM $\gtrsim 2500$ km s^{-1}) lines typical of the He/N spectroscopic class; however, a small fraction of these systems (e.g., M31N 2007-10a, 2007-10b, and 2007-11b) are characterized by relatively narrow line widths (FWHM $\lesssim 2000$ km s^{-1}). We refer to the latter systems as narrow-line He/N, or He/Nn, novae. The relative percentages of Fe II and He/N (and related) novae are similar to those found for Galactic novae (Shafter 2007; Della Valle & Livio 1998).

• We have presented photometric observations with sufficient coverage to determine light-curve parameters (peak brightness and rate of decline) for most of the novae in our spectroscopic survey, and for approximately half of all novae with known spectroscopic classifications. These data have allowed us to confirm that novae in the He/N and He/Nn classes have generally faster light-curve evolution than the more common Fe II objects. When the light-curve parameters for the entire sample are considered, we find that the brighter novae generally fade the fastest; they are consistent with an MMRD relation. Similarly, we find that the ejection velocities inferred from line widths are higher for the faster novae, as is the case for their Galactic counterparts.

• Under the assumption that there exist two separate populations of novae (bulge and disk populations), it is believed that the disk population, with their generally more massive white dwarfs, should produce novae that are on average brighter and faster than their counterparts

in the bulge population (Duerbeck 1990; Della Valle et al. 1992). To test this prediction further, we have explored the photometric behavior (specifically t_2) of novae as a function of spatial position in M31. After supplementing photometric data from our survey with decline rates from the "high quality" light-curve sample given by Capaccioli et al. (1989), we were able to generate a sample of 74 M31 novae with well-determined fade rates. This sample was subsequently divided into two groups: those with $t_2 \leq 25$ days (the "fast" sample) and those with $t_2 > 25$ days (the "slow" sample). A comparison of the spatial distributions for the two samples shows that the fast novae are in fact more spatially extended from the core of M31 than the slow novae, as expected in the two-population scenario.

• We have also explored the possibility that the spectroscopic class of M31 novae varies with spatial position in the galaxy, as would be expected if the He/N and related novae contain more massive white dwarfs. Surprisingly, as shown in Figures 21 and 22, the spatial distribution shows only a hint that Fe II objects may be more centrally concentrated (i.e., associated with the bulge of M31), and there is no compelling evidence for a dependence on spectroscopic class. Specifically, a KS test shows a 81% probability that the Fe II and He/N distributions would differ more than what is observed if they were drawn from the same overall distribution. This result suggests that the average white dwarf mass in nova systems may not be as strongly dependent on spatial position (and hence stellar population) in M31 as suggested by the photometric data.

Taken together, our spectroscopic and photometric data do not provide compelling evidence in support of the hypothesis that there exist two populations of novae in M31. Nevertheless, our light-curve data can be interpreted as mildly suggestive of a weak dependence of nova-speed class on spatial position (stellar population) within the galaxy. Furthermore, our spectra are not inconsistent with the possibility that spectroscopic type may be sensitive to stellar population. Whatever sensitivity there may be, however, appears to be weak, if it exists at all.

A major step forward in the understanding of nova populations generally, and the spectroscopic classification specifically, will likely require additional spectra and light-curve data for novae erupting in galaxies spanning a range of morphological types. For example, a sample of light curves and spectra from novae arising in the extreme Population II environment of an elliptical galaxy will be particularly instructive. The Large Synoptic Survey Telescope, when it becomes operational, will generate a large sample of Virgo cluster nova light curves that will undoubtedly shed new light on the question of nova populations. Spectra of novae in Virgo cluster galaxies can then be obtained with low-resolution spectrographs currently available on 10-m class telescopes.

The work presented here was made possible through observations obtained from facilities based throughout the world. Spectra were obtained with the Lick Observatory Shane 3-m telescope operated by the University of California and with the Marcario Low-Resolution Spectrograph on the Hobby-Eberly Telescope, which is operated by McDonald Observatory on behalf of the University of Texas at Austin, the Pennsylvania State University, Stanford University, the Ludwig-Maximillians-Universität, Munich, and the George-August-Universität, Göttingen. Photometric observations were made using the Liverpool Telescope, which is operated on the island of La Palma by Liverpool John Moores University (LJMU) in the Spanish Observatorio del Roque de los Muchachos of the Instituto de Astrofisica de Canarias with financial support from the UK Science and Technology Facilities Council. Faulkes Telescope North (FTN) is operated by the Las Cumbres Observatory Global Telescope network. Data from FTN were obtained as part of a joint programme between Las Cumbres Observatory and the LJMU Astrophysics Research Institute. Photometric observations were also obtained at the Centro Astronómico Hispano Alemán (CAHA) Observatory at Calar Alto, operated jointly by the Max-Planck Institut für Astronomie and the Instituto de Astrofísica de Andalucía (CSIC), with the 6-m telescope of the Special Astrophysical Observatory (SAO) of the Russian Academy of Sciences (RAS), operated under the financial support of the Science Department of Russia (registration number 01-43), with the Vatican Advanced Technology Telescope (the Alice P. Lennon Telescope and the Thomas J. Bannan Astrophysics Facility), with the 1.3-m McGraw-Hill and the 2.4-m Hiltner telescopes at the MDM Observatory, with the 2.5-m Isaac Newton Telescope operated on the island of La Palma by the Isaac Newton Group in the Spanish Observatorio del Roque de los Muchachos of the Instituto de Astrofsica de Canarias, with the 2.1-m telescope of the Kitt Peak National Observatory, National Optical Astronomy Observatory, which is operated by the Association of Universities for Research in Astronomy (AURA), Inc., under cooperative agreement with the National Science Foundation, and with the 0.84-m telescope of the Observatorio Astronómico Nacional, San Pedro Mártir. We wish to thank the staff of all these facilities for their assistance in obtaining the observations reported here.

Finally, we would like to thank the following individuals for contributing images of M31: V. L. Afanasiev, Z. Bardon, M. Burleigh, P. Cagaš, S. Casewell, S. N. Dodonov, T. Farnham, A. Galád, J. Gallagher, P. Garnavich, J. Gorosabel, T. Henych, M. Jelínek, A. Karska, C. Kennedy, R. Khan, P. Kubánek, P. Kušnirák, D. Mackey, K. Morhig, B. Mueller, O. Pejcha, J. Prieto, N. Samarasinha, L. Šarounová, P. Šedinová, O. N. Sholukhova, K. Thorne, B. Tucker, M. Tukinská, A. Valeev, M. Wolf, and P. Zasche. We are also grateful to the following for assistance with the Lick spectroscopic observations and reductions: A. Coil, R. J. Foley, M. Ganeshalingam, S. Jha, L. C. Ho, J. Hoffman, D. C. Leonard, W. Li, M. Papenkova, F. J. D. Serduke, J. C. Shields, and J. M. Silverman. Photometric reduction

software was kindly provided by P. Cagaš (SIMS), F. Hroch (Munipack), and M. Velen and P. Pravec (Aphot). This research has made use of the SIMBAD database, operated at CDS, Strasbourg, France, and of NASA's Astrophysics Data System Bibliographic Services. A.V.F.'s group at UC Berkeley is grateful for the financial support of the National Science Foundation (most recently through grant AST-0908886) and the TABASGO Foundation. A.W.S. is grateful to the University of Victoria for hospitality during a recent sabbatical leave while this work was being completed, and to the NSF for financial support through grants AST-0607682 and AST-1009566.

REFERENCES

Arp, H. 1961, ApJ, 133, 869

Barsukova, E., et al. 2007, ATel, 1186, 1

Barsukova, E., Afanasiev, V., Fabrika, S., Valeev, A., Hornoch, K., & Pietsch, W. 2009b, ATel, 2251

Barsukova, E., Sholukhova, O., Valeev, A., Fabrika, S., Goranskij, V., Pietsch, W., & Hornoch, K. 2008, ATel, 1773

Barsukova, E., Valeev, A., Fabrika, S., Burwitz, V., & Pietsch, W. 2007b, ATel, 1314

Barsukova, E., Valeev, A., Sholukhova, O., Medvedev, A., Hornoch, K., Pietsch, W., & Fabrika, S. 2009a, ATel, 2205

Barth, A. J. 2001, in Astronomical Data Analysis Software and Systems X, ed. F. R. Harnden, Jr., F. A. Primini, & H. E. Payne (San Francisco: ASP, Conf. Ser. Vol. 238), 385

Bryan, J., Filippenko, A. V., & Shields, J. C. 1990, IAUC, 5135

Bryan, J., Wren, W., Filippenko, A. V., Matheson, T., & Ho, L. C. 1992, IAUC, 5658

Burrows, D. N. et al. 2005, SSRv, 120, 165

Bode, M. F., & Evans, A. 1982, MNRAS, 200, 175

Bode, M. F., & Evans, A. 1983, MNRAS, 203, 285

Bode, M. F., & Evans, A. 1989, in Classical Novae, 1st ed., ed. M. F. Bode & A. Evans (Chichester: J. Wiley), 163

Bode, M. F., Darnley, M. J., Shafter, A. W., Page, K. L., Smirnova, O., Anupama, G. C., & Hilton, T. 2009, ApJ, 705, 1056

Burgdorf, M. J., Bramich, D. M., Dominik, M., Bode, M. F., Horne, K. D., Steele, I. A., Rattenbury, N., & Tsapras, Y. 2007, P&SS, 55, 582

Burwitz, V., Pietsch, W., Updike, A., Hartmann, D., Milne, P., & Williams, G. 2007, ATel, 1238

Capaccioli, M., Della Valle, M., Rosino, L., & D'Onofrio, M. 1989, AJ, 97, 1622

Chornock, R., Silverman, J. M., George, M. R., & Filippenko, A. V. 2008, ATel, 1708

Ciardullo, R., Ford, H. C., & Jacoby, G. H. 1983, ApJ, 272, 92

Ciardullo, R., Ford, H. C., Neill, J. D., Jacoby, G. H., & Shafter, A. W. 1987, ApJ, 318, 520

Ciardullo, R., Shafter, A. W., Ford, H. C., Neill, J. D., Shara, M. M., & Tomaney, A. B. 1990b, ApJ, 356, 472

Ciardullo, R., Tamblyn, P. Jacoby, G. H., Ford, H. C., & Williams, R. E. 1990a, AJ, 99, 1079.

Ciroi, S., Di Mille, F., Rafanelli, P., & Temporin, S. 2007, ATel, 1292

Darnley, M. J., et al. 2004, MNRAS, 353, 571

Darnley, M. J., et al. 2006, MNRAS, 369, 257

Della Valle, M., Bianchini, A., Livio, M., & Orio, M. 1992, A&A, 266, 232

Della Valle, M., & Duerbeck, H. W. 1993, A&A, 271, 175

Della Valle, M., & Livio, M. 1998, ApJ, 506, 818

Della Valle, M., Rosino, L., Bianchini, A., & Livio, M. 1994, ApJ, 287, 403.

Di Mille, F., Ciroi, S., Rafanelli, P., Navasardyan, H., & Bufano, F. 2007, ATel, 1325

Di Mille, F., Orio, M., Ciroi, S., Bianchini, A., Rafanelli, P., & Nelson, T. 2008a, AN, 331, 197

Di Mille, F., Orio, M., Ciroi, S., Bianchini, A., Rafanelli, P., & Nelson, T. 2010, AN, 331, 197

Di Mille, F., Ciroi, S., Navasardyan, H., Orio, M., Rafanelli, P., & Bianchini, A. 2009a, ATel, 2171

Di Mille, F., Ciroi, S., Orio, M., Rafanelli, P., Bianchini, A., Nelson, T., & Andreuzzi, G. 2008b, ATel, 1818

Di Mille, F., et al. 2009, ATel, 2248

Downes, R. A., & Duerbeck, H. W. 2000, AJ, 120, 2007

Duerbeck, H. W. 1984, Ap&SS, 99, 363

Duerbeck, H. W. 1990, in Physics of Classical Novae, ed. A. Cassatella & R. Viotti (New York: Springer-Verlag), 96

Fabrika, S., Sholukhova, O., Valeev, A., Hornoch, K., & Pietsch, W. 2009a, ATel, 2239

Fabrika, S., Sholukhova, O., Valeev, A., Hornoch, K., & Pietsch, W. 2009b, ATel, 2240

Ferrarese, L., Côté, P., & Jordán, A. 2003, ApJ, 599, 1302

Foley, R. J., et al. 2003, PASP, 115, 1220

Freedman, W. L. 2001, ApJ, 553, 47

Gal-Yam, A., & Quimby, R. 2007, ATel, 1236

Hachisu, I., & Kato, M. 2006, ApJS, 167, 59

Haiman, Z., et al., 1994, A&A, 286, 725

Hatano, K., Branch, D., Fisher, A., & Starrfield, S. 1997, ApJ, 487, L45

Hatzidimitriou, D., Reig, P., Manousakis, A., Pietsch, W., Burwitz, V., & Papamastorakis, I. 2007, A&A, 464, 1075

Henze, M., Pietsch, W., Updike, A., Hartmann, D., Milne, P., & Williams, G. 2007, ATel, 1336

Henze, M., et al. 2010, A&A, 523, 89

Henze, M., et al. 2011, A&A, in press.

Hill, G. J., Nicklas, H. E., MacQueen, P. J., Tejada, C., Cobos Duenas, F. J., & Mitsch, W. 1998, Proc. SPIE, 3355, 375

Holwerda, B. W., Gonzalez, R. A., Allen, R. J., & van der Kruit, P. C. 2005, AJ, 129, 1396

Horne, K. 1986, PASP, 98, 609

Hornoch, K. 2005, IAUC, 8461.

Hornoch, K. 2009, CBET, 1971

Hornoch, K., & Pejcha, O. 2009d, CBET, 2061

Hornoch, K., Pejcha, O., & Kusnirak, P. 2009c, CBET, 2058

Hornoch, K., Pejcha, O., & Wolf, M. 2009a, CBET, 2062

Hornoch, K., Pejcha, O., Zasche, P., & Kusnirak, P. 2009b, CBET, 2057

Hubble, E. P. 1929, ApJ, 69, 103

Humason, M. L. 1932, PASP, 44, 381

Jordi, K., Grebel, E. K., & Ammon, K. 2006, A&A, 460, 339

Joshi, Y. C., Pandley, A. K., Narasimha, D., Giraud-Héeraud, Y., Sagar, R., & Kaplan, J. 2004, A&A, 415, 471

Kasliwal, M. M. 2009, CBET, 2015

Kasliwal, M. M., Cenko, S. B., Kulkarni, S. R., Ofek, E. O., Quimby, R. & Rau, A. 2011, ApJ, in press.

Kasliwal, M. M., Rau, A., Salvato, M., Cenko, S. B., Ofek, E. O., Quimby, R., & Kulkarni, S. R. 2008, ATel, 1886

Kent, S. M. 1987, AJ, 95, 306

Kong, A. K. H., & Di Stefano, R. D. 2008, ATel, 1360

Landolt, 1992, AJ, 104, 340

Livio, M. 1992, ApJ, 393, 516

Miller, J. S., & Stone, R. P. S. 1987, Lick Observatory Technical Reports, Vol. 48 (Santa Cruz, CA: Lick Obs.)

Miller, J. S., & Stone, R. P. S. 1993, Lick Observatory Technical Reports, Vol. 66 (Santa Cruz, CA: Lick Obs.)

Magnier, E. A. et al.,1992, A&AS, 96, 379

Massey, P., et al., 2006, AJ, 131, 2478

Matheson, T., Filippenko, A. V., Ho, L. C., Barth, A. J., & Leonard, D. C. 2000, AJ, 120, 1499

Medvedev, A., et al. 2009, ATel, 2213

McLaughlin, D. B. 1945, PASP, 57, 69

McLaughlin, D. B. 1960, in Stellar Atmospheres, ed. J. L. Greenstein (Chicago: Univ. of Chicago Press)

Ovcharov, E., Valcheva, A., Kostov, A., Nikolov, Y., Georgiev, Ts., & Nedialkov, P. 2007, ATel, 1312

Pietsch, W., Burwitz, V., Stoss, R., & Sanchez, S. 2005, ATel, 520

Pietsch, W., et al. 2007a, ATel, 1009

Pietsch, W., Burwitz, V., Greiner, J., Haberl. F, Henze, M., & Sala, G. 2007b, ATel, 1294

Pietsch, W., Burwitz, V., Stefanescu, A., Hatzidimitriou, D., Ppsel, J., Binnewies, S., Ruder, H., Papamastorakis, G. 2007c, ATel, 1201

Pietsch, W., Burwitz, V., Updike, A., Milne, P., Williams, G., & Hartmann, D. 2007d, ATel, 1257

Pietsch, W., et al., 2007e, A&A, 465, 375

Quimby, R. 2006 ATel, 887

Quimby, R., Mondol, P., Hoeflich, P., Wheeler, J. C., & Gerardy, C. 2005, ATel, 600

Quimby, R., et al. 2007, ATel, 1118

Rau, A. 2007, ATel, 1276

Rau, A., Burwitz, V., Cenko, S. B., Updike, A., Hartmann, D., Milne, P., & Williams, G. 2007b, ATel, 1242

Rau, A., Burwitz, V., Hatzidimitriou, D., & Cenko, S. B. 2007a, ATel, 1153

Rau, A., & Cenko, S. B. 2007, ATel, 1331

Rau, A., Kasliwal, M. M., & Burwitz, V. 2008, ATel, 1568

Reig, P., Primak, N., Akras, S., Hatzidimitriou, D., Pietsch, W., & Papamastorakis, G. 2008, ATel, 1612

Rodríguez-Gil, P., Ferrando, R., Rodríguez, D., Bode, M. F., Huxor, A., Giles, P., & Mackey, D. 2009, ATel, 2166

Rosino, L. 1964, AnAp, 27, 498

Rosino, L. 1973, A&AS, 9, 347

Schlegel, D. J., Finkbeiner, D. P., & Davis, M. 1998, ApJ, 500, 525

Shafter, A. W. 1997, ApJ, 487, 226

Shafter, A. W. 2002, in Classical Nova Explosions, ed. M. Hernanz & J. José (New York: AIP, Conf. Proc. 637)

Shafter, A. W. 2007, BAAS, 211.5115

Shafter, A. W. 2008, in Classical Novae, 2nd ed., ed. M. Bode & A. Evans (Cambridge: Cambridge Univ. Press), 335

Shafter, A. W., Bode, M. F., Darnley, M. J., Misselt, K. A., Rubin, M., & Hornoch, K. 2011, ApJ, 727, 50

Shafter, A. W., Ciardullo, R., Bode, M. F., Darnley, M. J., Misselt, K. A., Nishiyama, K., & Kabashima, F. 2008 ATel, 1834

Shafter, A. W., Ciardullo, R., & Pritchet, C. J. 2000, ApJ, 530, 193

Shafter, A. W., Coelho, E. A., Misselt, K. A., Bode, M. F., Darnley, M. J., & Quimby, R. 2006, ATel, 923

Shafter, A. W., & Irby, B. K. 2001, ApJ, 563, 749

Shafter, A. W., Rau, A., Quimby, R. M., Kasliwal, M. M., Bode, M. F., Darnley, M. J., & Misselt, K. A. 2009, ApJ, 690, 1148

Shafter, A. W. & Quimby, R. M 2007, ApJ, 671, 121

Shafter, A. W., & Williams, S. J. 2004, ApJ, 612, 867

Shafter, A. W., et al. 2007, ATel, 1851.

Sharov, A. S. 1993, Ast.L., 19, 7

Sharov, A. S., & Alksnis, A. 1992, Ap&SS, 190, 119

Starrfield, S., Iliadis, C., & Hix, R. 2008, in Classical Novae, 2nd ed., ed. M. Bode & A. Evans (Cambridge: Cambridge Univ. Press), 77

Steele, I. A., et al., 2004, SPIE, 5489, 679

Tomaney, A. B., & Shafter, A. W. 1992, ApjS, 81, 683

Townsley, D. M., & Bildsten, L. 2005, ApJ, 628, 395

Tutukov, A. V., & Yungelson, L. R. 1995, in Cataclysmic Variables, ed. A. Bianchini, M. Della Valle, & M. Orio (Dordrecht: Kluwer), 495

Valeev, A., Barsukova, E., Sholukhova, O., Medvedev, A., Hornoch, K., Kusnirak, P., Pietsch, W., & Fabrika, S. 2009, ATel, 2208

Wade, R. A., & Horne, K. 1988, ApJ, 324, 411

Warner, B. 1995, in Cataclysmic Variable Stars, (Cambridge: Cambridge Univ. Press)

Warner, B. 2008, in Classical Novae, 2nd ed., ed. M. Bode & A. Evans (Cambridge: Cambridge Univ. Press), 16

Williams, R. E. 1992, AJ, 104, 725

Yuan, F., Rykoff, E., Aretakis, J., Akerlof, C., & Quimby, R. 2007, ATel, 1158

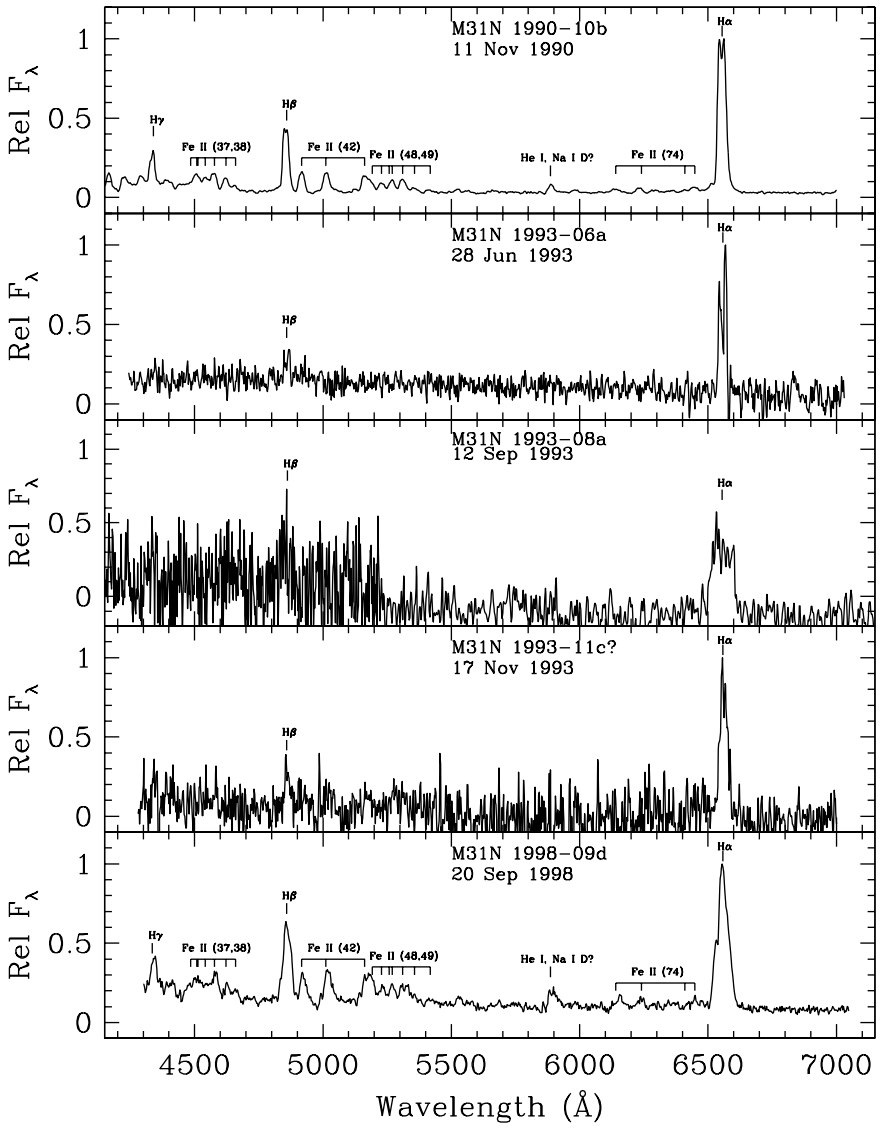

Fig. 1.— Spectra of the M31 novae M31N 1990-10b, 1993-06a, 1993-08a, 1993-11c (ID uncertain; see text), and 1998-09d, taken 19, 25, 37, 9, and 9 days post discovery, respectively. All are Fe II systems with the possible exception of M31N 1993-08a, which has a broad Hα emission line characteristic of the He/N novae.

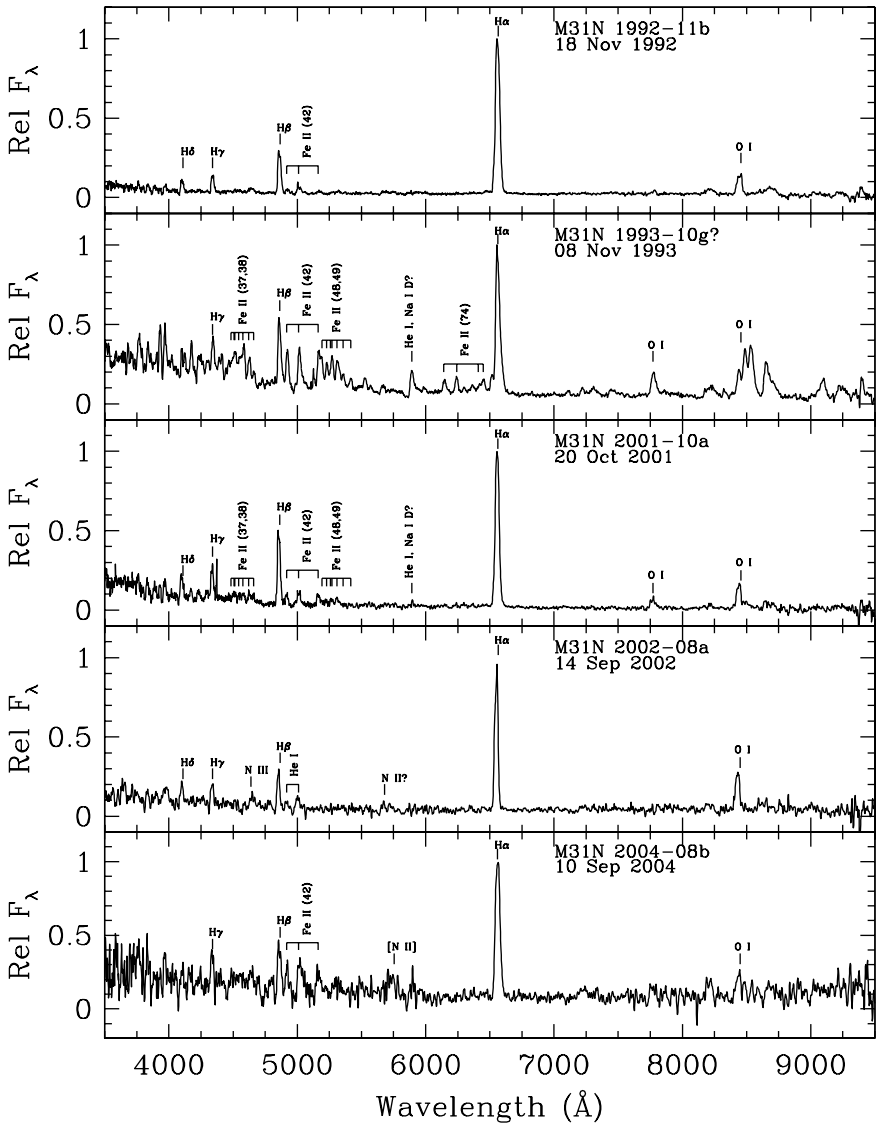

Fig. 2.— Spectra of the M31 novae M31N 1992-11b, 1993-10g (ID uncertain, see text), 2001-10a, 2002-08a, and 2004-08b obtained 10, 21, 17, 40, and 34 days post discovery, respectively. All are Fe II systems with the possible exception of 2002-08a, which was observed well past maximum light and has a spectrum similar to that of an He/Nn nova.

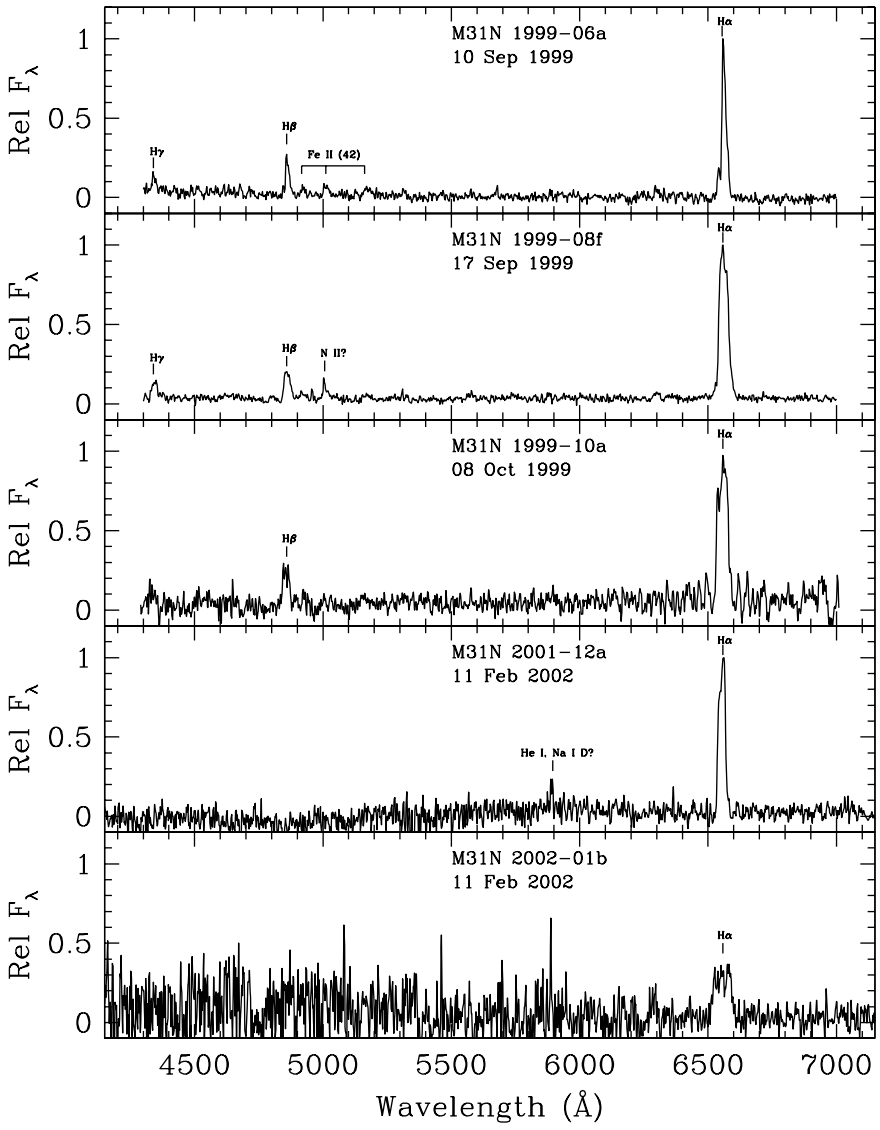

Fig. 3.— Spectra of the M31 novae M31N 1999-06a, 1999-08f, 1999-10a, 2001-12a, and 2002-01b, taken 75, 19, 6, 58, and 35 days post discovery, respectively. All are Fe II novae with the exception of 1999-08f, where the type is uncertain, and 2002-01b, where the broad Hα line suggests that the object may be a He/N system.

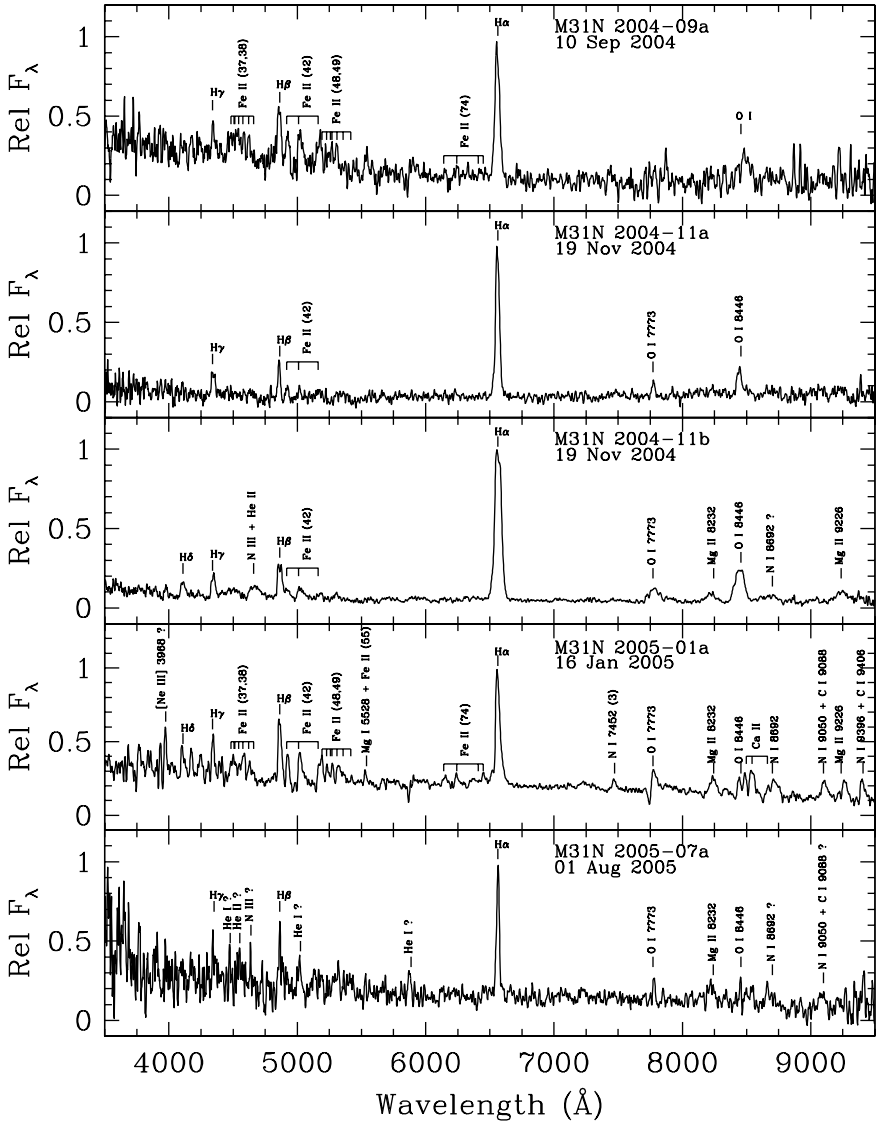

Fig. 4.— Spectra of the M31 novae M31N 2004-09a, 2004-11a, 2004-11b, 2005-01a, and 2005-07a taken 8, 14, 14, 8, and 2 days post discovery, respectively. All are Fe II novae with the possible exception of 2004-11b, which has a spectrum characterized by relatively broad Balmer and N III emission similar to that of an Fe IIb, or hybrid nova, and M31N 2005-07a, which might be a He/Nn system.

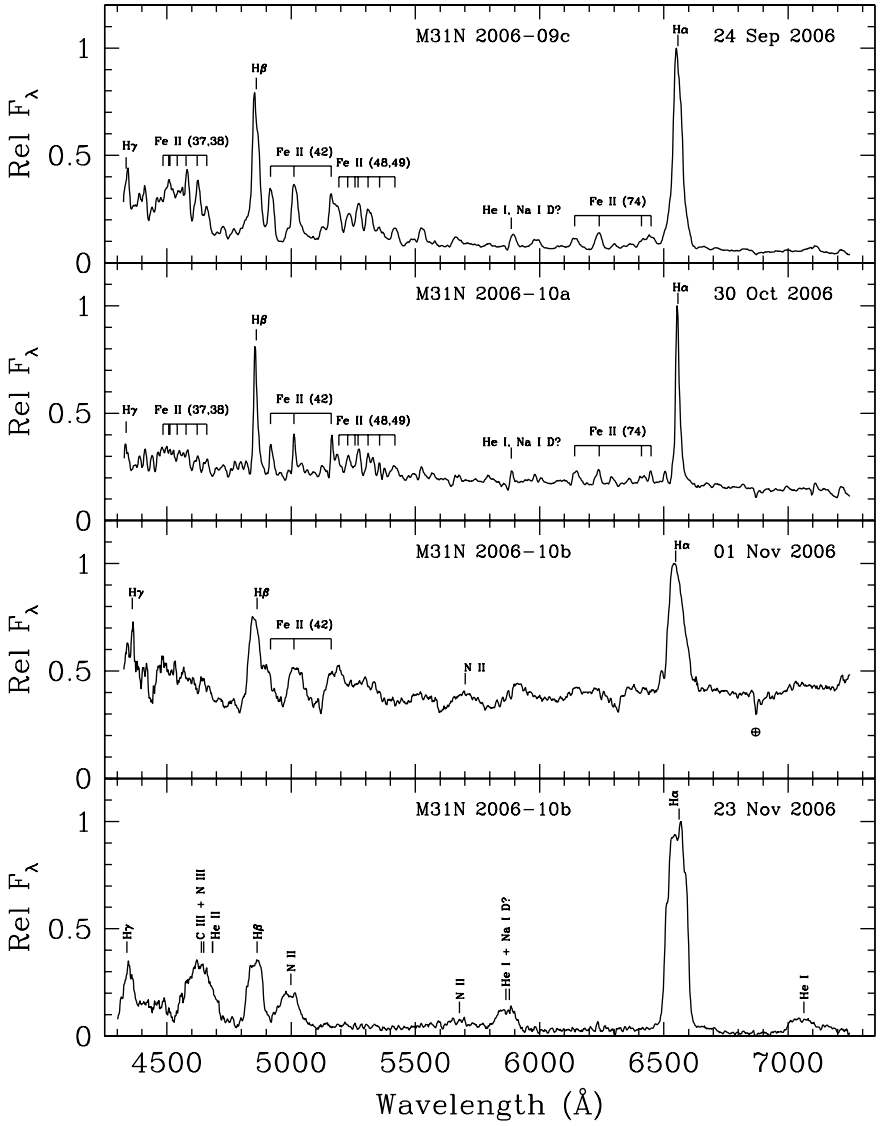

Fig. 5.— Spectra of the M31 novae M31N 2006-09c, 2006-10a, and two observations of 2006-10b taken 7, 8, 2, and 24 days post discovery, respectively. Both M31N 2006-09c and M31N 2006-10a are typical Fe II novae, while M31N 2006-10b (observed twice) is an example of a hybrid or Fe IIb nova. By the time of the second spectrum, M31N 2006-10b had evolved into a classic He/N nova.

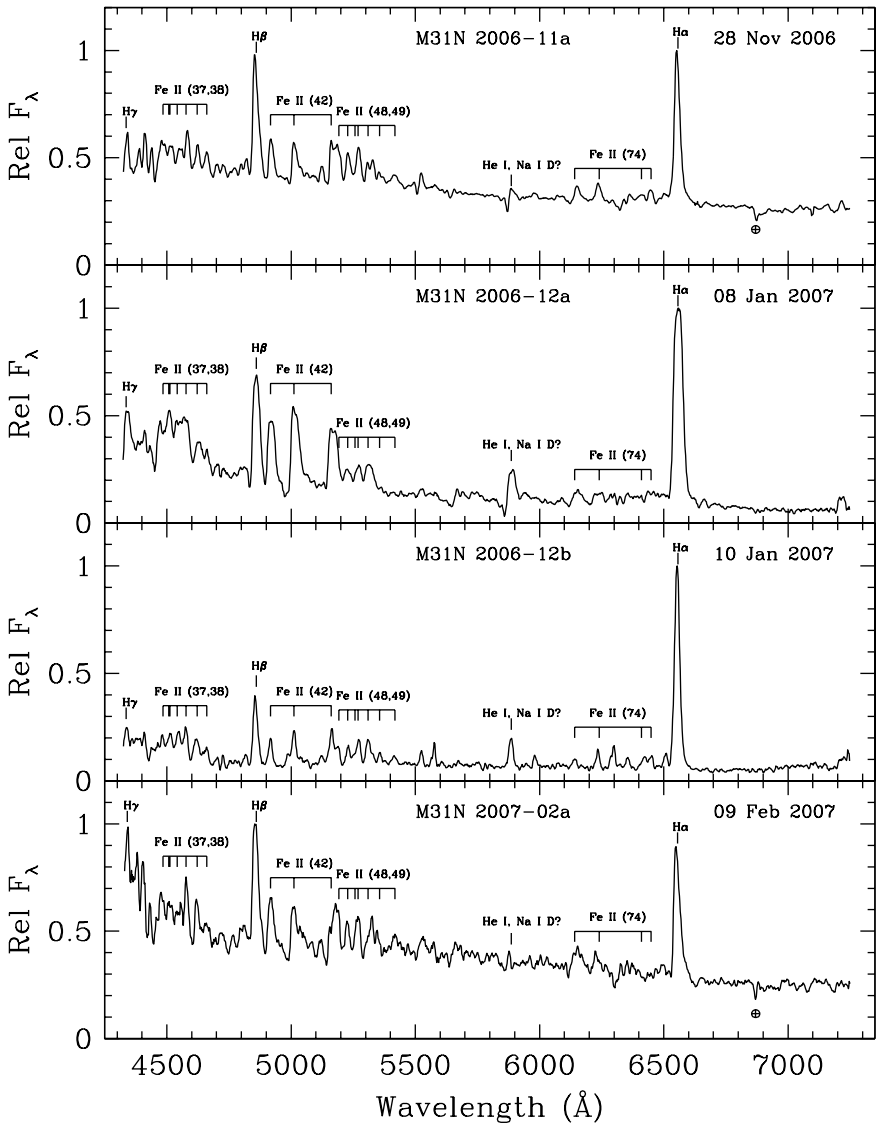

Fig. 6.— Spectra of the M31 novae M31N 2006-11a, 2006-12a, 2006-12b, and 2007-02a, taken 4, 24, 18, and 3 days post discovery, respectively. All four novae are typical members of the Fe II class.

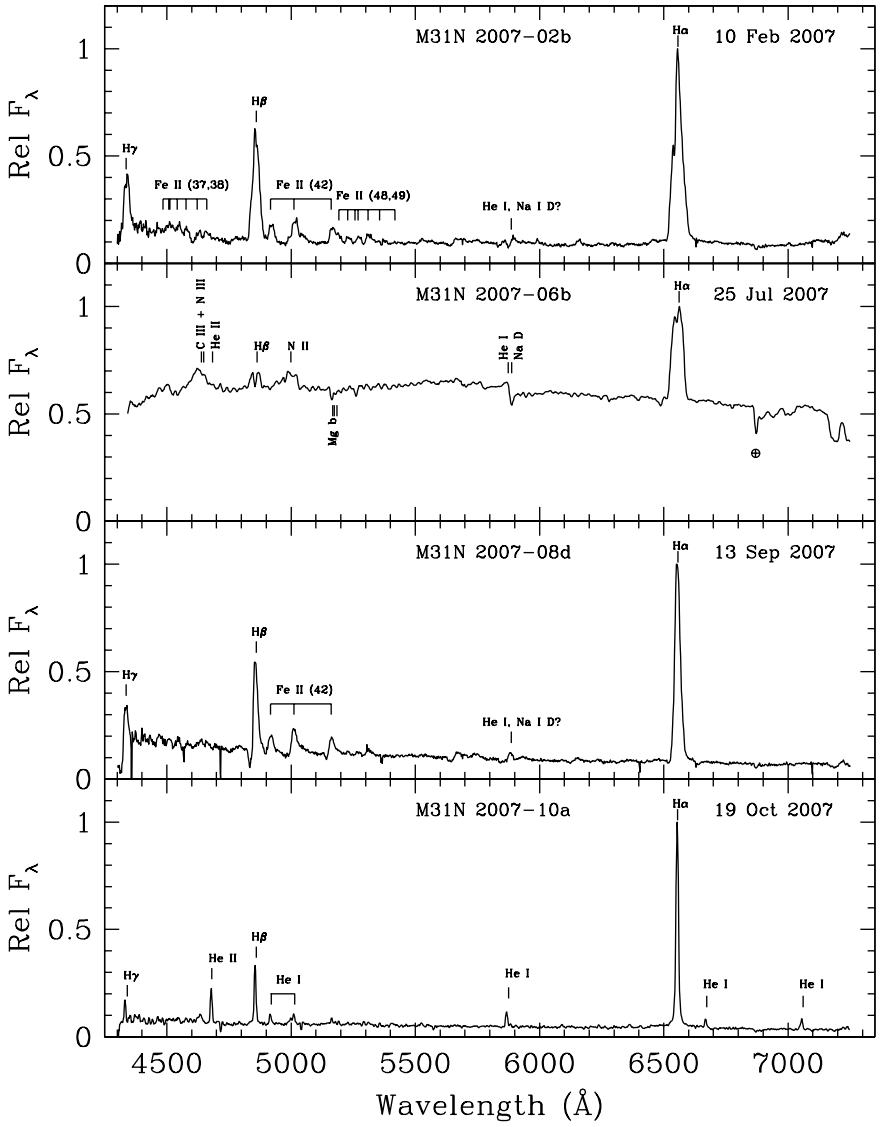

Fig. 7.— Spectra of the M31 novae M31N 2007-02b, 2007-06b, 2007-08d and 2007-10a, taken 7, 37, 21, and 14 days post discovery, respectively. M31N 2007-02b is likely to be an Fe II system, although the broad component in the Balmer lines is often seen in hybrid novae. M31N 2007-06b is a He/N nova that originated in the M31 globular cluster Bol 111 (Shafter & Quimby 2007). M31N 2007-08d is a Fe II system. M31N 2007-10a is an unusual nova displaying prominent Balmer and He I lines. The nova is not typical of either the Fe II class (no Fe II lines) or the He/N class (the lines are narrow and there is no sign of nitrogen lines). This is the prototype of our new class of the narrow-lined He novae (He/Nn).

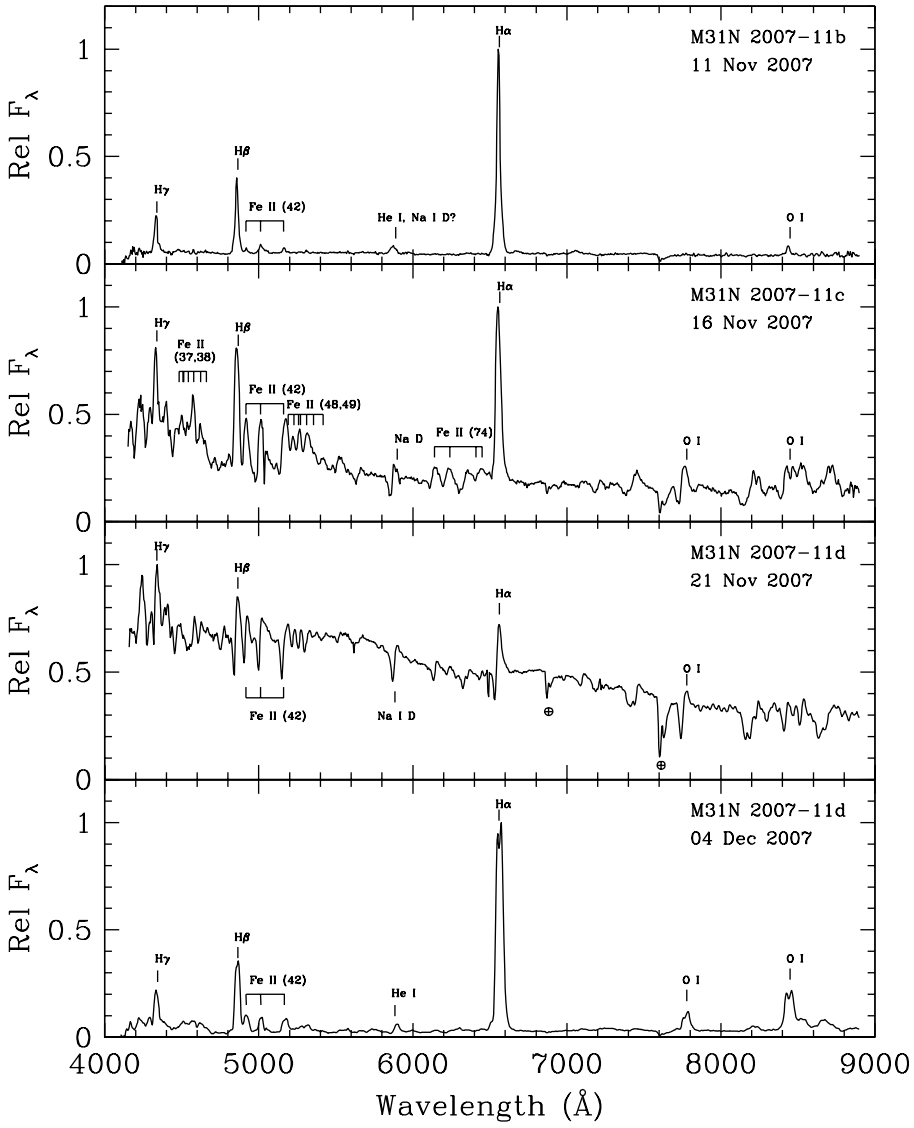

Fig. 8.— Spectra of the M31 novae M31N 2007-11b, 2007-11c, and 2007-11d (two spectra), taken 11, 5, 5, and 18 days post discovery, respectively. All are Fe II novae. M31N 2007-11d was observed twice, shortly after eruption when the P Cyg line profiles were clearly evident, and roughly two weeks later after the continuum had faded considerably.

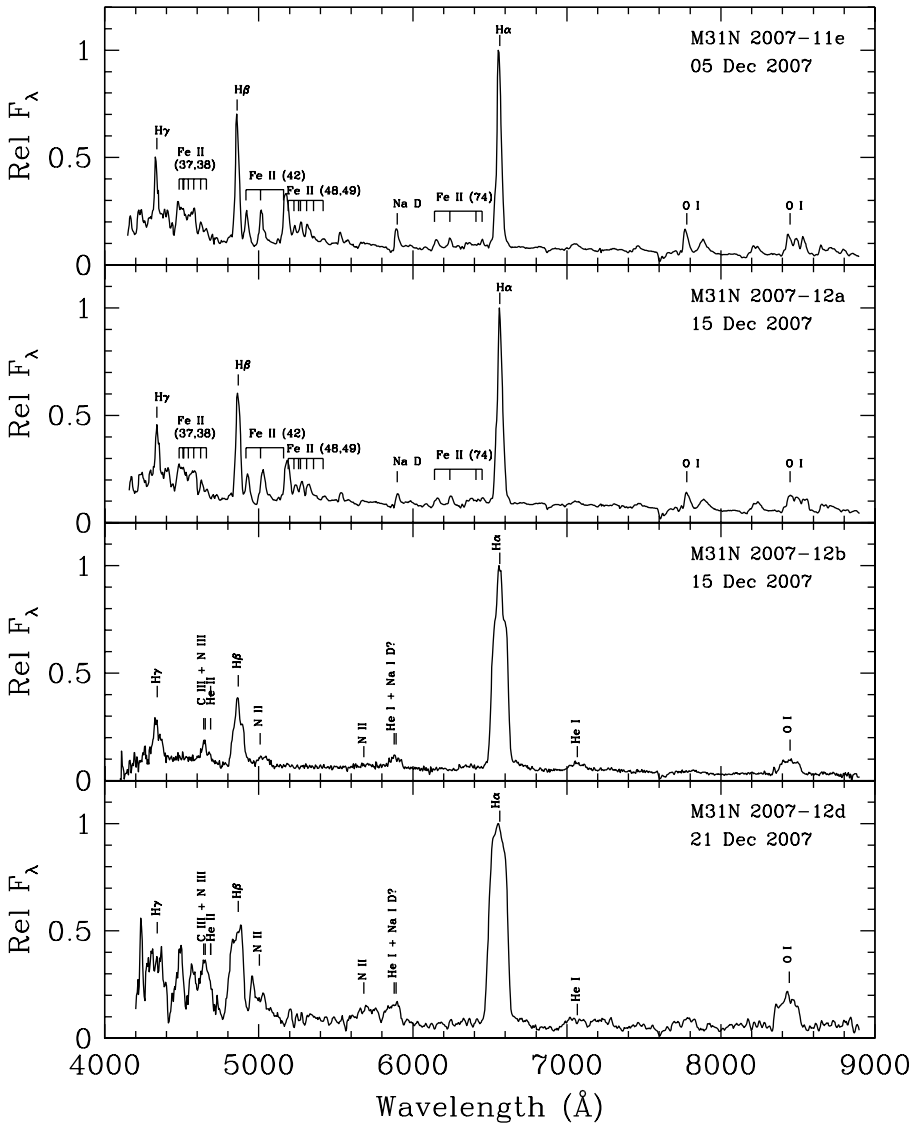

Fig. 9.— Spectra of the M31 novae M31N 2007-11e, 2007-12a, 2007-12b, and 2007-12d, taken 8, 10, 6, and 4 days post discovery, respectively. M31N 2007-11e and M31N 2007-11a are typical Fe II novae, while M31N 2007-12b and M31N 2007-12d are both examples of He/N novae.

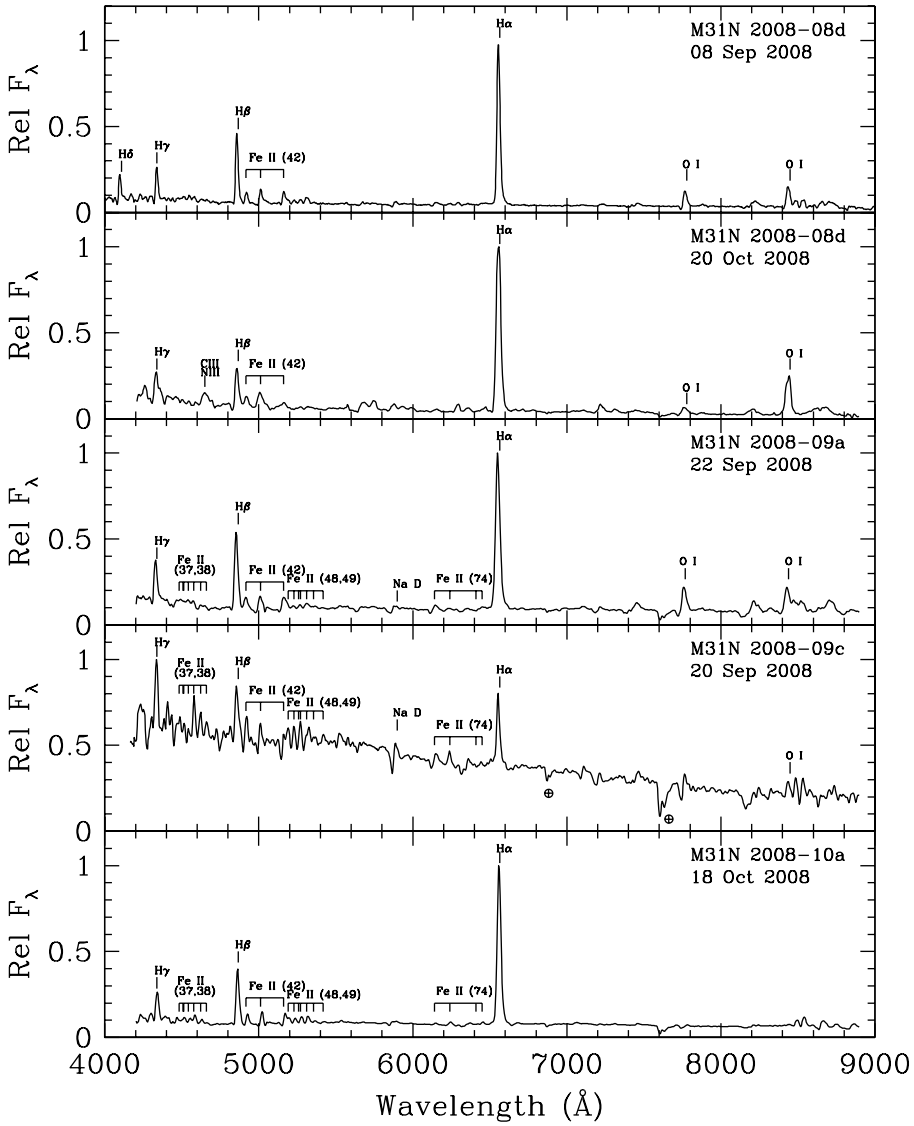

Fig. 10.— Spectra of the M31 novae M31N 2008-08d (two spectra), 2008-09a, 2008-09c, and 2008-10a, taken 14, 57, 10, 6, and 11 days post discovery, respectively. All four novae are of the Fe II spectral type.

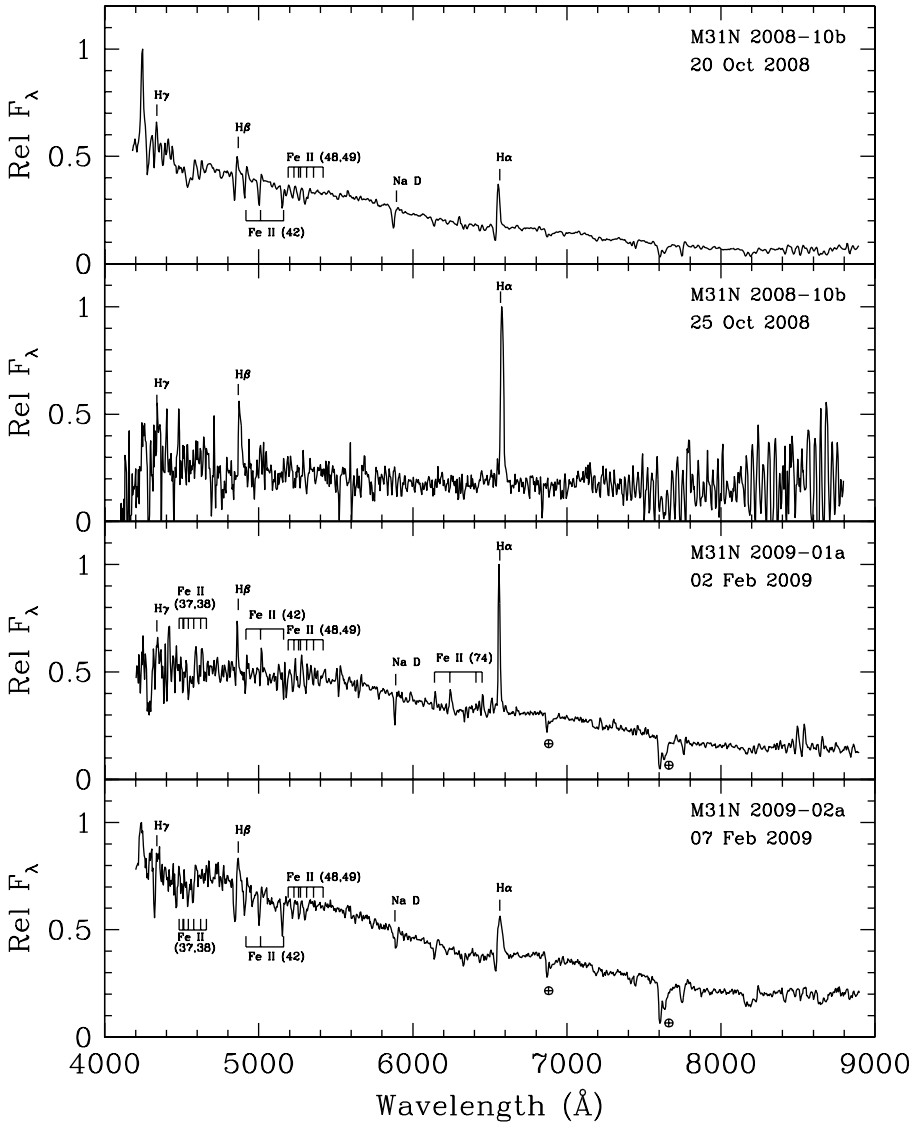

Fig. 11.— Spectra of the M31 novae M31N 2008-10b (two spectra), 2009-01a, and 2009-02a, taken 15, 20, 6, and 2 days, respectively. M31N 2008-10b is a Fe II nova that was observed twice. The first spectrum of M31N 2008-10b and the spectra of and M31N 2009-01a and M31N 2009-02a display P Cyg profiles indicating that they were observed shortly after eruption.

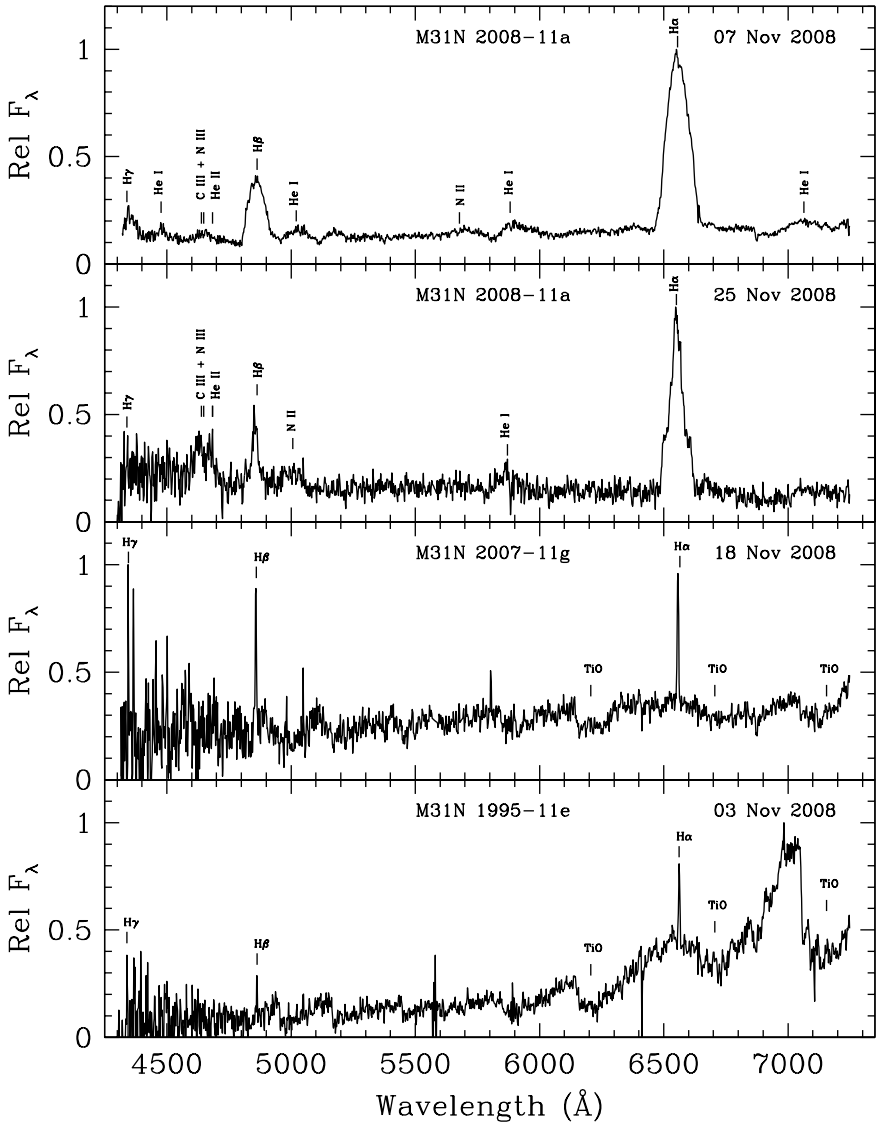

Fig. 12.— Spectra of the M31 nova M31N 2008-11a, a classic He/N nova, taken 4 and 22 days post discovery. The final two objects, M31N 2007-11g and M31N 1995-11e, are examples of long-period variable stars that were mistakenly classified as novae.

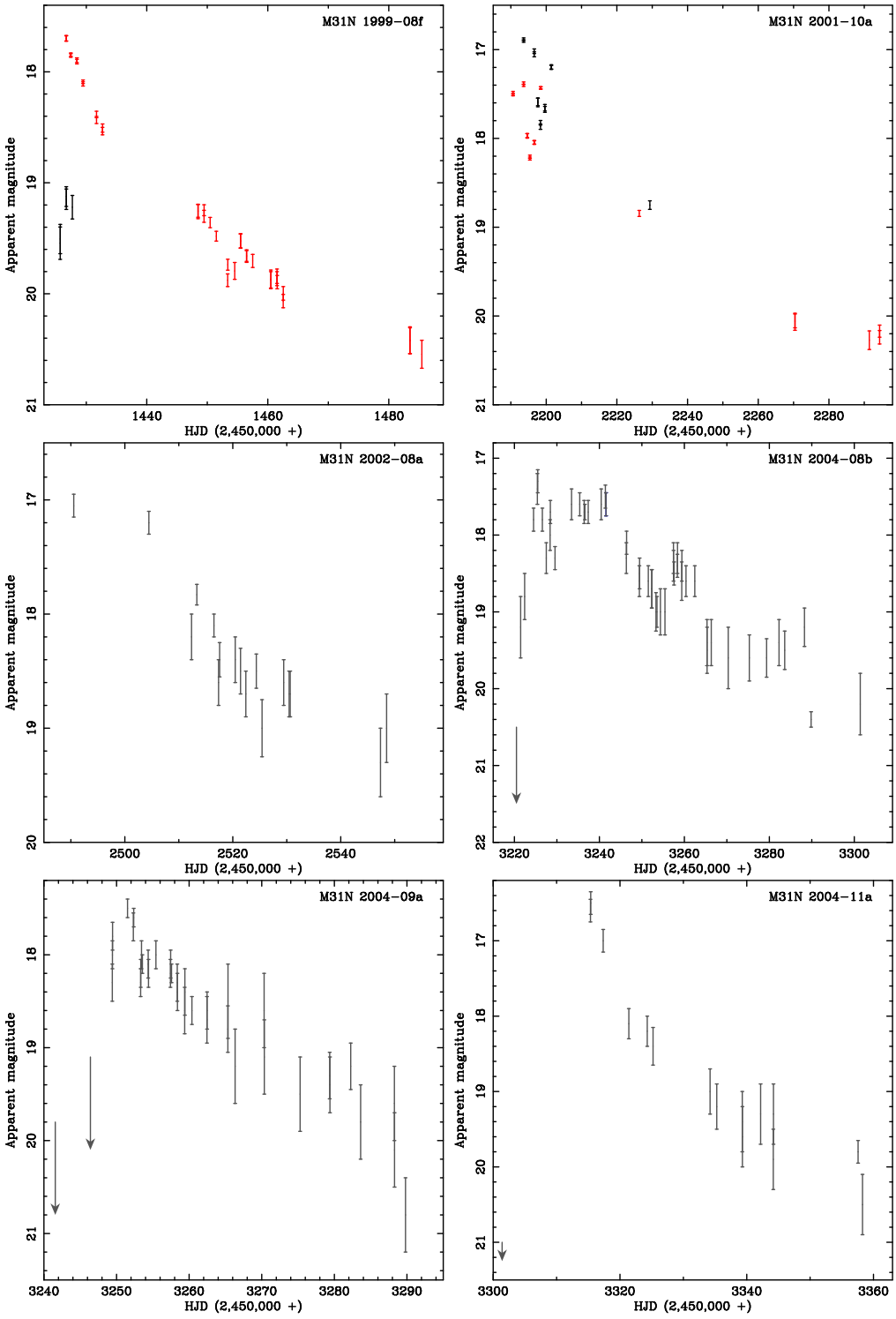

Fig. 13.— Nova light curves. The uncertainties in the photometric measurements are shown as vertical bars with the following colors representing the different bandpasses: B – blue; V – green; R – dark grey; r' – red; i' – black; z' – light grey. Upper flux limits are indicated by downward facing arrows.

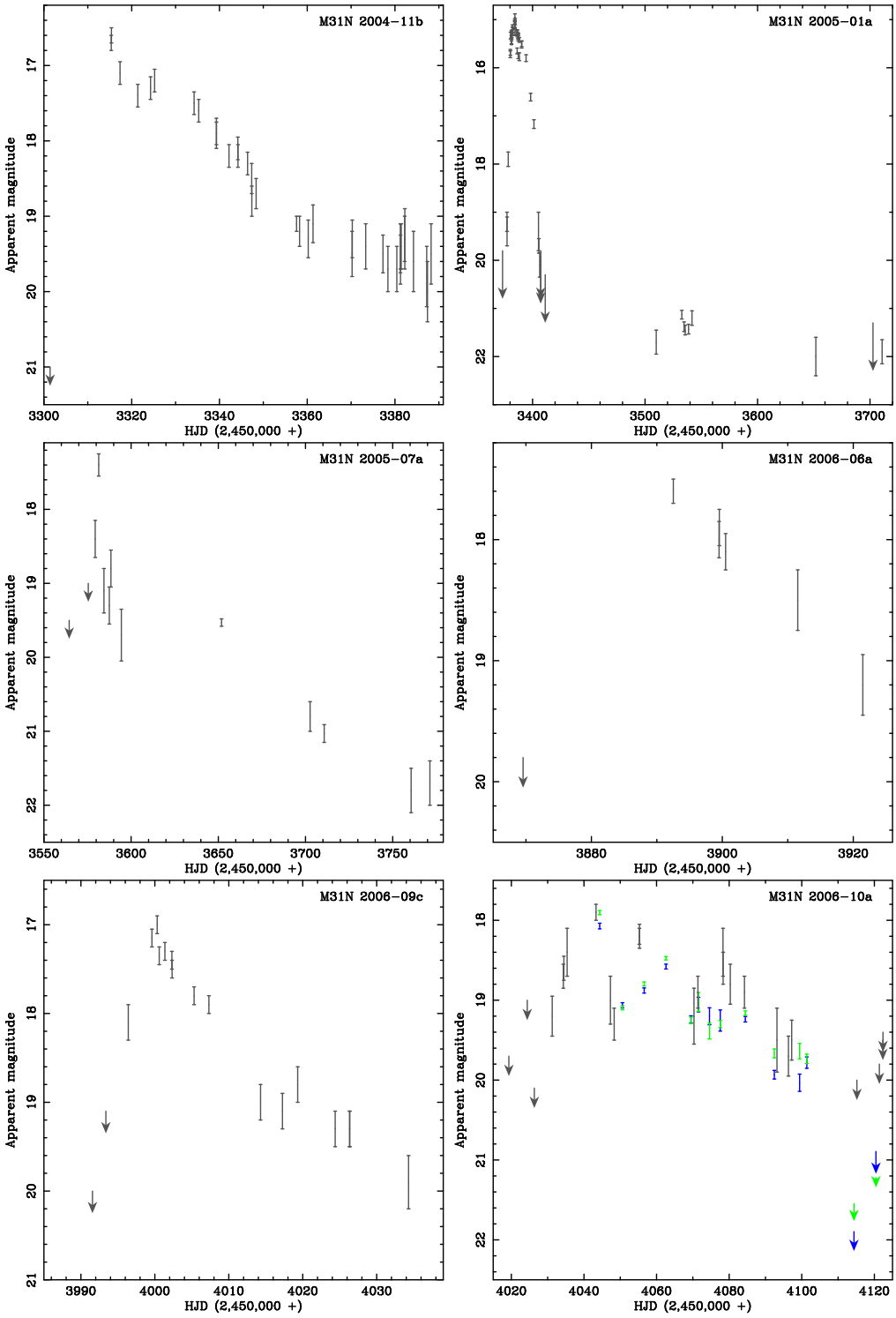

Fig. 14.— Nova light curves (continued). See Fig. 13 for details.

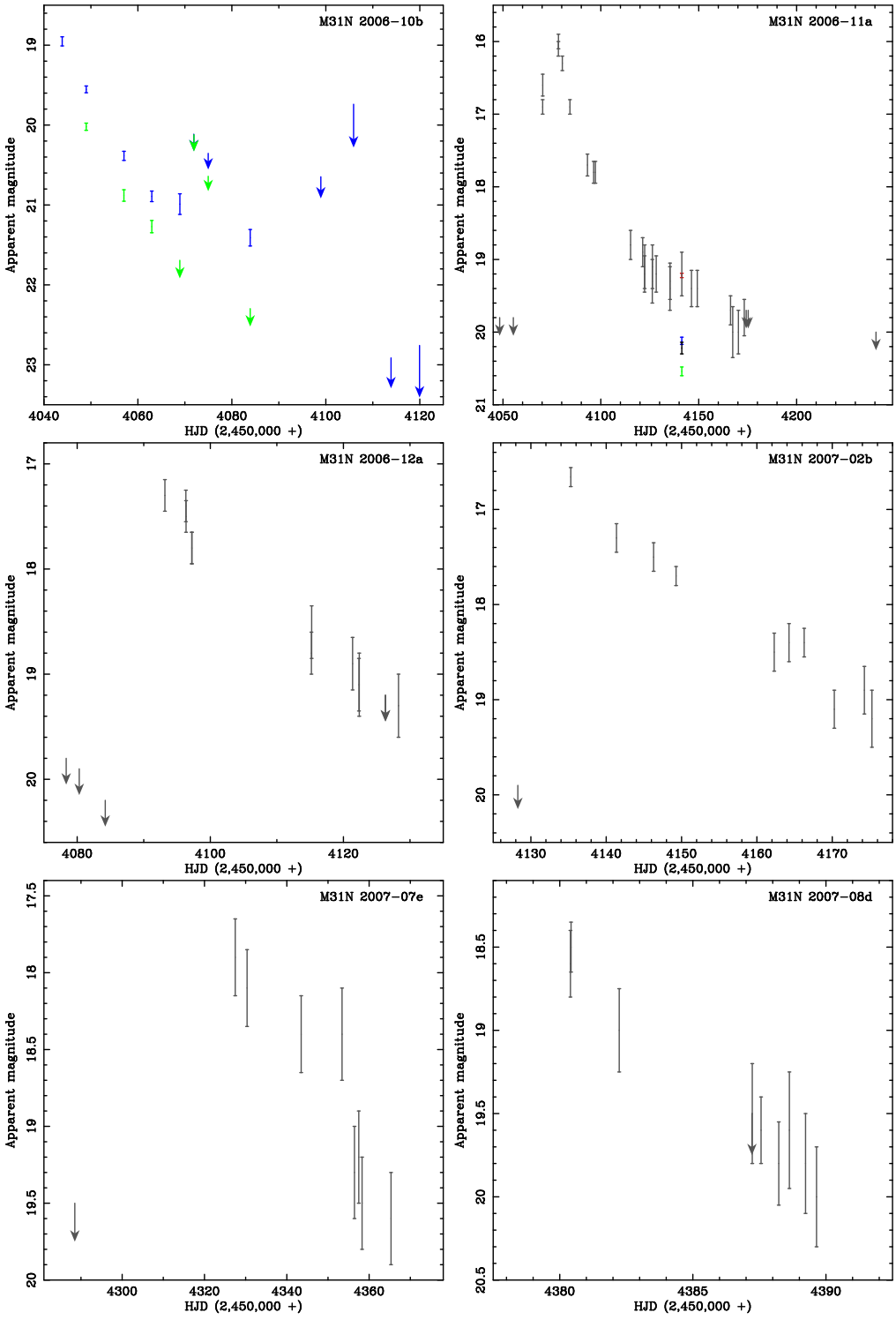

Fig. 15.— Nova light curves (continued). See Fig. 13 for details.

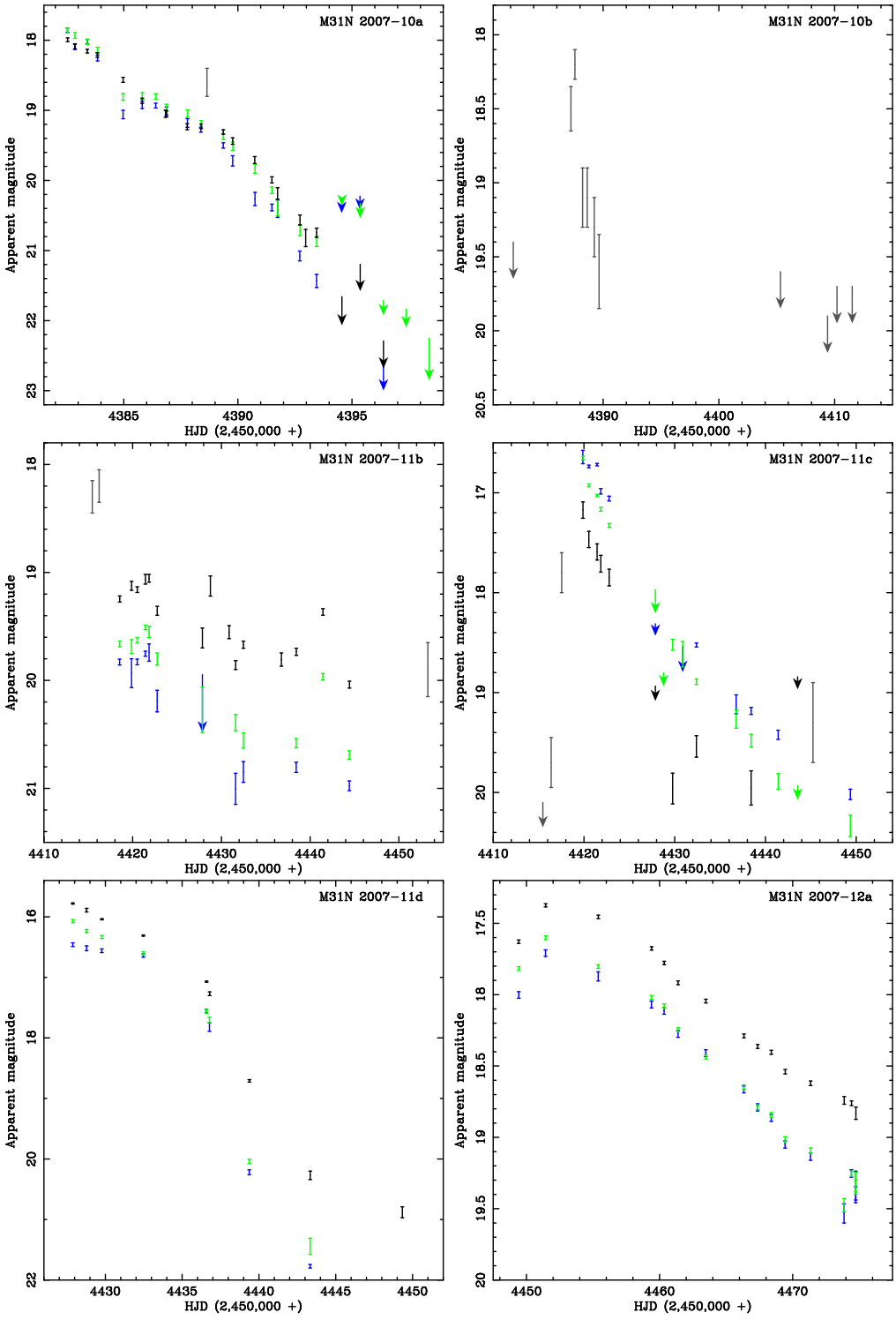

Fig. 16.— Nova light curves (continued). See Fig. 13 for details.

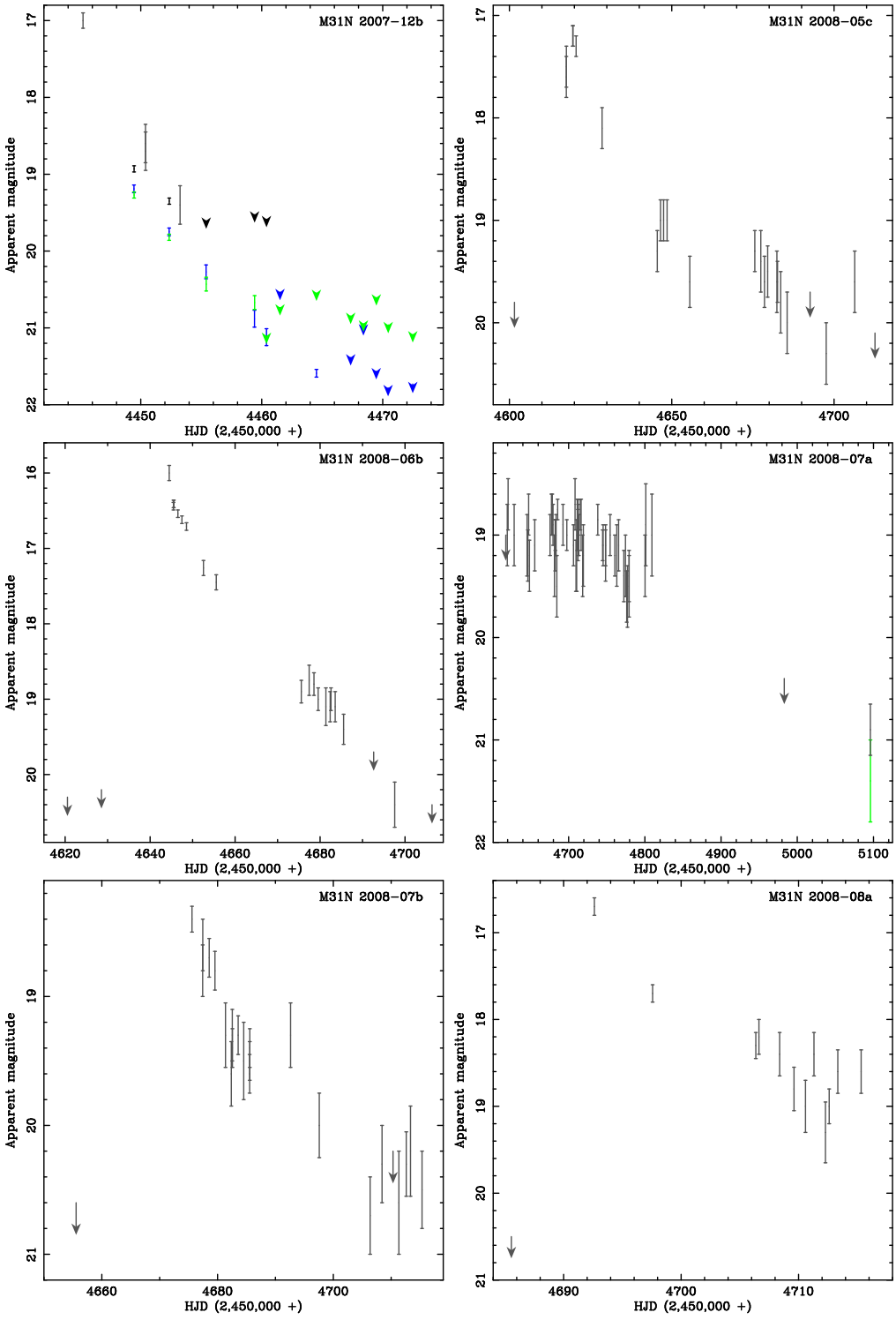

Fig. 17.— Nova light curves (continued). See Fig. 13 for details.

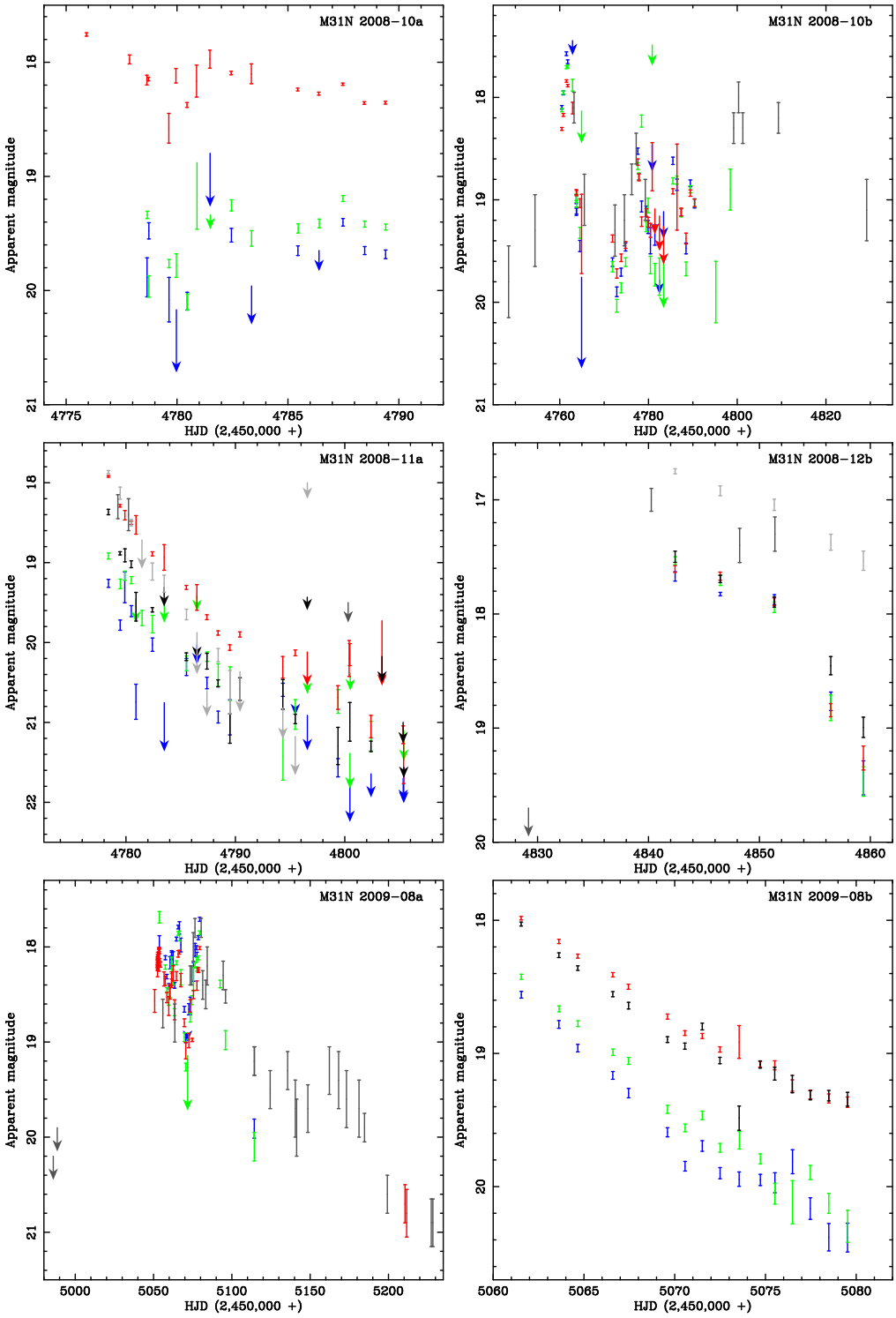

Fig. 18.— Nova light curves (continued). See Fig. 13 for details.

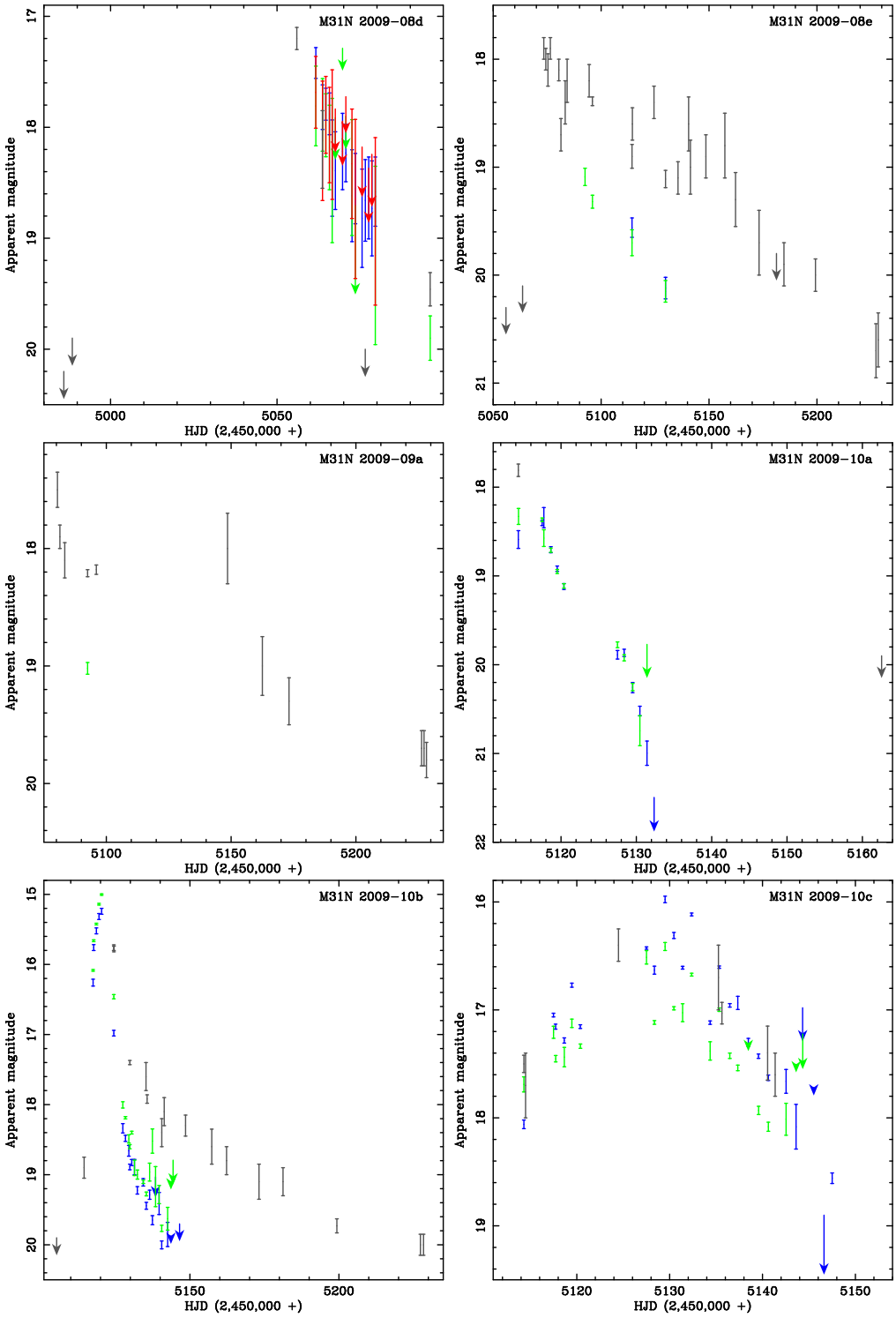

Fig. 19.— Nova light curves (continued). See Fig. 13 for details.

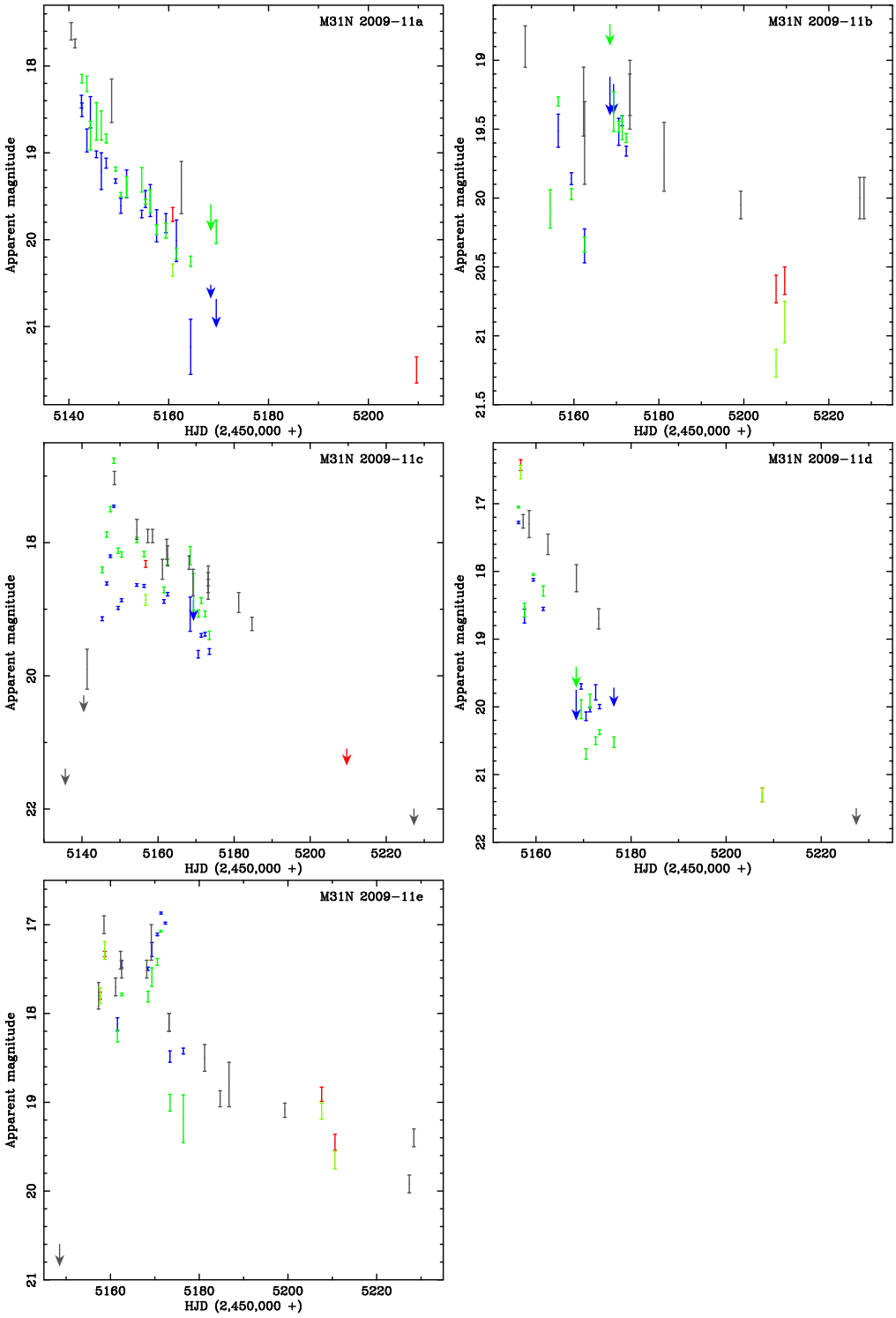

Fig. 20.— Nova light curves (continued). See Fig. 13 for details.

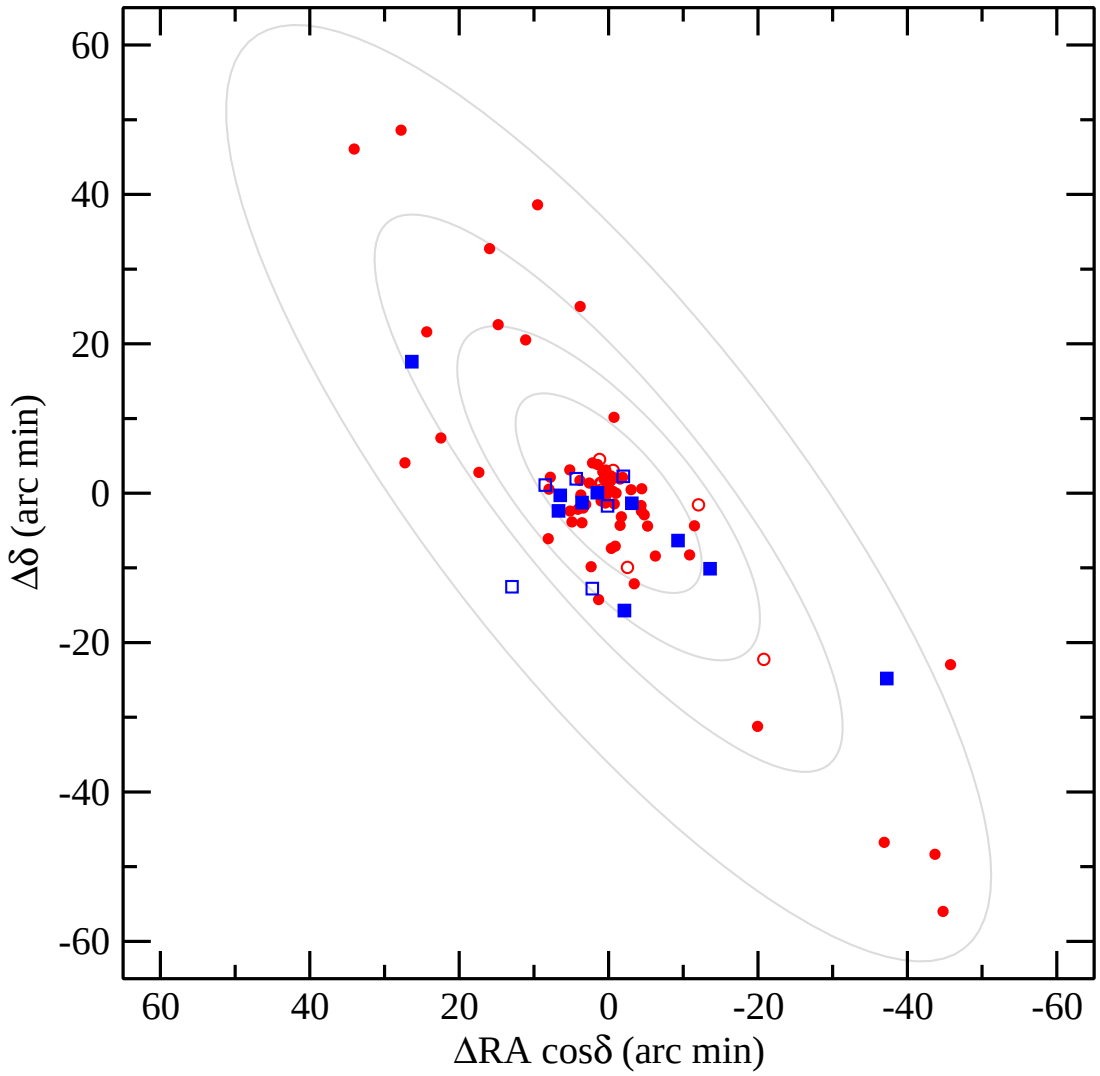

Fig. 21.— The spatial distribution of the 91 M31 novae with known spectroscopic class (see Table 4). The Fe II and Fe II: novae are indicated by filled and open red circles, respectively. The He/N and He/N: novae are represented by filled and open blue squares, respectively. The gray ellipses represent elliptical isophotes from the surface photometry of Kent (1987).

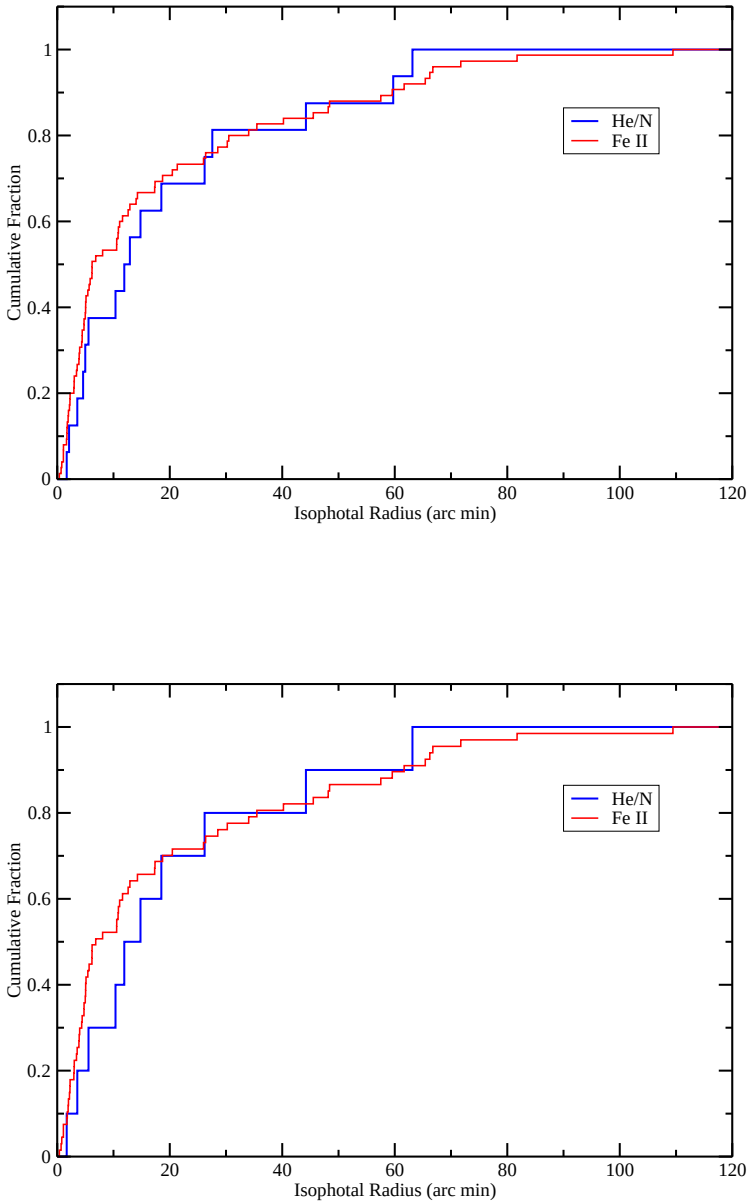

Fig. 22.— The cumulative distributions of Fe II novae compared with that for He/N and related novae. The top panel shows the Fe II and Fe II: systems (red) compared with the He/N + hybrid and He/N: systems (blue). The bottom panel compares only the well-established Fe II and He/N + hybrid novae. A KS test indicates a 81% (73% for bottom panel) probability that the distributions would differ by more than they do if both distributions come from the same parent population.

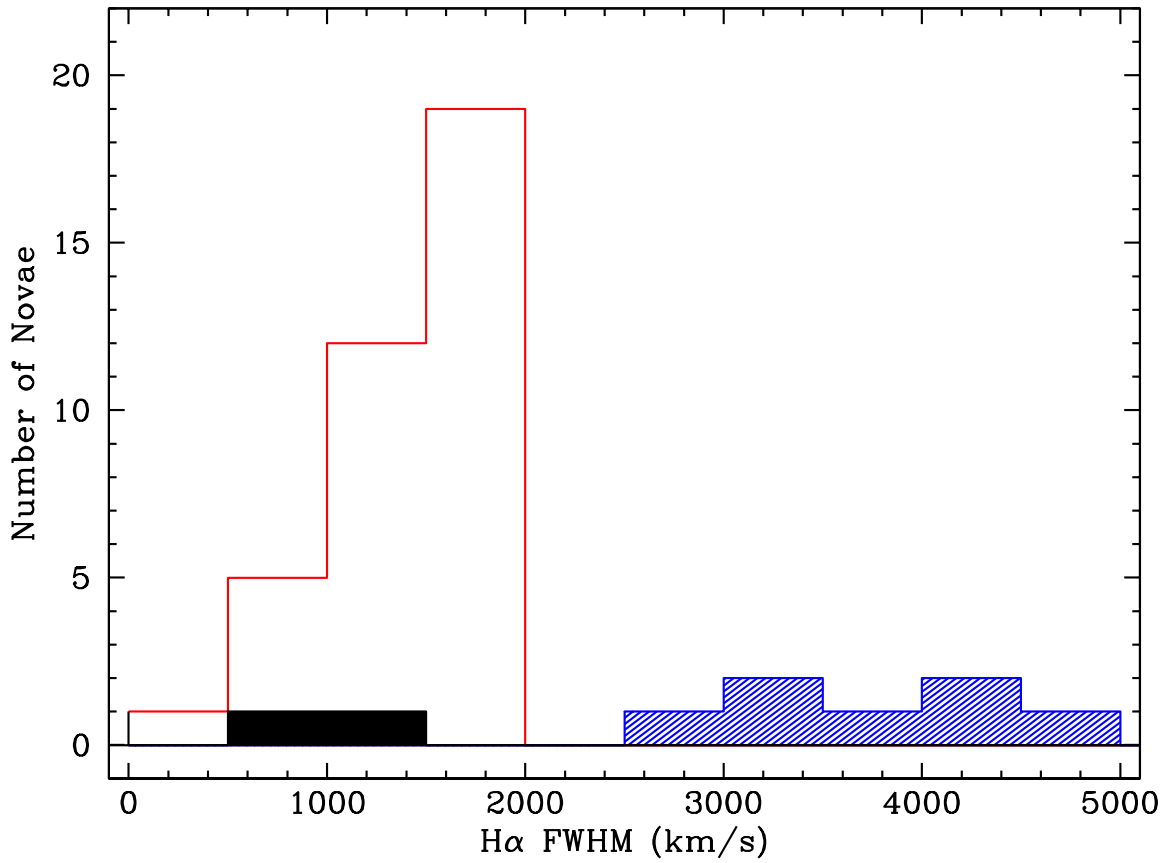

Fig. 23.— The distribution of Hα emission-line FWHM values from the novae in our sample. The novae classified as He/N (cross-hatched blue histogram) are clearly segregated from their Fe II counterparts (red open histogram), with the latter systems having FWHM $\lesssim$ 2500 km s^{-1}. Notable exceptions are two peculiar novae classified as He/Nn for which we have FWHM measurements that are represented by the filled region.

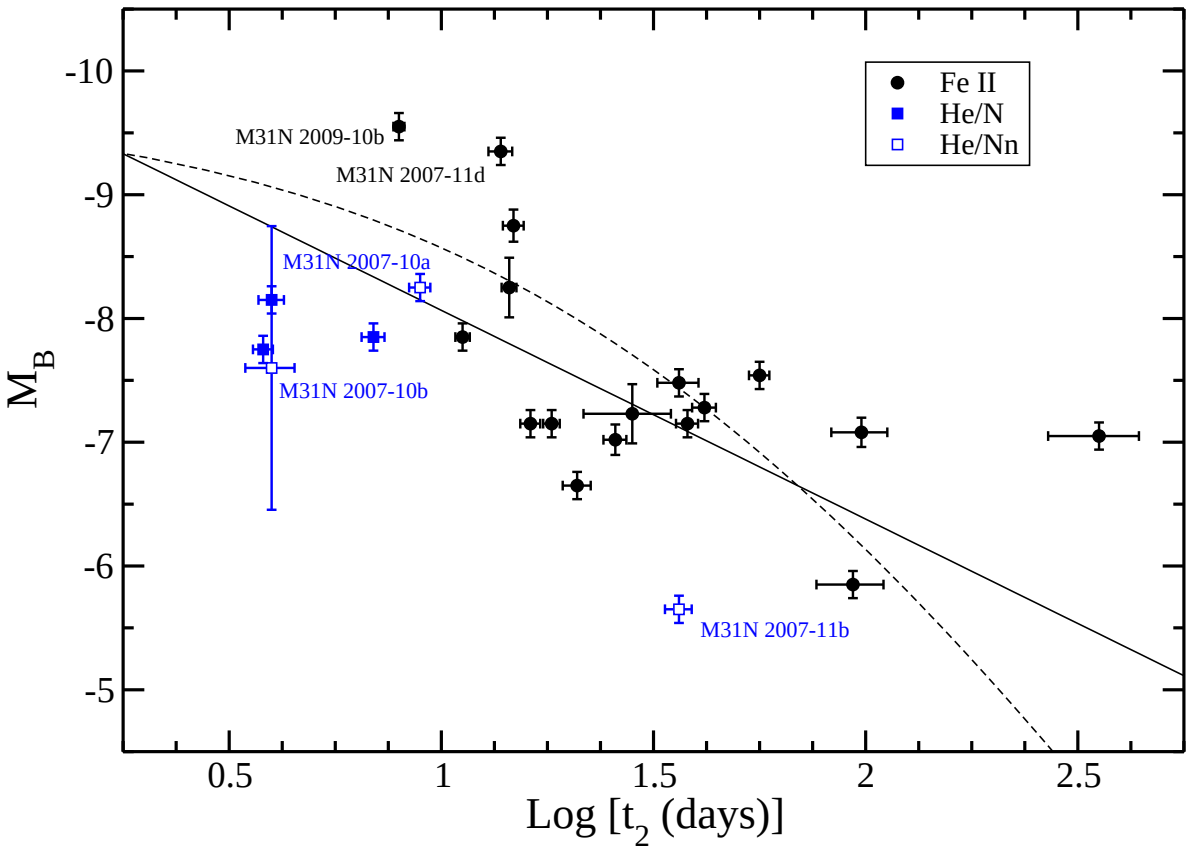

Fig. 24.— The *B*-band maximum-magnitude vs. rate-of-decline relation (MMRD) from our photometric survey. The Fe II, He/N, and He/Nn novae are represented by filled red circles, filled blue squares, and open blue squares, respectively. The solid line represents the best-fit relation determined from a weighted linear least-squares analysis (Equation 1), while the dashed line represents the theoretical relation from Livio (1992). Despite the considerable scatter, the data follow the expected trend with the brightest novae generally fading the fastest.

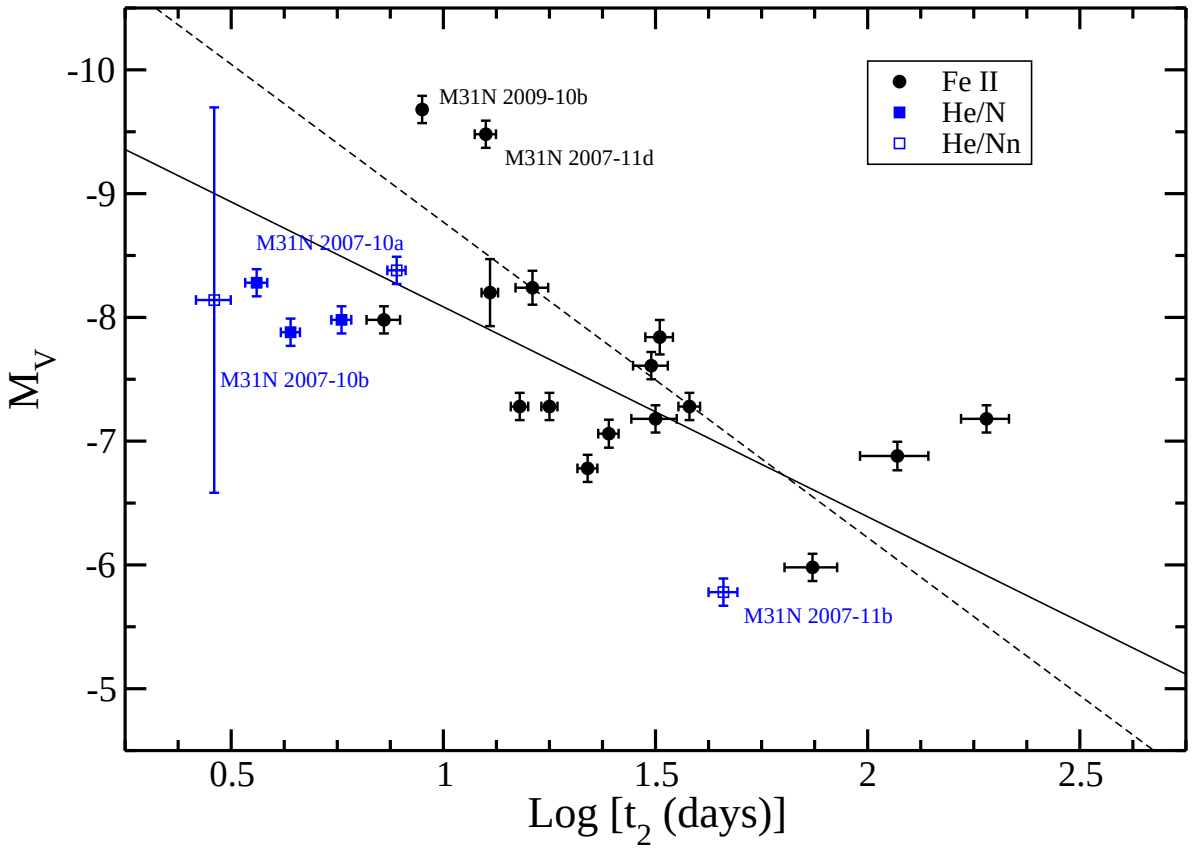

Fig. 25.— The V-band MMRD relation from our photometric survey. The symbols have the same meaning as in Fig. 24. The solid line is the best-fit relation given by Equation 2, while the dashed line represents the Galactic V-band relation from Downes & Duerbeck (2000).

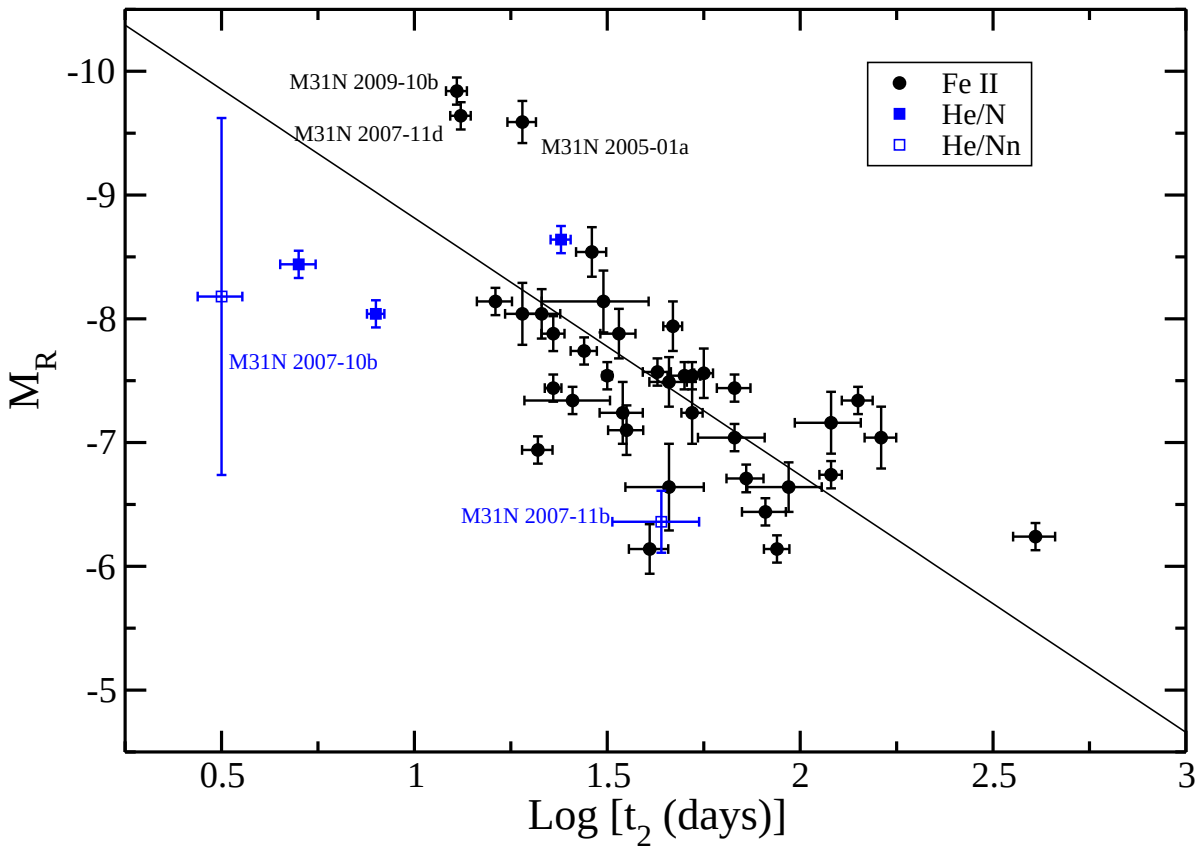

Fig. 26.— The R-band MMRD relation. The symbols have the same meaning as in Fig. 24. The best-fit relation is given by Equation 3. Note the tight group of luminous Fe II novae (M31N 2005-01a, 2007-11d, and 2009-10b) with $M_V \lesssim -9$ mag.

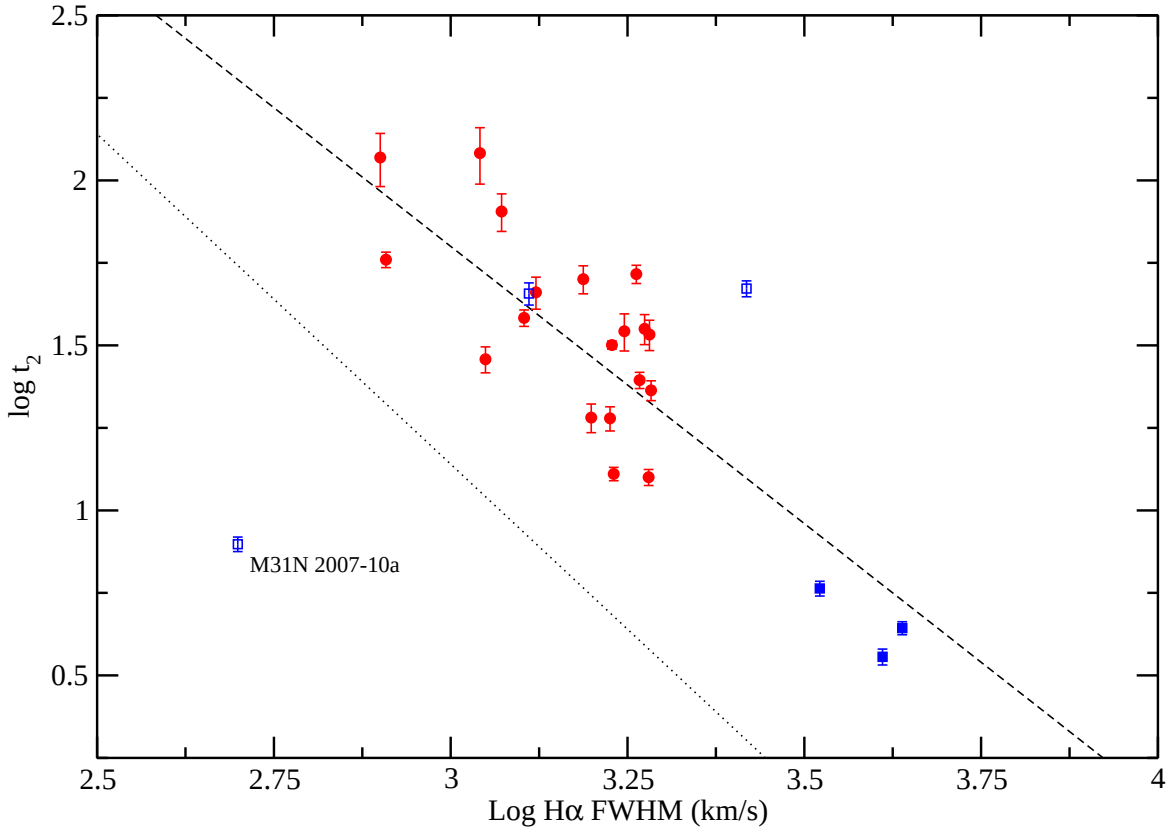

Fig. 27.— The dependence of the light-curve parameter t_2 on nova expansion velocity (as reflected by the FWHM of Hα). With the exception of M31N 2007-10a, there is a clear trend of decreasing t_2 with increasing Hα emission-line width. The red filled circles represent Fe II novae, while the filled (open) blue squares represent He/N (He/Nn and He/N:) novae, respectively. The dashed line reflects the best-fit relation given in Equation 5, while the dotted line gives the Galactic relation of McLaughlin (1960).

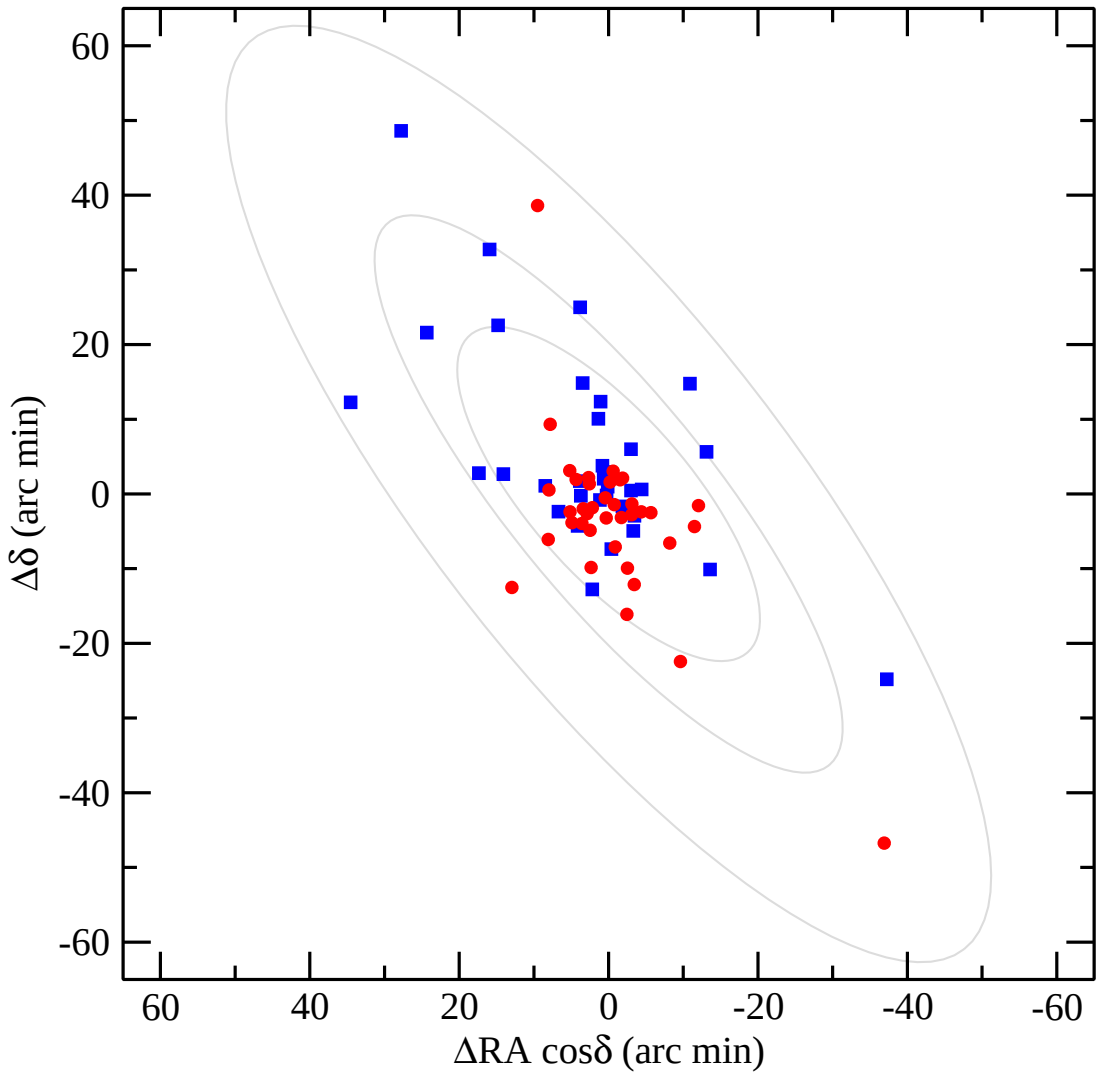

Fig. 28.— The spatial distribution of the 47 M31 novae with measured decline rates from our survey supplemented by 27 decline rates from the "high quality" light-curve sample from the Hubble, Arp, and Rosino surveys Capaccioli et al. (1989). The "very fast" and "fast" novae ($t_2 \leq 25$ days) are indicated by blue squares, with the slower novae ($t_2 > 25$ days) are indicated by red circles. The gray ellipses represent elliptical isophotes from the surface photometry of Kent (1987).

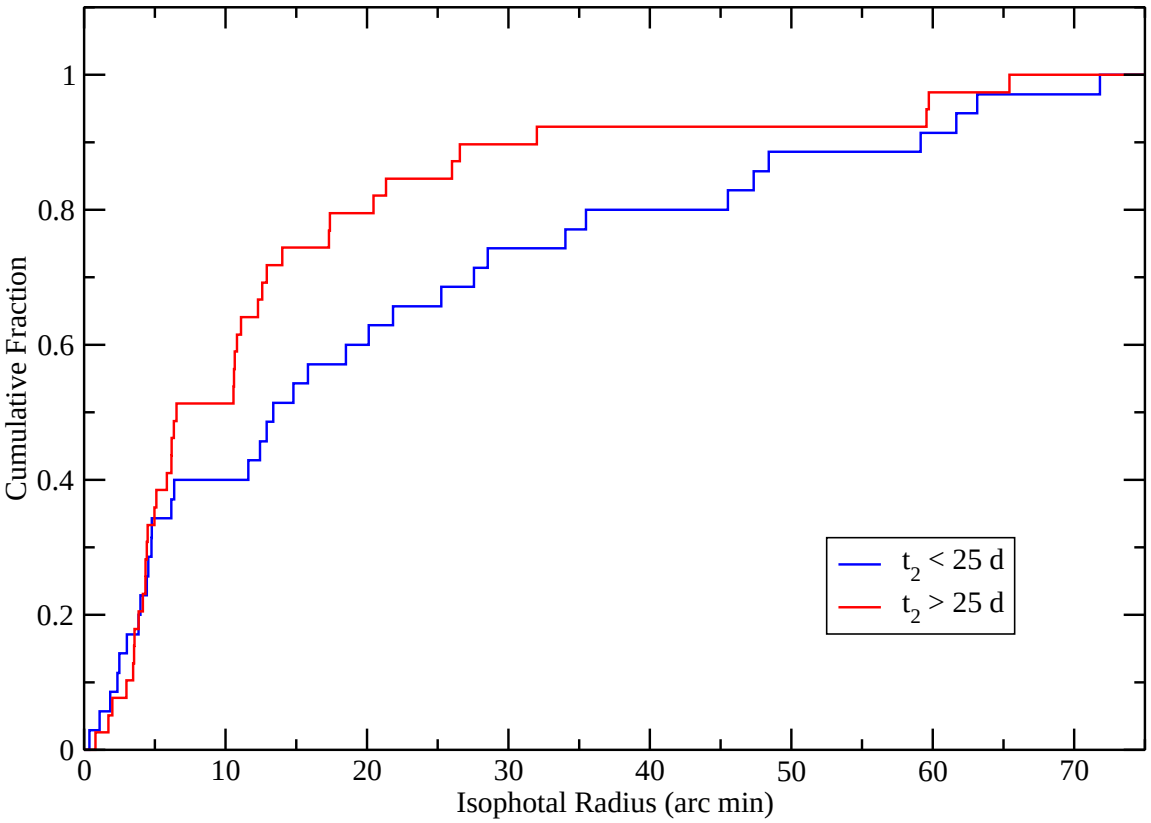

Fig. 29.— The cumulative distributions of the two nova samples from Figure 28. The blue distribution represents "very fast" and "fast" novae ($t_2 \leq 25$ days), with the red distribution (broken lines) representing slower novae ($t_2 > 25$ days). A KS test indicates a 23% probability that the distributions would differ by more than they do if both distributions come from the same parent population. Thus, it appears possible that the faster novae are more extended compared with the slower declining systems.

Table 1. Summary of Lick Spectroscopic Observations[a]

Nova	R.A. (J2000.0)	Decl. (J2000.0)	UT Date	Coverage (Å)
M31N 1990-10b	$00^h42^m36.2^s$	$41°11'54.0''$	11 Nov. 1990	3900–7100
M31N 1992-11b	00 42 36.2	41 11 54.0	18 Nov. 1992	3500–9500
M31N 1993-06a	00 42 49.2	41 17 27.5	28 Jun. 1993	4200–7100
M31N 1993-08a	00 42 45.1	41 14 27.0	12 Sep. 1993	3500–9500
M31N 1993-10g[b]	00 42 47.7	41 18 01.0	08 Nov. 1993	3500–9500
M31N 1993-11c[b]	00 42 50.1	41 17 28.0	17 Nov. 1993	4300–7100
M31N 1998-09d	00 42 46.6	41 14 49.2	20 Sep. 1998	4300–7000
M31N 1999-06a	00 42 49.7	41 15 05.6	10 Sep. 1999	4300–7000
M31N 1999-08f	00 42 41.1	41 19 12.2	17 Sep. 1999	4300–7000
M31N 1999-10a	00 42 49.7	41 16 32.0	08 Oct. 1999	4300–7000
M31N 2001-10a	00 43 03.3	41 12 11.5	20 Oct. 2001	3500–9500
M31N 2001-12a	00 42 41.4	41 16 24.5	11 Feb. 2002	3300–7900
M31N 2002-01b	00 42 33.9	41 18 23.9	11 Feb. 2002	3300–7900
M31N 2002-08a	00 42 30.92	41 06 13.1	13 Sep. 2002	3500–9500
M31N 2004-08b	00 43 26.84	41 16 40.8	10 Sep. 2004	3500–9500
M31N 2004-09a	00 42 40.27	41 14 42.5	10 Sep. 2004	3500–9500
M31N 2004-11a	00 42 42.81	41 18 27.9	19 Nov. 2004	3500–9500
M31N 2004-11b	00 43 07.45	41 18 04.7	19 Nov. 2004	3500–9500
M31N 2005-01a	00 42 28.39	41 16 36.2	16 Jan. 2005	3500–9500
M31N 2005-07a	00 42 50.79	41 20 39.8	01 Aug. 2005	3500–9500
M31N 2008-08d	00 45 48.25	43 02 22.2	08 Sep. 2008	3500–9500

[a]All observations obtained with the Shane 3-m reflector.

[b]Due to ambiguity in the data logs from November 1993, it is possible that the dates of observation (and thus the spectra) for these two novae are reversed.

Table 2. Summary of HET Spectroscopic Observations

Nova	R.A. (J2000.0)	Decl. (J2000.0)	UT Date	Exp. (sec)	Coverage (Å)	Weather
M31N 1995-11e	$00^{h}45^{m}09.9^{s}$	$41°52'03.0''$	03.30 Nov. 2008	1200	4275–7250	Spec
M31N 2006-09c	00 42 42.38	41 08 45.5	24.18 Sep. 2006	1800	4275–7250	Spec
M31N 2006-10a	00 41 43.23	41 11 45.9	30.31 Oct. 2006	1500	4275–7250	Spec
M31N 2006-10b	00 39 27.38	40 51 09.8	01.09 Nov. 2006	1800	4275–7250	Spec
			23.24 Nov. 2006	1200	4275–7250	Phot
M31N 2006-11a	00 42 56.81	41 06 18.4	28.23 Nov. 2006	1200	4275–7250	Spec
M31N 2006-12a	00 42 21.09	41 13 45.3	08.13 Jan. 2007	1200	4275–7250	Spec
M31N 2006-12b	00 42 11.14	41 07 43.8	10.11 Jan. 2007	3200	4275–7250	Cldy
M31N 2007-02a	00 40 59.02	40 44 52.7	09.07 Feb. 2007	900	4275–7250	Spec
M31N 2007-02b	00 41 40.32	41 14 33.5	10.06 Feb. 2007	900	4275–7250	Phot
M31N 2007-06b	00 42 33.14	41 00 25.9	25.34 Jul. 2007	3600	4275–7250	Spec
M31N 2007-08d	00 39 30.27	40 29 14.2	13.44 Sep. 2007	1200	4275–7250	Spec
M31N 2007-10a	00 42 55.95	41 03 22.0	19.13 Oct. 2007	1400	4275–7250	Phot
M31N 2007-11b	00 43 52.99	41 03 36.2	11.30 Nov. 2007	1200	4100–8900	Spec
M31N 2007-11c	00 43 04.14	41 15 54.3	16.28 Nov. 2007	1200	4100–8900	Spec
M31N 2007-11d	00 44 54.60	41 37 40.0	21.27 Nov. 2007	600	4100–8900	Phot
			04.22 Dec. 2007	1200	4100–8900	Phot
M31N 2007-11e	00 45 47.74	42 02 03.5	05.23 Dec. 2007	1200	4100–8900	Phot
M31N 2007-11g	00 44 15.80	41 13 50.3	18.28 Nov. 2008	1200	4275–7250	Spec
M31N 2007-12a	00 44 03.51	41 38 41.1	15.20 Dec. 2007	1200	4100–8900	Phot
M31N 2007-12b	00 43 19.94	41 13 46.6	15.18 Dec. 2007	1000	4100–8900	Phot
M31N 2007-12d	00 41 54.96	41 09 47.3	21.17 Dec. 2007	1800	4100–8900	Spec
M31N 2008-08d	00 45 48.25	43 02 22.2	20.13 Oct. 2008	1200	4100–8900	Phot
M31N 2008-09a	00 41 46.72	41 07 52.1	22.41 Sep. 2008	1200	4100–8900	Spec
M31N 2008-09c	00 42 51.42	41 01 54.0	20.18 Sep. 2008	1200	4100–8900	Spec
M31N 2008-10a	00 43 35.46	41 54 44.2	18.34 Oct. 2008	1200	4100–8900	Phot
M31N 2008-10b	00 43 02.42	41 14 09.9	20.11 Oct. 2008	1200	4100–8900	Phot
			25.33 Oct. 2008	1200	4100–8900	Spec
M31N 2008-11a	00 41 32.26	41 06 01.0	07.29 Nov. 2008	1200	4275–7250	Phot
			25.25 Nov. 2008	1800	4275–7250	Spec
M31N 2009-01a	00 44 44.03	41 23 28.3	02.07 Feb. 2009	1350	4100–8900	Phot
M31N 2009-02a	00 43 43.81	41 36 38.8	07.07 Feb. 2009	900	4100–8900	Spec

Table 3. Photometric Observations

JD (2,450,000+)	Mag	Filter	Notes[a]
	M31N 1999-08f		
1427.686	17.700 ± 0.024	r'	(29)
1427.690	17.697 ± 0.025	r'	(29)
1428.444	17.853 ± 0.016	r'	(29)
1428.452	17.845 ± 0.015	r'	(29)
1429.452	17.895 ± 0.021	r'	(29)
1429.456	17.908 ± 0.021	r'	(29)
1430.467	18.090 ± 0.016	r'	(29)
1430.471	18.109 ± 0.019	r'	(29)
1432.686	18.384 ± 0.029	r'	(29)
1432.690	18.434 ± 0.032	r'	(29)
1433.678	18.534 ± 0.034	r'	(29)
1433.686	18.507 ± 0.037	r'	(29)
1449.467	19.258 ± 0.065	r'	(29)
1449.471	19.253 ± 0.057	r'	(29)
1450.463	19.302 ± 0.054	r'	(29)
1450.467	19.247 ± 0.049	r'	(29)
1451.475	19.358 ± 0.046	r'	(29)
1452.491	19.481 ± 0.044	r'	(29)
1454.374	19.878 ± 0.057	r'	(29)
1454.389	19.738 ± 0.049	r'	(29)
1455.538	19.794 ± 0.076	r'	(29)
1456.495	19.523 ± 0.063	r'	(29)
1456.499	19.525 ± 0.065	r'	(29)
1457.495	19.664 ± 0.053	r'	(29)
1457.499	19.656 ± 0.052	r'	(29)
1458.506	19.704 ± 0.059	r'	(29)
1461.510	19.877 ± 0.076	r'	(29)
1461.514	19.867 ± 0.081	r'	(29)
1462.530	19.864 ± 0.063	r'	(29)
1462.534	19.842 ± 0.065	r'	(29)
1462.561	19.895 ± 0.060	r'	(29)
1463.549	20.066 ± 0.060	r'	(29)
1463.557	19.996 ± 0.061	r'	(29)
1484.499	20.424 ± 0.117	r'	(29)
1484.502	20.418 ± 0.120	r'	(29)
1486.456	20.545 ± 0.126	r'	(29)
1426.694	19.544 ± 0.146	i'	(29)
1426.702	19.507 ± 0.132	i'	(29)
1427.690	19.124 ± 0.089	i'	(29)
1427.698	19.148 ± 0.092	i'	(29)
1428.702	19.220 ± 0.106	i'	(29)

Table 3—Continued

JD (2,450,000+)	Mag	Filter	Notes[a]
	M31N 2001-10a		
2191.616	17.512 ± 0.008	r'	(29)
2191.620	17.481 ± 0.011	r'	(29)
2194.620	17.378 ± 0.014	r'	(29)
2194.624	17.402 ± 0.013	r'	(29)
2195.640	17.968 ± 0.021	r'	(29)
2195.643	17.971 ± 0.026	r'	(29)
2196.382	18.227 ± 0.017	r'	(29)
2196.386	18.207 ± 0.018	r'	(29)
2197.628	18.043 ± 0.020	r'	(29)
2197.632	18.047 ± 0.020	r'	(29)
2199.452	17.430 ± 0.013	r'	(29)
2199.456	17.433 ± 0.013	r'	(29)
2227.339	18.845 ± 0.034	r'	(29)
2271.405	20.056 ± 0.078	r'	(29)
2271.409	20.065 ± 0.096	r'	(29)
2292.429	20.273 ± 0.105	r'	(29)
2295.343	20.171 ± 0.068	r'	(29)
2295.350	20.240 ± 0.076	r'	(29)
2194.612	16.903 ± 0.014	i'	(29)
2194.620	16.883 ± 0.015	i'	(29)
2197.620	17.018 ± 0.026	i'	(29)
2197.624	17.053 ± 0.028	i'	(29)
2198.636	17.588 ± 0.043	i'	(29)
2198.640	17.595 ± 0.048	i'	(29)
2199.382	17.868 ± 0.030	i'	(29)
2199.386	17.824 ± 0.026	i'	(29)
2200.628	17.654 ± 0.037	i'	(29)
2200.632	17.673 ± 0.033	i'	(29)
2202.448	17.194 ± 0.024	i'	(29)
2202.456	17.201 ± 0.022	i'	(29)
2230.331	18.751 ± 0.048	i'	(29)
	M31N 2002-08a		
2490.523	17.05 ± 0.1	R	(2)
2504.452	17.2 ± 0.1	R	(2)
2512.360	18.2 ± 0.2	R	(2)
2513.344	17.83 ± 0.09	R	(2)
2516.506	18.1 ± 0.1	R	(32)
2517.368	18.6 ± 0.2	R	(2)
2517.560	18.4 ± 0.15	R	(32)

Table 3—Continued

JD (2,450,000+)	Mag	Filter	Notes[a]
2520.452	18.4 ± 0.2	R	(2)
2521.433	18.5 ± 0.2	R	(2)
2522.414	18.7 ± 0.2	R	(2)
2524.358	18.5 ± 0.15	R	(32)
2525.417	19.0 ± 0.25	R	(2)
2529.435	18.6 ± 0.2	R	(2)
2530.438	18.7 ± 0.2	R	(2)
2530.637	18.7 ± 0.2	R	(32)
2547.365	19.3 ± 0.3	R	(2)
2548.505	19.0 ± 0.3	R	(2)
	M31N 2004-08b		
3241.563	17.6 ± 0.15	V	(32)
3220.474	> 20.5	R	(32)
3221.460	19.2 ± 0.4	R	(2)
3222.401	18.8 ± 0.3	R	(2)
3224.497	17.8 ± 0.15	R	(32)
3225.405	17.4 ± 0.2	R	(2)
3225.482	17.3 ± 0.15	R	(32)
3226.570	17.8 ± 0.15	R	(32)
3227.505	18.3 ± 0.2	R	(2)
3228.393	18.0 ± 0.2	R	(2)
3228.456	17.7 ± 0.15	R	(2)
3229.557	18.3 ± 0.15	R	(32)
3233.443	17.6 ± 0.2	R	(2)
3235.370	17.6 ± 0.15	R	(2)
3236.410	17.7 ± 0.15	R	(2)
3236.586	17.7 ± 0.1	R	(32)
3237.375	17.7 ± 0.15	R	(2)
3240.429	17.6 ± 0.2	R	(2)
3241.402	17.5 ± 0.15	R	(2)
3241.560	17.6 ± 0.15	R	(32)
3246.342	18.3 ± 0.2	R	(2)
3246.399	18.1 ± 0.15	R	(2)
3249.415	18.6 ± 0.2	R	(2)
3249.464	18.5 ± 0.2	R	(2)
3251.518	18.6 ± 0.2	R	(32)
3252.312	18.7 ± 0.25	R	(2)
3252.368	18.7 ± 0.25	R	(2)
3253.319	19.0 ± 0.25	R	(2)
3253.558	19.0 ± 0.2	R	(32)
3254.362	19.0 ± 0.3	R	(2)
3255.430	19.0 ± 0.3	R	(2)

Table 3—Continued

JD (2,450,000+)	Mag	Filter	Notes[a]
3257.429	18.3 ± 0.2	R	(2)
3257.453	18.4 ± 0.2	R	(2)
3257.571	18.5 ± 0.15	R	(32)
3258.363	18.4 ± 0.15	R	(2)
3258.393	18.3 ± 0.2	R	(2)
3259.384	18.6 ± 0.25	R	(2)
3259.413	18.4 ± 0.2	R	(2)
3260.385	18.6 ± 0.2	R	(32)
3262.453	18.6 ± 0.2	R	(2)
3265.332	19.4 ± 0.3	R	(2)
3265.352	19.5 ± 0.3	R	(2)
3266.335	19.4 ± 0.3	R	(2)
3270.330	19.6 ± 0.4	R	(2)
3275.290	19.6 ± 0.3	R	(2)
3279.356	19.6 ± 0.25	R	(32)
3282.281	19.4 ± 0.3	R	(2)
3283.619	19.5 ± 0.25	R	(32)
3288.272	19.2 ± 0.25	R	(2)
3289.828	20.40 ± 0.1	R	(33)
3301.408	20.2 ± 0.4	R	(32)
	M31N 2004-09a		
3241.560	> 19.8	R	(32)
3246.399	> 19.1	R	(2)
3249.415	18.3 ± 0.2	R	(2)
3249.438	18.0 ± 0.15	R	(2)
3249.452	17.8 ± 0.15	R	(2)
3251.518	17.5 ± 0.1	R	(32)
3252.312	17.7 ± 0.15	R	(2)
3252.368	17.6 ± 0.1	R	(2)
3253.319	18.3 ± 0.15	R	(2)
3253.341	18.2 ± 0.15	R	(2)
3253.441	18.0 ± 0.15	R	(2)
3253.558	18.1 ± 0.1	R	(32)
3254.362	18.1 ± 0.15	R	(2)
3254.400	18.2 ± 0.15	R	(2)
3255.430	18.0 ± 0.15	R	(2)
3257.429	18.2 ± 0.15	R	(2)
3257.453	18.1 ± 0.15	R	(2)
3257.571	18.2 ± 0.1	R	(32)
3258.363	18.3 ± 0.2	R	(2)
3258.393	18.4 ± 0.2	R	(2)
3259.384	18.6 ± 0.25	R	(2)
3259.413	18.4 ± 0.25	R	(2)

Table 3—Continued

JD (2,450,000+)	Mag	Filter	Notes[a]
3260.385	18.6 ± 0.15	R	(32)
3262.453	18.7 ± 0.25	R	(2)
3262.472	18.6 ± 0.2	R	(2)
3265.332	18.8 ± 0.25	R	(2)
3265.352	18.5 ± 0.4	R	(2)
3266.335	19.2 ± 0.4	R	(2)
3270.330	18.6 ± 0.4	R	(2)
3270.351	19.1 ± 0.4	R	(2)
3275.290	19.5 ± 0.4	R	(2)
3279.356	19.3 ± 0.25	R	(32)
3279.398	19.4 ± 0.3	R	(2)
3282.257	19.2 ± 0.25	R	(2)
3283.619	19.8 ± 0.4	R	(32)
3288.272	19.6 ± 0.4	R	(2)
3288.292	20.1 ± 0.4	R	(2)
3289.802	20.8 ± 0.4	R	(33)
	M31N 2004-11a		
3301.408	> 21.0	R	(2)
3315.347	16.6 ± 0.15	R	(2)
3315.390	16.5 ± 0.15	R	(2)
3317.352	17.0 ± 0.15	R	(2)
3321.404	18.1 ± 0.2	R	(2)
3324.305	18.2 ± 0.2	R	(2)
3325.218	18.4 ± 0.25	R	(2)
3334.218	19.0 ± 0.3	R	(2)
3335.273	19.2 ± 0.3	R	(2)
3339.296	19.4 ± 0.4	R	(2)
3339.318	19.6 ± 0.4	R	(2)
3342.192	19.3 ± 0.4	R	(32)
3344.192	19.9 ± 0.4	R	(2)
3344.214	19.3 ± 0.4	R	(2)
3357.568	19.8 ± 0.15	R	(37)
3358.260	20.5 ± 0.4	R	(32)
	M31N 2004-11b		
3381.253	19.5 ± 0.4	V	(32)
3301.408	> 21.0	R	(2)
3315.347	16.7 ± 0.1	R	(2)
3315.390	16.6 ± 0.1	R	(2)
3317.352	17.1 ± 0.15	R	(2)
3321.404	17.4 ± 0.15	R	(2)

Table 3—Continued

JD (2,450,000+)	Mag	Filter	Notes[a]
3324.305	17.3 ± 0.15	R	(2)
3325.218	17.2 ± 0.15	R	(2)
3334.218	17.5 ± 0.15	R	(2)
3335.273	17.6 ± 0.15	R	(2)
3339.296	17.9 ± 0.2	R	(2)
3339.318	17.9 ± 0.15	R	(2)
3342.172	18.2 ± 0.15	R	(32)
3344.192	18.1 ± 0.15	R	(2)
3344.214	18.2 ± 0.15	R	(2)
3346.410	18.3 ± 0.15	R	(2)
3347.344	18.5 ± 0.2	R	(2)
3347.370	18.8 ± 0.2	R	(2)
3348.359	18.7 ± 0.2	R	(2)
3357.568	19.1 ± 0.1	R	(37)
3358.260	19.2 ± 0.2	R	(32)
3360.236	19.3 ± 0.25	R	(2)
3361.324	19.1 ± 0.25	R	(2)
3370.230	19.5 ± 0.3	R	(2)
3370.267	19.3 ± 0.25	R	(2)
3373.321	19.4 ± 0.3	R	(32)
3377.266	19.5 ± 0.25	R	(32)
3378.391	19.7 ± 0.3	R	(2)
3380.426	19.7 ± 0.3	R	(2)
3381.249	19.5 ± 0.25	R	(32)
3381.276	19.4 ± 0.3	R	(2)
3381.417	19.4 ± 0.3	R	(2)
3382.219	19.3 ± 0.3	R	(2)
3382.246	19.3 ± 0.4	R	(32)
3384.212	19.6 ± 0.4	R	(2)
3387.231	19.8 ± 0.4	R	(32)
3387.400	20.0 ± 0.4	R	(2)
3388.224	19.5 ± 0.4	R	(32)
	M31N 2005-01a		
3381.253	15.45 ± 0.05	V	(32)
3382.251	15.26 ± 0.05	V	(32)
3384.333	15.26 ± 0.07	V	(32)
3386.305	15.65 ± 0.06	V	(32)
3387.237	15.75 ± 0.06	V	(32)
3388.233	15.77 ± 0.08	V	(32)
3373.321	> 19.8	R	(32)
3377.266	19.2 ± 0.2	R	(32)
3377.293	19.4 ± 0.3	R	(2)

Table 3—Continued

JD (2,450,000+)	Mag	Filter	Notes[a]
3378.391	17.9 ± 0.15	R	(2)
3380.224	15.72 ± 0.07	R	(2)
3380.253	15.68 ± 0.06	R	(2)
3380.437	15.33 ± 0.07	R	(2)
3381.249	15.48 ± 0.04	R	(32)
3381.266	15.32 ± 0.06	R	(2)
3381.286	15.27 ± 0.05	R	(2)
3381.306	15.30 ± 0.04	R	(2)
3381.408	15.34 ± 0.07	R	(2)
3381.426	15.31 ± 0.06	R	(2)
3382.219	15.16 ± 0.05	R	(2)
3382.246	15.21 ± 0.05	R	(32)
3382.257	15.21 ± 0.06	R	(2)
3384.212	15.05 ± 0.05	R	(2)
3384.252	15.10 ± 0.06	R	(2)
3384.326	15.12 ± 0.05	R	(32)
3384.405	15.04 ± 0.07	R	(2)
3386.202	15.27 ± 0.06	R	(2)
3386.228	15.26 ± 0.05	R	(2)
3386.300	15.27 ± 0.04	R	(32)
3386.424	15.31 ± 0.05	R	(2)
3387.212	15.36 ± 0.04	R	(2)
3387.231	15.39 ± 0.05	R	(32)
3387.249	15.34 ± 0.06	R	(2)
3387.400	15.34 ± 0.05	R	(2)
3388.224	15.42 ± 0.05	R	(32)
3390.287	15.52 ± 0.07	R	(2)
3390.327	15.50 ± 0.06	R	(2)
3394.234	15.80 ± 0.07	R	(2)
3398.274	16.61 ± 0.08	R	(2)
3401.212	17.17 ± 0.09	R	(2)
3405.273	19.4 ± 0.4	R	(32)
3405.633	19.7 ± 0.15	R	(20)
3406.326	20.1 ± 0.25	R	(32)
3407.231	> 19.9	R	(2)
3407.283	> 19.8	R	(2)
3509.952	21.7 ± 0.25	R	(33)
3411.257	> 20.3	R	(32)
3532.699	21.13 ± 0.09	R	(38)
3534.701	21.38 ± 0.1	R	(38)
3535.681	21.45 ± 0.1	R	(38)
3538.697	21.43 ± 0.1	R	(38)
3541.718	21.2 ± 0.15	R	(38)
3651.821	22.0 ± 0.4	R	(35)
3702.638	> 21.3	R	(33)

Table 3—Continued

JD (2,450,000+)	Mag	Filter	Notes[a]
3710.730	21.9 ± 0.25	R	(36)
3996.839	> 23.0	R	(37)
3384.315	14.95 ± 0.07	I	(2)
	M31N 2005-07a		
3564.493	> 19.5	R	(32)
3575.429	> 19.0	R	(2)
3579.409	18.4 ± 0.25	R	(2)
3581.419	17.4 ± 0.15	R	(2)
3584.404	19.1 ± 0.3	R	(2)
3587.509	19.3 ± 0.25	R	(32)
3588.415	18.8 ± 0.25	R	(2)
3594.390	19.7 ± 0.35	R	(32)
3651.862	19.53 ± 0.05	R	(32)
3702.638	20.8 ± 0.2	R	(33)
3710.730	21.03 ± 0.12	R	(36)
3760.586	21.8 ± 0.3	R	(36)
3771.346	21.7 ± 0.3	R	(21)
	M31N 2006-06a		
3771.264	> 19.2	R	(2)
3771.346	> 22	R	(21)
3869.565	> 19.8	R	(1)
3892.518	17.6 ± 0.1	R	(3)
3899.502	18.0 ± 0.15	R	(1)
3899.540	17.9 ± 0.15	R	(1)
3900.502	18.1 ± 0.15	R	(1)
3911.522	18.5 ± 0.25	R	(2)
3921.464	19.2 ± 0.25	R	(2)
	M31N 2006-09c		
4256.677	> 21.2	B	(30)
4260.700	> 21.7	B	(30)
4260.705	> 21.0	V	(30)
3892.967	> 21.1	R	(14)
3991.566	> 20.0	R	(4)
3993.376	> 19.1	R	(2)
3996.404	18.1 ± 0.2	R	(3)
3999.609	17.15 ± 0.1	R	(3)

Table 3—Continued

JD (2,450,000+)	Mag	Filter	Notes[a]
4000.317	17.0 ± 0.1	R	(2)
4000.590	17.35 ± 0.1	R	(4)
4001.360	17.3 ± 0.1	R	(2)
4002.302	17.4 ± 0.1	R	(2)
4002.329	17.5 ± 0.1	R	(2)
4005.312	17.8 ± 0.1	R	(2)
4007.312	17.9 ± 0.1	R	(2)
4014.295	19.0 ± 0.2	R	(2)
4017.258	19.1 ± 0.2	R	(2)
4019.319	18.8 ± 0.2	R	(2)
4024.383	19.3 ± 0.2	R	(2)
4026.330	19.3 ± 0.2	R	(2)
4026.364	19.3 ± 0.2	R	(2)
4034.312	19.9 ± 0.3	R	(2)
4260.690	> 21.4	r'	(30)
4260.695	21.800 ± 0.500	i'	(30)
	M31N 2006-10a		
4044.337	18.072 ± 0.035	B	(30)
4050.589	19.064 ± 0.033	B	(30)
4056.585	18.879 ± 0.032	B	(30)
4062.606	18.579 ± 0.030	B	(30)
4069.484	19.240 ± 0.044	B	(30)
4071.549	19.055 ± 0.091	B	(30)
4074.575	19.201 ± 0.106	B	(30)
4077.542	19.255 ± 0.132	B	(30)
4084.460	19.239 ± 0.034	B	(30)
4092.454	19.933 ± 0.054	B	(30)
4099.407	20.033 ± 0.108	B	(30)
4101.393	19.781 ± 0.071	B	(30)
4114.372	> 21.896	B	(30)
4120.432	> 20.893	B	(30)
4254.685	> 17.6	B	(30)
4044.334	17.904 ± 0.026	V	(30)
4050.586	19.096 ± 0.024	V	(30)
4056.582	18.797 ± 0.025	V	(30)
4062.604	18.475 ± 0.021	V	(30)
4069.481	19.253 ± 0.039	V	(30)
4071.546	19.022 ± 0.118	V	(30)
4074.572	19.387 ± 0.099	V	(30)
4077.539	19.299 ± 0.045	V	(30)

Table 3—Continued

JD (2,450,000+)	Mag	Filter	Notes[a]
4084.457	19.161 ± 0.027	V	(30)
4092.451	19.666 ± 0.055	V	(30)
4099.404	19.638 ± 0.096	V	(30)
4101.391	19.734 ± 0.058	V	(30)
4114.370	> 21.545	V	(30)
4120.429	> 21.221	V	(30)
4254.692	> 18.4	V	(30)
3771.346	> 22	R	(21)
4019.319	> 19.7	R	(2)
4024.383	> 19.0	R	(2)
4026.330	> 20.1	R	(2)
4031.251	19.2 ± 0.25	R	(2)
4034.312	18.7 ± 0.15	R	(2)
4034.470	18.6 ± 0.15	R	(3)
4035.360	18.4 ± 0.3	R	(2)
4043.331	17.9 ± 0.1	R	(2)
4047.288	19.0 ± 0.3	R	(2)
4048.324	19.3 ± 0.2	R	(2)
4055.296	18.2 ± 0.15	R	(2)
4055.262	18.2 ± 0.1	R	(23)
4070.308	19.2 ± 0.35	R	(6)
4071.385	18.9 ± 0.2	R	(3)
4078.308	18.4 ± 0.3	R	(2)
4078.343	18.6 ± 0.2	R	(2)
4080.306	18.8 ± 0.25	R	(2)
4084.212	18.9 ± 0.2	R	(2)
4093.174	$19.5 : \pm 0.4$	R	(2)
4096.325	19.7 ± 0.25	R	(2)
4097.222	19.5 ± 0.25	R	(2)
4115.194	> 20.0	R	(2)
4121.381	> 19.8	R	(2)
4122.331	> 19.5	R	(2)
4122.377	> 19.4	R	(2)
4254.671	> 19.0	r'	(30)
	M31N 2006-10b		
4044.388	18.952 ± 0.057	B	(30)
4049.501	19.553 ± 0.042	B	(30)
4057.534	20.385 ± 0.057	B	(30)
4063.463	20.892 ± 0.066	B	(30)
4069.445	20.989 ± 0.129	B	(30)
4072.440	> 20.144	B	(30)

Table 3—Continued

JD (2,450,000+)	Mag	Filter	Notes[a]
4075.473	> 20.354	B	(30)
4084.411	21.410 ± 0.103	B	(30)
4099.438	> 20.647	B	(30)
4106.415	> 19.739	B	(30)
4114.383	> 22.913	B	(30)
4120.458	> 21.830	B	(30)
4248.704	> 22.422	B	(30)
4049.498	20.021 ± 0.045	V	(30)
4054.317	> 17.332	V	(30)
4057.531	20.881 ± 0.072	V	(30)
4063.460	21.271 ± 0.077	V	(30)
4069.442	> 21.692	V	(30)
4072.437	> 20.121	V	(30)
4075.470	> 20.641	V	(30)
4084.408	> 22.297	V	(30)
4099.436	> 20.506	V	(30)
4102.385	> 20.134	V	(30)
4106.412	> 17.613	V	(30)
4108.486	> 18.404	V	(30)
4114.380	> 21.955	V	(30)
4120.455	> 22.758	V	(30)
4248.709	> 22.304	V	(30)
4248.693	> 22.9	r'	(30)
4248.699	> 21.5	i'	(30)
	M31N 2006-11a		
4141.368	20.120 ± 0.050	B	(30)
4141.372	20.540 ± 0.060	V	(30)
3771.346	> 22	R	(21)
4048.324	> 19.8	R	(2)
4055.296	> 19.8	R	(2)
4070.263	16.9 ± 0.1	R	(6)
4070.308	16.6 ± 0.15	R	(6)
4078.308	16.1 ± 0.1	R	(2)
4078.343	16.0 ± 0.1	R	(2)
4080.306	16.3 ± 0.1	R	(2)
4084.212	16.9 ± 0.1	R	(2)
4093.174	17.7 ± 0.15	R	(2)
4096.325	17.8 ± 0.15	R	(2)

Table 3—Continued

JD (2,450,000+)	Mag	Filter	Notes[a]
4097.222	17.8 ± 0.15	R	(2)
4115.194	18.8 ± 0.2	R	(2)
4121.381	18.9 ± 0.2	R	(2)
4122.331	19.2 ± 0.25	R	(2)
4122.377	19.1 ± 0.3	R	(2)
4126.289	19.3 ± 0.3	R	(2)
4126.339	19.1 ± 0.3	R	(2)
4128.275	19.2 ± 0.25	R	(2)
4135.298	19.4 ± 0.3	R	(2)
4135.334	19.3 ± 0.25	R	(2)
4141.362	19.2 ± 0.3	R	(2)
4146.295	19.4 ± 0.25	R	(2)
4149.273	19.4 ± 0.25	R	(2)
4166.247	19.7 ± 0.2	R	(1)
4167.366	20.0 ± 0.35	R	(1)
4170.264	20.0 ± 0.3	R	(1)
4173.269	19.8 ± 0.25	R	(25)
4174.268	> 19.7	R	(2)
4175.267	> 19.7	R	(4)
4240.561	> 20.0	R	(1)
4141.356	19.220 ± 0.030	r'	(30)
4141.362	20.220 ± 0.080	i'	(30)
	M31N 2006-12a		
3771.346	> 22	R	(21)
4078.343	> 19.8	R	(2)
4080.306	> 19.9	R	(2)
4084.212	> 20.2	R	(2)
4093.174	17.3 ± 0.15	R	(2)
4096.325	17.4 ± 0.15	R	(2)
4096.357	17.5 ± 0.15	R	(2)
4097.222	17.8 ± 0.15	R	(2)
4097.241	17.8 ± 0.15	R	(2)
4115.194	18.8 ± 0.2	R	(2)
4115.226	18.6 ± 0.25	R	(2)
4121.381	18.9 ± 0.25	R	(2)
4122.331	19.1 ± 0.25	R	(2)
4122.377	19.1 ± 0.3	R	(2)
4126.289	> 19.2	R	(2)
4126.339	> 19.2	R	(2)
4128.275	19.3 ± 0.3	R	(2)

Table 3—Continued

JD (2,450,000+)	Mag	Filter	Notes[a]
M31N 2007-02b			
3771.346	> 22	R	(21)
4128.275	> 19.9	R	(2)
4135.298	16.66 ± 0.1	R	(2)
4141.362	17.3 ± 0.15	R	(2)
4146.295	17.5 ± 0.15	R	(2)
4149.273	17.7 ± 0.1	R	(2)
4162.295	18.5 ± 0.2	R	(1)
4164.263	18.4 ± 0.2	R	(1)
4166.274	18.4 ± 0.15	R	(1)
4170.274	19.1 ± 0.2	R	(1)
4174.268	18.9 ± 0.25	R	(2)
4175.267	19.2 ± 0.3	R	(4)
4238.560	> 19.7	R	(1)
M31N 2007-07c			
3771.346	> 22	R	(21)
4288.506	> 20.0	R	(1)
4327.469	19.2 ± 0.25	R	(1)
4330.344	19.2 ± 0.25	R	(1)
M31N 2007-07e			
3771.346	> 22	R	(21)
4288.506	> 19.5	R	(1)
4327.469	17.9 ± 0.25	R	(1)
4330.344	18.1 ± 0.25	R	(1)
4343.487	18.4 ± 0.25	R	(4)
4353.409	18.4 ± 0.3	R	(1)
4356.430	19.3 ± 0.3	R	(1)
4357.473	19.2 ± 0.3	R	(1)
4358.284	19.5 ± 0.3	R	(1)
4365.319	19.6 ± 0.3	R	(3)
M31N 2007-08d			
3771.346	> 22	R	(21)
4380.401	18.6 ± 0.2	R	(24)
4380.424	18.5 ± 0.15	R	(24)
4382.235	19.0 ± 0.25	R	(24)
4387.219	> 19.5	R	(24)
4387.231	19.5 ± 0.3	R	(24)
4387.561	19.6 ± 0.2	R	(1)

Table 3—Continued

JD (2,450,000+)	Mag	Filter	Notes[a]
4388.227	19.8 ± 0.25	R	(24)
4388.626	19.6 ± 0.35	R	(1)
4389.233	19.8 ± 0.3	R	(24)
4389.646	20.0 ± 0.3	R	(1)
	M31N 2007-10a		
4383.529	17.856 ± 0.031	B	(30)
4384.398	18.019 ± 0.031	B	(30)
4387.398	18.932 ± 0.034	B	(30)
4389.384	19.276 ± 0.035	B	(30)
4390.355	19.501 ± 0.038	B	(30)
4392.486	20.386 ± 0.048	B	(30)
4393.714	21.077 ± 0.070	B	(30)
4394.448	21.434 ± 0.093	B	(30)
4395.553	> 20.359	B	(30)
4396.352	> 20.224	B	(30)
4397.375	> 22.588	B	(30)
4398.367	> 22.575	B	(30)
4399.380	> 21.985	B	(30)
4400.693	> 20.718	B	(30)
4402.606	> 22.359	B	(30)
4405.649	> 22.927	B	(30)
4406.679	> 21.795	B	(30)
4407.573	> 22.505	B	(30)
4410.416	> 22.726	B	(30)
4383.860	18.091 ± 0.041	B	(31)
4384.846	18.253 ± 0.042	B	(31)
4385.970	19.059 ± 0.060	B	(31)
4386.811	18.922 ± 0.052	B	(31)
4387.869	19.009 ± 0.057	B	(31)
4388.786	19.180 ± 0.062	B	(31)
4389.991	17.651 ± 0.037	B	(31)
4390.773	19.720 ± 0.073	B	(31)
4391.745	20.264 ± 0.094	B	(31)
4392.739	20.398 ± 0.129	B	(31)
4393.971	> 21.016	B	(3)
4394.793	> 21.294	B	(31)
4383.532	17.859 ± 0.036	V	(30)
4384.401	18.021 ± 0.037	V	(30)
4387.403	18.802 ± 0.040	V	(30)
4389.386	19.188 ± 0.040	V	(30)
4390.358	19.372 ± 0.041	V	(30)

Table 3—Continued

JD (2,450,000+)	Mag	Filter	Notes[a]
4392.489	20.141 ± 0.048	V	(30)
4393.717	20.709 ± 0.077	V	(30)
4394.451	20.871 ± 0.072	V	(30)
4395.555	> 20.255	V	(30)
4396.355	> 20.328	V	(30)
4397.378	> 21.711	V	(30)
4398.370	> 21.835	V	(30)
4399.383	> 22.252	V	(30)
4400.696	> 21.472	V	(30)
4402.609	> 21.735	V	(30)
4405.652	> 22.490	V	(30)
4406.682	> 22.278	V	(30)
4407.576	> 21.828	V	(30)
4410.419	> 21.934	V	(30)
4383.862	17.933 ± 0.041	V	(31)
4384.849	18.141 ± 0.042	V	(31)
4385.973	18.808 ± 0.048	V	(31)
4386.813	18.796 ± 0.047	V	(31)
4387.872	18.962 ± 0.049	V	(31)
4388.789	19.047 ± 0.053	V	(31)
4389.994	18.163 ± 0.042	V	(31)
4390.777	19.512 ± 0.058	V	(31)
4391.748	19.834 ± 0.063	V	(31)
4392.742	20.394 ± 0.107	V	(31)
4393.975	> 21.105	V	(31)
4394.796	> 20.904	V	(31)
3771.346	> 22	R	(21)
4388.644	18.6 ± 0.2	R	(1)
4383.535	17.994 ± 0.027	i'	(30)
4384.404	18.155 ± 0.027	i'	(30)
4389.389	19.227 ± 0.032	i'	(30)
4390.361	19.309 ± 0.032	i'	(30)
4392.492	19.992 ± 0.044	i'	(30)
4393.720	20.565 ± 0.071	i'	(30)
4394.453	20.746 ± 0.066	i'	(30)
4395.558	> 21.657	i'	(30)
4396.358	> 21.196	i'	(30)
4397.381	> 22.289	i'	(30)
4398.373	> 21.485	i'	(30)
4399.386	> 21.672	i'	(30)
4400.698	> 21.071	i'	(30)
4402.612	> 21.385	i'	(30)

Table 3—Continued

JD (2,450,000+)	Mag	Filter	Notes[a]
4405.655	> 21.920	i'	(30)
4406.685	> 21.647	i'	(30)
4407.578	> 21.377	i'	(30)
4410.422	> 21.955	i'	(30)
4383.857	18.089 ± 0.032	i'	(31)
4384.844	18.211 ± 0.033	i'	(31)
4385.967	18.565 ± 0.035	i'	(31)
4386.808	18.863 ± 0.037	i'	(31)
4387.835	19.048 ± 0.051	i'	(31)
4387.866	19.050 ± 0.042	i'	(31)
4388.783	19.233 ± 0.043	i'	(31)
4389.988	18.186 ± 0.031	i'	(31)
4390.771	19.438 ± 0.046	i'	(31)
4391.743	19.709 ± 0.049	i'	(31)
4392.736	20.186 ± 0.082	i'	(31)
4393.968	20.821 ± 0.123	i'	(31)
4394.790	> 20.323	i'	(31)
4395.810	> 20.778	i'	(31)
	M31N 2007-10b		
4389.507	19.603 ± 0.049	B	(30)
4392.397	> 22.280	B	(30)
4393.519	> 21.828	B	(30)
4394.436	> 22.276	B	(30)
4395.483	> 21.807	B	(30)
4389.504	19.927 ± 0.038	V	(30)
4392.394	> 21.704	V	(30)
4393.516	> 21.935	V	(30)
4394.433	> 22.293	V	(30)
4395.480	> 22.240	V	(30)
3771.346	> 22	R	(21)
4382.235	> 19.4	R	(1)
4387.219	18.5 ± 0.15	R	(24)
4387.561	18.2 ± 0.1	R	(1)
4388.227	19.1 ± 0.2	R	(24)
4388.626	19.1 ± 0.2	R	(1)
4389.233	19.3 ± 0.2	R	(24)
4389.646	19.6 ± 0.25	R	(1)
4405.318	> 19.6	R	(28)
4409.388	> 19.9	R	(1)
4410.204	$> 19.7 \pm 0.25$	R	(27)

Table 3—Continued

JD (2,450,000+)	Mag	Filter	Notes[a]
4411.517	$> 19.7 \pm 0.25$	R	(27)
4389.501	20.148 ± 0.062	i'	(30)
4390.406	20.649 ± 0.096	i'	(30)
4392.391	> 20.840	i'	(30)
4393.513	> 20.811	i'	(30)
4394.430	> 21.046	i'	(30)
4395.477	> 20.406	i'	(30)
	M31N 2007-11b		
4418.534	19.830 ± 0.027	B	(30)
4420.510	19.829 ± 0.026	B	(30)
4421.434	19.753 ± 0.023	B	(30)
4431.597	21.004 ± 0.144	B	(30)
4432.478	20.848 ± 0.096	B	(30)
4438.431	20.805 ± 0.047	B	(30)
4444.422	20.976 ± 0.045	B	(30)
4419.872	19.933 ± 0.134	B	(31)
4421.846	19.742 ± 0.080	B	(31)
4422.762	20.191 ± 0.100	B	(31)
4427.856	> 19.946	B	(31)
4418.537	19.662 ± 0.026	V	(30)
4420.513	19.628 ± 0.024	V	(30)
4421.437	19.509 ± 0.021	V	(30)
4431.602	20.391 ± 0.075	V	(30)
4432.481	20.557 ± 0.070	V	(30)
4438.434	20.581 ± 0.043	V	(30)
4441.433	19.966 ± 0.030	V	(30)
4444.424	20.691 ± 0.039	V	(30)
4419.874	19.687 ± 0.064	V	(31)
4421.849	19.551 ± 0.051	V	(31)
4422.765	19.802 ± 0.056	V	(31)
4427.859	20.272 ± 0.210	V	(31)
3771.346	> 21.0	R	(21)
4415.446	18.3 ± 0.15	R	(1)
4416.223	18.2 ± 0.15	R	(1)
4453.263	19.9 ± 0.25	R	(1)
4418.540	19.246 ± 0.028	i'	(30)
4420.516	19.159 ± 0.026	i'	(30)

Table 3—Continued

JD (2,450,000+)	Mag	Filter	Notes[a]
4421.440	19.063 ± 0.045	i'	(30)
4431.607	19.858 ± 0.041	i'	(30)
4432.484	19.669 ± 0.033	i'	(30)
4438.437	19.735 ± 0.033	i'	(30)
4441.436	19.366 ± 0.030	i'	(30)
4444.427	20.039 ± 0.032	i'	(30)
4419.877	19.124 ± 0.041	i'	(31)
4421.852	19.054 ± 0.036	i'	(31)
4422.768	19.355 ± 0.041	i'	(31)
4427.862	19.607 ± 0.092	i'	(31)
4428.758	19.126 ± 0.093	i'	(31)
4430.869	19.553 ± 0.060	i'	(31)
4436.765	19.807 ± 0.061	i'	(31)
	M31N 2007-11c		
4419.883	16.642 ± 0.067	B	(31)
4420.536	16.736 ± 0.013	B	(30)
4421.447	16.718 ± 0.012	B	(30)
4421.858	16.985 ± 0.027	B	(31)
4422.774	17.058 ± 0.024	B	(31)
4427.868	> 18.311	B	(31)
4430.875	> 18.536	B	(31)
4432.385	18.524 ± 0.020	B	(30)
4436.771	19.117 ± 0.094	B	(30)
4438.418	19.184 ± 0.035	B	(30)
4441.397	19.423 ± 0.046	B	(30)
4443.534	> 20.583	B	(30)
4449.347	20.019 ± 0.052	B	(30)
4419.886	16.651 ± 0.016	V	(31)
4420.539	16.926 ± 0.014	V	(30)
4421.450	17.028 ± 0.011	V	(30)
4421.860	17.165 ± 0.019	V	(31)
4422.776	17.327 ± 0.019	V	(31)
4427.870	> 17.968	V	(31)
4428.767	> 18.804	V	(31)
4429.766	18.521 ± 0.054	V	(31)
4430.878	18.616 ± 0.127	V	(31)
4432.388	18.891 ± 0.028	V	(30)
4436.773	19.266 ± 0.091	V	(31)
4438.421	19.482 ± 0.064	V	(30)
4441.400	19.890 ± 0.079	V	(30)
4443.537	> 19.933	V	(30)

Table 3—Continued

JD (2,450,000+)	Mag	Filter	Notes[a]
4449.350	20.334 ± 0.107	V	(30)
3771.346	> 21.5	R	(21)
4415.475	> 20.1	R	(1)
4416.387	19.7 ± 0.25	R	(1)
4417.547	17.8 ± 0.2	R	(1)
4445.234	$19.3 : \pm 0.4$	R	(1)
4419.888	17.173 ± 0.082	i'	(31)
4420.542	17.467 ± 0.081	i'	(30)
4421.453	17.592 ± 0.081	i'	(30)
4421.863	17.710 ± 0.084	i'	(31)
4422.779	17.848 ± 0.083	i'	(31)
4427.873	> 18.935	i'	(31)
4429.769	19.961 ± 0.154	i'	(31)
4432.391	19.539 ± 0.107	i'	(30)
4438.424	19.955 ± 0.171	i'	(30)
4443.540	> 18.842	i'	(30)
4449.352	> 20.690	i'	(30)
	M31N 2007-11d		
4427.880	16.460 ± 0.030	B	(30)
4428.780	16.520 ± 0.040	B	(30)
4429.770	16.560 ± 0.030	B	(30)
4432.470	16.639 ± 0.027	B	(31)
4436.580	17.558 ± 0.028	B	(31)
4436.780	17.820 ± 0.070	B	(30)
4439.370	20.220 ± 0.040	B	(31)
4443.330	21.772 ± 0.029	B	(31)
4427.880	16.071 ± 0.024	V	(30)
4428.780	16.236 ± 0.026	V	(30)
4429.780	16.334 ± 0.024	V	(30)
4432.470	16.603 ± 0.023	V	(31)
4436.590	17.563 ± 0.031	V	(31)
4436.780	17.703 ± 0.043	V	(30)
4439.370	20.039 ± 0.036	V	(31)
4443.340	21.443 ± 0.133	V	(31)
4427.880	15.780 ± 0.010	i'	(30)
4428.780	15.890 ± 0.030	i'	(30)
4429.780	16.040 ± 0.010	i'	(30)
4432.470	16.310 ± 0.010	i'	(31)
4436.590	17.070 ± 0.010	i'	(31)

Table 3—Continued

JD (2,450,000+)	Mag	Filter	Notes[a]
4436.790	17.270 ± 0.030	i'	(30)
4439.380	18.710 ± 0.020	i'	(31)
4443.340	20.270 ± 0.070	i'	(31)
4449.340	20.880 ± 0.090	i'	(31)
	M31N 2007-12a		
4449.415	18.002 ± 0.023	B	(30)
4451.434	17.709 ± 0.023	B	(30)
4455.392	17.872 ± 0.032	B	(30)
4459.390	18.069 ± 0.024	B	(30)
4460.344	18.114 ± 0.023	B	(30)
4461.386	18.275 ± 0.024	B	(30)
4463.473	18.410 ± 0.024	B	(30)
4466.335	18.664 ± 0.024	B	(30)
4467.367	18.790 ± 0.025	B	(30)
4468.388	18.864 ± 0.024	B	(30)
4469.432	19.050 ± 0.025	B	(30)
4471.343	19.135 ± 0.026	B	(30)
4473.862	19.533 ± 0.067	B	(31)
4474.413	19.253 ± 0.026	B	(30)
4474.732	19.402 ± 0.056	B	(31)
4474.741	19.338 ± 0.101	B	(31)
4449.418	17.817 ± 0.013	V	(30)
4451.437	17.601 ± 0.013	V	(30)
4455.395	17.803 ± 0.013	V	(30)
4459.393	18.020 ± 0.014	V	(30)
4460.347	18.079 ± 0.014	V	(30)
4461.389	18.246 ± 0.014	V	(30)
4463.476	18.436 ± 0.015	V	(30)
4466.338	18.647 ± 0.015	V	(30)
4467.370	18.789 ± 0.016	V	(30)
4468.391	18.842 ± 0.016	V	(30)
4469.435	19.013 ± 0.017	V	(30)
4471.346	19.093 ± 0.018	V	(30)
4473.865	19.475 ± 0.046	V	(31)
4474.416	19.255 ± 0.018	V	(30)
4474.734	19.349 ± 0.049	V	(31)
4474.744	19.314 ± 0.069	V	(31)
4449.421	17.629 ± 0.012	i'	(30)
4451.439	17.374 ± 0.011	i'	(30)
4455.398	17.455 ± 0.012	i'	(30)
4459.396	17.676 ± 0.012	i'	(30)

Table 3—Continued

JD (2,450,000+)	Mag	Filter	Notes[a]
4460.350	17.778 ± 0.012	i'	(30)
4461.392	17.917 ± 0.013	i'	(30)
4463.479	18.045 ± 0.013	i'	(30)
4466.341	18.289 ± 0.013	i'	(30)
4467.373	18.363 ± 0.014	i'	(30)
4468.394	18.404 ± 0.014	i'	(30)
4469.437	18.540 ± 0.015	i'	(30)
4471.349	18.621 ± 0.016	i'	(30)
4473.868	18.741 ± 0.027	i'	(31)
4474.419	18.761 ± 0.016	i'	(30)
4474.747	18.831 ± 0.043	i'	(31)
	M31N 2007-12b		
4449.440	19.190 ± 0.050	B	(30)
4452.350	19.750 ± 0.050	B	(30)
4455.400	20.270 ± 0.090	B	(30)
4459.400	20.880 ± 0.110	B	(30)
4460.390	21.120 ± 0.110	B	(30)
4461.510	> 20.54	B	(30)
4464.520	21.590 ± 0.050	B	(30)
4467.350	> 21.4	B	(30)
4468.400	> 21.01	B	(30)
4469.460	> 21.63	B	(30)
4470.440	> 21.78	B	(30)
4472.480	> 21.73	B	(30)
4449.450	19.270 ± 0.040	V	(30)
4452.350	19.820 ± 0.040	V	(30)
4455.410	20.430 ± 0.090	V	(30)
4459.410	20.670 ± 0.090	V	(30)
4460.390	> 21.11	V	(30)
4461.510	> 20.74	V	(30)
4464.520	> 20.55	V	(30)
4467.350	> 20.88	V	(30)
4468.400	> 20.97	V	(30)
4469.470	> 20.62	V	(30)
4470.450	> 20.96	V	(30)
4472.480	> 21.09	V	(30)
3771.346	> 21.5	R	(21)
4417.547	> 19.1	R	(1)
4445.234	17.0 ± 0.1	R	(1)
4450.392	18.6 ± 0.25	R	(1)
4450.402	18.7 ± 0.25	R	(1)

Table 3—Continued

JD (2,450,000+)	Mag	Filter	Notes[a]
4453.250	19.4 ± 0.25	R	(1)
4449.450	18.930 ± 0.040	i'	(30)
4452.360	19.350 ± 0.040	i'	(30)
4455.410	> 19.65	i'	(30)
4459.410	> 19.58	i'	(30)
4460.390	> 19.64	i'	(30)
	M31N 2007-12d		
3771.346	> 21.5	R	(21)
4453.238	17.8 ± 0.2	R	(1)
	M31N 2008-05c		
4528.246	> 19.6	R	(1)
4601.558	> 19.8	R	(28)
4617.523	17.6 ± 0.2	R	(1)
4617.549	17.5 ± 0.2	R	(1)
4619.529	17.2 ± 0.1	R	(1)
4619.554	17.2 ± 0.1	R	(1)
4620.543	17.3 ± 0.1	R	(1)
4628.541	18.1 ± 0.2	R	(3)
4645.550	19.3 ± 0.2	R	(1)
4646.535	19.0 ± 0.2	R	(1)
4647.492	19.0 ± 0.2	R	(1)
4648.557	19.0 ± 0.2	R	(1)
4655.567	19.6 ± 0.25	R	(3)
4675.581	19.3 ± 0.2	R	(3)
4677.432	19.4 ± 0.3	R	(1)
4678.562	19.6 ± 0.25	R	(1)
4679.551	19.5 ± 0.25	R	(1)
4682.379	19.6 ± 0.3	R	(1)
4682.574	19.6 ± 0.2	R	(1)
4683.562	19.8 ± 0.3	R	(1)
4685.548	20.0 ± 0.3	R	(1)
4692.616	> 19.7	R	(28)
4697.573	20.3 ± 0.3	R	(3)
4706.362	19.6 ± 0.3	R	(1)
4712.608	> 20.1	R	(1)
	M31N 2008-06b		
4505.226	> 20.0	R	(1)
4620.542	> 20.3	R	(1)

Table 3—Continued

JD (2,450,000+)	Mag	Filter	Notes[a]
4628.541	> 20.2	R	(3)
4644.498	16.0 ± 0.1	R	(5)
4645.489	16.44 ± 0.05	R	(1)
4645.529	16.41 ± 0.05	R	(1)
4645.550	16.41 ± 0.05	R	(1)
4646.535	16.54 ± 0.05	R	(1)
4647.492	16.62 ± 0.05	R	(1)
4648.557	16.71 ± 0.05	R	(1)
4652.560	17.26 ± 0.1	R	(3)
4655.567	17.45 ± 0.1	R	(3)
4675.581	18.9 ± 0.15	R	(3)
4677.432	18.75 ± 0.2	R	(1)
4678.562	18.8 ± 0.15	R	(1)
4679.551	19.0 ± 0.15	R	(1)
4681.370	19.1 ± 0.25	R	(1)
4682.379	19.1 ± 0.2	R	(1)
4682.574	19.0 ± 0.15	R	(1)
4683.562	19.1 ± 0.2	R	(1)
4685.548	19.4 ± 0.2	R	(1)
4692.616	> 19.7	R	(28)
4697.573	20.4 ± 0.3	R	(3)
4706.362	> 20.4	R	(1)
	M31N 2008-07a		
5095.981	21.4 ± 0.4 V (13)		
4505.226	> 19.7	R	(1)
4617.523	> 19.0	R	(1)
4619.529	19.0 ± 0.3	R	(1)
4620.542	18.7 ± 0.25	R	(1)
4628.541	19.0 ± 0.3	R	(3)
4645.488	19.1 ± 0.3	R	(1)
4646.535	19.2 ± 0.25	R	(1)
4647.492	18.8 ± 0.2	R	(1)
4648.557	19.3 ± 0.25	R	(1)
4655.567	19.1 ± 0.25	R	(3)
4675.581	19.0 ± 0.2	R	(3)
4677.432	18.8 ± 0.2	R	(1)
4678.562	18.8 ± 0.2	R	(1)
4679.551	18.9 ± 0.2	R	(1)
4681.370	19.3 ± 0.3	R	(1)
4682.379	19.1 ± 0.25	R	(1)
4682.574	19.0 ± 0.15	R	(1)
4683.562	19.0 ± 0.2	R	(1)

Table 3—Continued

JD (2,450,000+)	Mag	Filter	Notes[a]
4684.525	19.5 ± 0.3	R	(1)
4685.548	18.75 ± 0.1	R	(1)
4692.616	18.9 ± 0.2	R	(28)
4697.573	19.0 ± 0.15	R	(3)
4706.362	19.1 ± 0.2	R	(1)
4708.387	18.7 ± 0.25	R	(1)
4709.613	19.3 ± 0.25	R	(1)
4710.589	19.2 ± 0.35	R	(1)
4711.310	18.9 ± 0.25	R	(1)
4712.291	19.0 ± 0.25	R	(1)
4712.337	18.8 ± 0.15	R	(1)
4712.608	18.85 ± 0.15	R	(1)
4713.343	19.0 ± 0.2	R	(1)
4715.330	18.8 ± 0.15	R	(1)
4716.334	18.9 ± 0.25	R	(1)
4718.378	19.3 ± 0.3	R	(3)
4719.299	19.2 ± 0.3	R	(3)
4738.221	18.85 ± 0.15	R	(3)
4744.604	19.1 ± 0.15	R	(1)
4745.257	19.1 ± 0.2	R	(1)
4748.472	19.1 ± 0.2	R	(7)
4748.485	19.2 ± 0.25	R	(7)
4754.400	19.0 ± 0.2	R	(3)
4760.628	19.2 ± 0.2	R	(3)
4763.219	19.2 ± 0.3	R	(1)
4765.545	19.1 ± 0.25	R	(1)
4772.448	19.4 ± 0.25	R	(1)
4774.545	19.3 ± 0.3	R	(1)
4776.228	19.6 ± 0.25	R	(1)
4777.215	19.6 ± 0.3	R	(1)
4779.283	19.4 ± 0.25	R	(1)
4779.318	19.5 ± 0.3	R	(1)
4800.301	19.3 ± 0.3	R	(1)
4801.226	$18.9 : \pm 0.4$	R	(1)
4809.285	$19.0 : \pm 0.4$	R	(1)
4982.972	> 20.4	R	(9)
5095.968	20.9 ± 0.25	R	(13)
	M31N 2008-07b		
4505.226	> 19.7	R	(1)
4655.567	> 20.6	R	(3)
4675.581	18.4 ± 0.1	R	(3)
4677.432	18.8 ± 0.2	R	(1)
4677.448	18.6 ± 0.2	R	(1)

Table 3—Continued

JD (2,450,000+)	Mag	Filter	Notes[a]
4678.562	18.7 ± 0.15	R	(1)
4679.551	18.8 ± 0.15	R	(1)
4681.370	19.3 ± 0.25	R	(1)
4682.379	19.6 ± 0.25	R	(1)
4682.550	19.3 ± 0.2	R	(1)
4682.574	19.4 ± 0.15	R	(1)
4683.562	19.3 ± 0.15	R	(1)
4684.525	19.5 ± 0.3	R	(1)
4685.548	19.6 ± 0.15	R	(1)
4685.564	19.5 ± 0.15	R	(1)
4685.577	19.4 ± 0.15	R	(1)
4692.616	19.3 ± 0.25	R	(28)
4697.573	20.0 ± 0.25	R	(3)
4706.362	20.7 ± 0.3	R	(1)
4708.424	20.3 ± 0.3	R	(1)
4710.323	> 20.2	R	(1)
4711.335	20.6 ± 0.4	R	(1)
4712.608	20.3 ± 0.25	R	(1)
4713.343	20.2 ± 0.35	R	(1)
4715.330	20.5 ± 0.3	R	(1)
M31N 2008-08a			
4685.548	> 20.5	R	(1)
4692.616	16.7 ± 0.1	R	(28)
4697.573	17.7 ± 0.1	R	(3)
4706.362	18.3 ± 0.15	R	(1)
4706.627	18.2 ± 0.2	R	(1)
4708.387	18.4 ± 0.25	R	(1)
4709.613	18.8 ± 0.25	R	(1)
4710.589	19.0 ± 0.3	R	(1)
4711.310	18.4 ± 0.25	R	(1)
4712.291	19.3 ± 0.35	R	(1)
4712.608	19.0 ± 0.2	R	(1)
4713.343	18.6 ± 0.25	R	(1)
4715.330	18.6 ± 0.25	R	(1)
M31N 2008-08b			
4685.548	> 20.5	R	(1)
4692.616	17.8 ± 0.1	R	(28)
4697.573	19.3 ± 0.2	R	(3)
M31N 2008-09a			

Table 3—Continued

JD (2,450,000+)	Mag	Filter	Notes[a]
4744.340	18.4 ± 0.2	R	(1)
	M31N 2008-10a		
4778.655	19.884 ± 0.171	B	(30)
4778.727	19.477 ± 0.071	B	(31)
4779.967	> 20.168	B	(31)
4779.637	20.080 ± 0.195	B	(30)
4780.463	20.093 ± 0.078	B	(30)
4781.491	> 18.797	B	(30)
4782.449	19.515 ± 0.060	B	(30)
4783.360	> 19.960	B	(30)
4785.451	19.651 ± 0.042	B	(30)
4786.404	> 19.649	B	(30)
4787.479	19.402 ± 0.033	B	(30)
4788.455	19.650 ± 0.035	B	(30)
4789.403	19.683 ± 0.038	B	(30)
4778.658	19.337 ± 0.032	V	(30)
4778.732	19.964 ± 0.094	V	(31)
4779.641	19.764 ± 0.036	V	(30)
4779.972	19.781 ± 0.103	V	(31)
4780.466	20.100 ± 0.070	V	(30)
4780.900	18.880 ± 0.582	V	(31)
4781.495	> 19.338	V	(30)
4782.453	19.254 ± 0.049	V	(30)
4783.364	19.543 ± 0.068	V	(30)
4785.456	19.456 ± 0.040	V	(30)
4786.407	19.412 ± 0.038	V	(30)
4787.483	19.194 ± 0.026	V	(30)
4788.458	19.418 ± 0.026	V	(30)
4789.406	19.444 ± 0.026	V	(30)
4775.921	17.756 ± 0.015	r'	(31)
4777.861	17.975 ± 0.039	r'	(31)
4778.644	18.156 ± 0.043	r'	(30)
4778.712	18.147 ± 0.016	r'	(31)
4779.626	18.578 ± 0.130	r'	(30)
4779.952	18.118 ± 0.063	r'	(31)
4780.452	18.374 ± 0.021	r'	(30)
4780.877	18.165 ± 0.140	r'	(31)
4781.480	17.973 ± 0.079	r'	(30)
4782.438	18.094 ± 0.016	r'	(30)
4783.349	18.101 ± 0.087	r'	(30)
4785.440	18.239 ± 0.012	r'	(30)

Table 3—Continued

JD (2,450,000+)	Mag	Filter	Notes[a]
4786.393	18.275 ± 0.013	r'	(30)
4787.468	18.192 ± 0.010	r'	(30)
4788.444	18.357 ± 0.011	r'	(30)
4789.392	18.354 ± 0.012	r'	(30)
	M31N 2008-10b		
4716.407	> 20.1	R	(1)
4748.479	19.8 ± 0.35	R	(4)
4754.419	19.3 ± 0.35	R	(3)
4763.218	18.1 ± 0.15	R	(1)
4765.546	19.0 ± 0.25	R	(1)
4772.448	19.3 ± 0.25	R	(1)
4774.571	19.2 ± 0.25	R	(1)
4776.228	18.8 ± 0.15	R	(1)
4777.229	18.5 ± 0.15	R	(1)
4779.283	19.0 ± 0.2	R	(1)
4795.192	19.9 ± 0.3	V	(1)
4798.431	18.9 ± 0.2	V	(5)
4799.199	18.3 ± 0.15	R	(1)
4800.301	18.0 ± 0.15	R	(1)
4801.267	18.3 ± 0.15	R	(1)
4809.285	18.2 ± 0.15	R	(1)
4829.183	19.1 ± 0.3	R	(1)
4760.472	18.098 ± 0.018	B	(30)
4761.514	17.574 ± 0.018	B	(30)
4764.549	19.451 ± 0.055	B	(30)
4777.584	18.525 ± 0.030	B	(30)
4778.441	19.065 ± 0.053	B	(30)
4779.485	19.113 ± 0.052	B	(30)
4780.429	19.399 ± 0.128	B	(30)
4781.435	19.343 ± 0.100	B	(30)
4782.461	> 19.780	B	(30)
4783.401	> 19.115	B	(30)
4785.495	18.619 ± 0.036	B	(30)
4786.422	18.853 ± 0.055	B	(30)
4787.370	19.123 ± 0.036	B	(30)
4788.467	19.475 ± 0.053	B	(30)
4789.418	18.839 ± 0.033	B	(30)
4790.383	19.035 ± 0.044	B	(30)
4760.793	17.956 ± 0.019	B	(31)
4761.793	17.652 ± 0.018	B	(31)
4762.894	> 17.446	B	(31)

Table 3—Continued

JD (2,450,000+)	Mag	Filter	Notes[a]
4763.727	18.993 ± 0.044	B	(31)
4763.740	19.117 ± 0.035	B	(31)
4763.793	19.105 ± 0.034	B	(31)
4764.919	> 19.756	B	(31)
4771.889	19.609 ± 0.042	B	(31)
4772.862	19.898 ± 0.047	B	(31)
4773.835	19.706 ± 0.039	B	(31)
4774.842	19.460 ± 0.040	B	(31)
4777.843	18.774 ± 0.032	B	(31)
4779.922	19.266 ± 0.063	B	(31)
4780.835	> 18.461	B	(31)
4760.476	18.124 ± 0.016	V	(30)
4761.517	17.706 ± 0.014	V	(30)
4764.553	19.322 ± 0.054	V	(30)
4777.588	18.671 ± 0.033	V	(30)
4778.444	18.231 ± 0.059	V	(30)
4779.487	19.262 ± 0.049	V	(30)
4780.433	19.636 ± 0.085	V	(30)
4781.438	19.731 ± 0.110	V	(30)
4782.465	19.750 ± 0.182	V	(30)
4783.405	> 19.558	V	(30)
4785.499	18.815 ± 0.030	V	(30)
4786.426	18.808 ± 0.039	V	(30)
4787.374	19.126 ± 0.041	V	(30)
4788.471	19.674 ± 0.067	V	(30)
4789.421	18.897 ± 0.035	V	(30)
4790.387	19.030 ± 0.038	V	(30)
4760.796	17.953 ± 0.016	V	(31)
4761.796	17.699 ± 0.015	V	(31)
4762.895	17.881 ± 0.057	V	(31)
4763.730	18.975 ± 0.031	V	(31)
4763.743	18.993 ± 0.032	V	(31)
4763.796	19.040 ± 0.033	V	(31)
4764.923	> 18.132	V	(31)
4771.892	19.653 ± 0.051	V	(31)
4772.865	20.034 ± 0.062	V	(31)
4773.837	19.859 ± 0.049	V	(31)
4774.845	19.608 ± 0.042	V	(31)
4777.846	18.773 ± 0.035	V	(31)
4779.925	19.055 ± 0.072	V	(31)
4780.838	> 17.488	V	(31)
4760.478	18.308 ± 0.014	r'	(30)

Table 3—Continued

JD (2,450,000+)	Mag	Filter	Notes[a]
4761.520	17.840 ± 0.012	r'	(30)
4764.556	19.033 ± 0.043	r'	(30)
4777.591	18.631 ± 0.030	r'	(30)
4778.448	19.213 ± 0.046	r'	(30)
4779.492	19.124 ± 0.037	r'	(30)
4780.437	19.298 ± 0.068	r'	(30)
4781.442	> 19.089	r'	(30)
4782.469	> 19.158	r'	(30)
4783.409	> 19.260	r'	(30)
4785.503	18.917 ± 0.026	r'	(30)
4786.430	18.876 ± 0.420	r'	(30)
4787.378	19.119 ± 0.038	r'	(30)
4788.474	19.378 ± 0.053	r'	(30)
4789.425	18.934 ± 0.031	r'	(30)
4790.391	19.029 ± 0.036	r'	(30)
4760.799	18.171 ± 0.014	r'	(31)
4761.799	17.885 ± 0.012	r'	(31)
4762.898	18.104 ± 0.057	r'	(31)
4763.733	18.926 ± 0.026	r'	(31)
4763.799	18.935 ± 0.025	r'	(31)
4764.925	19.333 ± 0.387	r'	(31)
4771.895	19.378 ± 0.035	r'	(31)
4772.868	19.719 ± 0.045	r'	(31)
4773.841	19.566 ± 0.037	r'	(31)
4774.848	19.441 ± 0.033	r'	(31)
4777.850	18.781 ± 0.033	r'	(31)
4779.928	19.219 ± 0.048	r'	(31)
4780.841	18.677 ± 0.235	r'	(31)
	M31N 2008-11a		
4778.400	19.259 ± 0.050	B	(30)
4779.472	19.783 ± 0.064	B	(30)
4779.891	19.309 ± 0.193	B	(31)
4780.486	19.607 ± 0.069	B	(30)
4780.907	20.742 ± 0.220	B	(31)
4782.418	20.027 ± 0.083	B	(30)
4783.496	> 20.753	B	(30)
4785.529	20.306 ± 0.107	B	(30)
4786.490	> 20.029	B	(30)
4787.404	20.507 ± 0.072	B	(30)
4788.428	20.933 ± 0.074	B	(30)
4789.503	20.936 ± 0.220	B	(30)
4794.344	20.592 ± 0.082	B	(30)

Table 3—Continued

JD (2,450,000+)	Mag	Filter	Notes[a]
4795.478	> 20.830	B	(30)
4796.581	> 20.911	B	(30)
4799.384	21.567 ± 0.114	B	(30)
4800.470	> 21.775	B	(30)
4802.396	> 21.644	B	(30)
4805.339	> 21.701	B	(30)
4805.395	> 21.562	B	(30)
4778.404	18.917 ± 0.038	V	(30)
4779.476	19.266 ± 0.060	V	(30)
4779.896	19.164 ± 0.057	V	(31)
4780.489	19.219 ± 0.044	V	(30)
4780.912	> 19.462	V	(31)
4781.472	19.693 ± 0.095	V	(30)
4782.422	19.770 ± 0.110	V	(30)
4783.499	> 19.457	V	(30)
4785.532	20.260 ± 0.092	V	(30)
4786.494	> 19.410	V	(30)
4787.407	20.177 ± 0.059	V	(30)
4788.432	20.407 ± 0.141	V	(30)
4789.508	20.515 ± 0.211	V	(30)
4794.348	21.413 ± 0.310	V	(30)
4795.482	20.900 ± 0.186	V	(30)
4796.585	> 20.561	V	(30)
4799.387	20.737 ± 0.147	V	(30)
4800.474	> 21.387	V	(30)
4800.498	> 20.384	V	(30)
4802.400	21.172 ± 0.185	V	(30)
4805.399	> 21.106	V	(30)
4744.340	> 19.9	R	(1)
4775.218	16.5 ± 0.1	R	(1)
4776.217	17.4 ± 0.1	R	(1)
4779.260	18.3 ± 0.15	R	(1)
4780.234	18.4 ± 0.2	R	(1)
4800.310	> 19.5	R	(1)
4778.389	17.920 ± 0.011	r'	(30)
4779.461	18.289 ± 0.016	r'	(30)
4779.901	18.407 ± 0.059	r'	(31)
4780.475	18.502 ± 0.020	r'	(30)
4780.917	18.528 ± 0.116	r'	(31)
4782.407	18.890 ± 0.025	r'	(30)
4783.485	18.935 ± 0.160	r'	(30)
4785.518	19.310 ± 0.025	r'	(30)

Table 3—Continued

JD (2,450,000+)	Mag	Filter	Notes[a]
4786.479	19.436 ± 0.160	r'	(30)
4787.393	19.683 ± 0.031	r'	(30)
4788.418	19.881 ± 0.027	r'	(30)
4789.492	20.063 ± 0.035	r'	(30)
4790.412	19.899 ± 0.032	r'	(30)
4794.333	20.310 ± 0.135	r'	(30)
4795.467	20.130 ± 0.036	r'	(30)
4796.570	> 20.119	r'	(30)
4799.373	20.689 ± 0.148	r'	(30)
4800.403	20.200 ± 0.225	r'	(30)
4800.459	20.152 ± 0.138	r'	(30)
4802.385	21.052 ± 0.140	r'	(30)
4803.398	> 19.727	r'	(30)
4805.328	21.155 ± 0.111	r'	(30)
4805.384	21.470 ± 0.295	r'	(30)
4778.393	18.367 ± 0.034	i'	(30)
4779.465	18.884 ± 0.020	i'	(30)
4779.906	18.909 ± 0.082	i'	(31)
4780.478	19.020 ± 0.043	i'	(30)
4780.922	19.552 ± 0.179	i'	(31)
4782.411	19.591 ± 0.028	i'	(30)
4783.489	> 19.309	i'	(30)
4785.521	20.178 ± 0.048	i'	(30)
4786.483	> 20.126	i'	(30)
4787.396	20.234 ± 0.099	i'	(30)
4788.421	20.511 ± 0.044	i'	(30)
4789.497	21.077 ± 0.184	i'	(30)
4790.415	20.583 ± 0.142	i'	(30)
4794.337	20.649 ± 0.186	i'	(30)
4795.471	20.957 ± 0.059	i'	(30)
4796.574	> 19.433	i'	(30)
4799.376	21.295 ± 0.233	i'	(30)
4800.464	20.993 ± 0.242	i'	(30)
4802.389	21.300 ± 0.066	i'	(30)
4803.401	> 20.175	i'	(30)
4805.331	> 21.000	i'	(30)
4805.388	> 21.564	i'	(30)
4778.396	17.866 ± 0.018	z'	(30)
4779.468	18.131 ± 0.076	z'	(30)
4780.482	18.500 ± 0.040	z'	(30)
4781.465	> 18.716	z'	(30)
4782.414	19.112 ± 0.107	z'	(30)
4783.492	19.264 ± 0.107	z'	(30)

Table 3—Continued

JD (2,450,000+)	Mag	Filter	Notes[a]
4785.525	19.649 ± 0.066	z'	(30)
4786.486	> 19.875	z'	(30)
4787.400	> 20.602	z'	(30)
4788.425	20.158 ± 0.083	z'	(30)
4789.499	20.621 ± 0.271	z'	(30)
4790.419	> 20.364	z'	(30)
4794.340	> 20.821	z'	(30)
4795.474	> 21.175	z'	(30)
4796.578	> 17.999	z'	(30)
	M31N 2008-12b		
4842.404	17.671 ± 0.041	B	(30)
4846.474	17.826 ± 0.015	B	(30)
4851.347	17.874 ± 0.043	B	(30)
4856.441	18.765 ± 0.081	B	(30)
4859.377	19.436 ± 0.149	B	(30)
4842.408	17.533 ± 0.035	V	(30)
4846.478	17.705 ± 0.045	V	(30)
4851.351	17.941 ± 0.046	V	(30)
4856.444	18.822 ± 0.112	V	(30)
4859.381	19.468 ± 0.129	V	(30)
4829.183	> 19.7	R	(1)
4840.253	17.0 ± 0.1	R	(4)
4848.217	17.4 ± 0.15	R	(11)
4851.394	17.3 ± 0.15	R	(1)
4842.394	17.606 ± 0.030	r'	(30)
4846.464	17.669 ± 0.036	r'	(30)
4851.337	17.893 ± 0.033	r'	(30)
4856.430	18.843 ± 0.058	r'	(30)
4859.366	19.262 ± 0.105	r'	(30)
4842.397	17.499 ± 0.049	i'	(30)
4846.467	17.693 ± 0.032	i'	(30)
4851.340	17.896 ± 0.044	i'	(30)
4856.433	18.453 ± 0.080	i'	(30)
4859.370	18.993 ± 0.089	i'	(30)
4842.400	16.750 ± 0.022	z'	(30)
4846.471	16.921 ± 0.043	z'	(30)
4851.344	17.044 ± 0.049	z'	(30)
4856.437	17.371 ± 0.070	z'	(30)

Table 3—Continued

JD (2,450,000+)	Mag	Filter	Notes[a]
4859.374	17.533 ± 0.084	z'	(30)
	M31N 2009-01a		
4872.241	> 19.3	R	(11)
	M31N 2009-02a		
4872.254	16.91 ± 0.1	R	(11)
	M31N 2009-08a		
5053.724	17.944 ± 0.062	B	(30)
5057.516	18.114 ± 0.021	B	(30)
5058.498	18.312 ± 0.023	B	(30)
5059.719	18.413 ± 0.027	B	(30)
5060.533	18.167 ± 0.065	B	(30)
5061.484	18.076 ± 0.022	B	(30)
5061.562	18.086 ± 0.047	B	(30)
5062.507	18.121 ± 0.070	B	(30)
5063.485	18.404 ± 0.030	B	(30)
5064.630	17.917 ± 0.020	B	(30)
5065.739	17.791 ± 0.019	B	(30)
5066.525	17.800 ± 0.065	B	(30)
5067.474	17.980 ± 0.072	B	(30)
5069.678	18.655 ± 0.031	B	(30)
5070.586	18.978 ± 0.029	B	(30)
5071.746	> 18.911	B	(30)
5072.526	18.655 ± 0.059	B	(30)
5073.467	18.620 ± 0.092	B	(30)
5075.501	18.263 ± 0.098	B	(30)
5076.459	18.030 ± 0.068	B	(30)
5077.718	18.077 ± 0.021	B	(30)
5077.487	18.009 ± 0.021	B	(30)
5078.572	17.903 ± 0.021	B	(30)
5079.469	17.710 ± 0.021	B	(30)
5114.306	19.91 ± 0.10	B	(17)
5053.729	17.688 ± 0.060	V	(30)
5057.520	18.212 ± 0.022	V	(30)
5058.501	18.453 ± 0.025	V	(30)
5059.723	18.520 ± 0.092	V	(30)
5060.536	18.463 ± 0.071	V	(30)
5061.488	18.169 ± 0.063	V	(30)
5061.566	18.231 ± 0.050	V	(30)

Table 3—Continued

JD (2,450,000+)	Mag	Filter	Notes[a]
5062.511	18.321 ± 0.079	V	(30)
5063.489	18.686 ± 0.037	V	(30)
5064.633	18.167 ± 0.021	V	(30)
5065.742	17.858 ± 0.019	V	(30)
5066.528	17.885 ± 0.052	V	(30)
5067.478	18.320 ± 0.080	V	(30)
5069.681	18.949 ± 0.046	V	(30)
5070.590	19.263 ± 0.041	V	(30)
5071.749	> 19.142	V	(30)
5072.529	18.940 ± 0.033	V	(30)
5073.470	18.745 ± 0.045	V	(30)
5074.483	18.560 ± 0.047	V	(30)
5075.504	18.338 ± 0.124	V	(30)
5076.463	18.195 ± 0.026	V	(30)
5077.721	18.233 ± 0.023	V	(30)
5077.490	18.134 ± 0.022	V	(30)
5078.575	18.115 ± 0.021	V	(30)
5079.472	17.852 ± 0.020	V	(30)
5092.525	18.39 ± 0.04	V	(17)
5095.981	18.98 ± 0.1	V	(13)
5114.308	20.1 ± 0.15	V	(17)
4985.974	> 20.2	R	(9)
4988.527	> 19.9	R	(1)
5055.923	18.7 ± 0.15	R	(8)
5063.605	18.8 ± 0.2	R	(22)
5073.441	18.3 ± 0.1	R	(1)
5074.366	18.3 ± 0.1	R	(1)
5075.384	18.0 ± 0.15	R	(1)
5076.478	17.8 ± 0.1	R	(1)
5080.413	17.8 ± 0.1	R	(1)
5081.393	18.4 ± 0.15	R	(1)
5083.357	18.5 ± 0.15	R	(1)
5084.267	18.2 ± 0.2	R	(1)
5094.451	18.3 ± 0.15	R	(3)
5095.968	18.52 ± 0.07	R	(13)
5114.304	19.2 ± 0.15	R	(17)
5114.486	19.2 ± 0.15	R	(3)
5124.491	19.5 ± 0.2	R	(3)
5135.632	19.3 ± 0.2	R	(12)
5140.546	19.7 ± 0.3	R	(1)
5141.359	19.9 ± 0.3	R	(1)
5148.536	19.7 ± 0.25	R	(1)
5162.281	19.3 ± 0.25	R	(5)
5168.173	19.4 ± 0.3	R	(7)

Table 3—Continued

JD (2,450,000+)	Mag	Filter	Notes[a]
5173.192	19.6 ± 0.3	R	(1)
5181.226	19.7 ± 0.3	R	(1)
5184.717	19.9 ± 0.15	R	(19)
5199.299	20.6 ± 0.2	R	(12)
5227.345	20.9 ± 0.25	R	(12)
5228.383	20.9 ± 0.25	R	(12)
5050.721	18.568 ± 0.120	r'	(30)
5052.551	18.194 ± 0.057	r'	(30)
5052.556	18.248 ± 0.066	r'	(30)
5052.570	18.170 ± 0.047	r'	(30)
5052.585	18.119 ± 0.042	r'	(30)
5052.591	18.198 ± 0.044	r'	(30)
5052.605	18.147 ± 0.042	r'	(30)
5052.620	18.202 ± 0.019	r'	(30)
5052.626	18.186 ± 0.020	r'	(30)
5052.640	18.171 ± 0.041	r'	(30)
5052.652	18.184 ± 0.046	r'	(30)
5052.660	18.098 ± 0.042	r'	(30)
5052.682	18.147 ± 0.043	r'	(30)
5052.711	18.152 ± 0.061	r'	(30)
5052.721	18.154 ± 0.045	r'	(30)
5052.728	18.152 ± 0.044	r'	(30)
5053.716	18.069 ± 0.054	r'	(30)
5053.505	18.160 ± 0.095	r'	(30)
5053.509	18.109 ± 0.084	r'	(30)
5053.514	18.037 ± 0.026	r'	(30)
5053.528	18.143 ± 0.068	r'	(30)
5053.532	18.064 ± 0.058	r'	(30)
5053.537	18.081 ± 0.057	r'	(30)
5053.541	18.101 ± 0.054	r'	(30)
5054.478	18.185 ± 0.028	r'	(30)
5056.718	18.337 ± 0.074	r'	(30)
5057.510	18.357 ± 0.049	r'	(30)
5058.491	18.532 ± 0.054	r'	(30)
5059.713	18.621 ± 0.099	r'	(30)
5060.526	18.472 ± 0.077	r'	(30)
5061.478	18.336 ± 0.073	r'	(30)
5061.555	18.383 ± 0.045	r'	(30)
5062.501	18.278 ± 0.079	r'	(30)
5063.479	18.661 ± 0.105	r'	(30)
5064.623	18.307 ± 0.047	r'	(30)
5065.733	18.073 ± 0.034	r'	(30)
5066.518	18.055 ± 0.020	r'	(30)
5067.468	18.349 ± 0.070	r'	(30)

Table 3—Continued

JD (2,450,000+)	Mag	Filter	Notes[a]
5069.672	18.797 ± 0.041	r'	(30)
5070.580	19.090 ± 0.087	r'	(30)
5072.519	18.984 ± 0.076	r'	(30)
5073.460	18.620 ± 0.065	r'	(30)
5074.733	18.978 ± 0.017	r'	(30)
5075.495	18.500 ± 0.044	r'	(30)
5077.712	18.407 ± 0.049	r'	(30)
5078.566	18.251 ± 0.018	r'	(30)
5078.515	18.235 ± 0.019	r'	(30)
5079.463	18.012 ± 0.016	r'	(30)
5210.587	20.7 ± 0.2	r'	(16)
5211.600	20.8 ± 0.25	r'	(16)
	M31N 2009-08b		
5061.546	18.559 ± 0.025	B	(30)
5063.625	18.782 ± 0.029	B	(30)
5064.662	18.960 ± 0.028	B	(30)
5066.594	19.165 ± 0.029	B	(30)
5067.459	19.298 ± 0.035	B	(30)
5069.600	19.592 ± 0.034	B	(30)
5070.567	19.847 ± 0.036	B	(30)
5071.522	19.695 ± 0.040	B	(30)
5072.496	19.899 ± 0.042	B	(30)
5073.554	19.944 ± 0.054	B	(30)
5074.717	19.950 ± 0.042	B	(30)
5075.517	19.971 ± 0.075	B	(30)
5076.485	19.813 ± 0.090	B	(30)
5077.471	20.165 ± 0.081	B	(30)
5078.492	20.380 ± 0.103	B	(30)
5079.523	20.383 ± 0.108	B	(30)
5061.549	18.424 ± 0.019	V	(30)
5063.628	18.665 ± 0.022	V	(30)
5064.665	18.776 ± 0.022	V	(30)
5066.596	18.991 ± 0.024	V	(30)
5067.462	19.056 ± 0.026	V	(30)
5069.603	19.420 ± 0.030	V	(30)
5070.570	19.559 ± 0.029	V	(30)
5071.523	19.465 ± 0.032	V	(30)
5072.499	19.709 ± 0.033	V	(30)
5073.556	19.652 ± 0.066	V	(30)
5074.719	19.792 ± 0.038	V	(30)
5075.520	20.053 ± 0.078	V	(30)
5076.487	20.117 ± 0.162	V	(30)

Table 3—Continued

JD (2,450,000+)	Mag	Filter	Notes[a]
5077.474	19.894 ± 0.053	V	(30)
5078.494	20.126 ± 0.075	V	(30)
5079.526	20.298 ± 0.120	V	(30)
5061.541	17.984 ± 0.013	r'	(30)
5063.620	18.159 ± 0.016	r'	(30)
5064.657	18.269 ± 0.015	r'	(30)
5066.588	18.409 ± 0.016	r'	(30)
5067.454	18.499 ± 0.019	r'	(30)
5069.595	18.723 ± 0.019	r'	(30)
5070.562	18.847 ± 0.018	r'	(30)
5071.516	18.869 ± 0.019	r'	(30)
5072.491	18.970 ± 0.020	r'	(30)
5073.548	18.914 ± 0.123	r'	(30)
5074.711	19.081 ± 0.021	r'	(30)
5075.512	19.089 ± 0.034	r'	(30)
5076.479	19.241 ± 0.043	r'	(30)
5077.466	19.308 ± 0.033	r'	(30)
5078.487	19.338 ± 0.034	r'	(30)
5079.518	19.366 ± 0.039	r'	(30)
5061.544	18.028 ± 0.015	i'	(30)
5063.622	18.262 ± 0.018	i'	(30)
5064.659	18.359 ± 0.017	i'	(30)
5066.591	18.555 ± 0.019	i'	(30)
5067.456	18.641 ± 0.025	i'	(30)
5069.598	18.896 ± 0.022	i'	(30)
5070.564	18.945 ± 0.023	i'	(30)
5071.517	18.798 ± 0.025	i'	(30)
5072.494	19.053 ± 0.024	i'	(30)
5073.551	19.486 ± 0.091	i'	(30)
5074.714	19.083 ± 0.027	i'	(30)
5075.514	19.152 ± 0.048	i'	(30)
5076.482	19.230 ± 0.065	i'	(30)
5077.469	19.314 ± 0.034	i'	(30)
5078.489	19.317 ± 0.039	i'	(30)
5079.521	19.344 ± 0.052	i'	(30)
	M31N 2009-08d		
5061.639	17.421 ± 0.139	B	(30)
5063.650	17.819 ± 0.201	B	(30)
5064.648	17.792 ± 0.144	B	(30)
5065.724	17.879 ± 0.188	B	(30)
5066.555	18.368 ± 0.434	B	(30)

Table 3—Continued

JD (2,450,000+)	Mag	Filter	Notes[a]
5067.499	18.391 ± 0.350	B	(30)
5069.658	18.218 ± 0.344	B	(30)
5070.656	18.232 ± 0.259	B	(30)
5071.730	> 15.710	B	(30)
5072.510	18.617 ± 0.414	B	(30)
5073.509	18.553 ± 0.317	B	(30)
5075.531	18.820 ± 0.443	B	(30)
5076.514	18.659 ± 0.368	B	(30)
5077.512	18.637 ± 0.369	B	(30)
5078.478	18.731 ± 0.428	B	(30)
5079.494	18.580 ± 0.312	B	(30)
5061.641	17.808 ± 0.359	V	(30)
5063.653	17.888 ± 0.327	V	(30)
5064.651	17.982 ± 0.284	V	(30)
5065.727	18.182 ± 0.381	V	(30)
5066.558	18.390 ± 0.650	V	(30)
5067.502	> 17.915	V	(30)
5069.661	> 17.288	V	(30)
5070.659	> 17.900	V	(30)
5072.513	18.453 ± 0.522	V	(30)
5073.512	> 18.705	V	(30)
5079.497	19.155 ± 0.804	V	(30)
5095.981	19.9 ± 0.2	V	(13)
4985.974	> 20.2	R	(9)
4988.527	> 19.9	R	(1)
5055.923	17.2 ± 0.1	R	(8)
5063.605	18.2 ± 0.35	R	(22)
5076.478	> 20.0	R	(1)
5095.968	19.46 ± 0.15	R	(13)
5061.633	17.685 ± 0.323	r'	(30)
5063.644	18.122 ± 0.538	r'	(30)
5064.643	17.888 ± 0.346	r'	(30)
5065.719	18.070 ± 0.430	r'	(30)
5066.550	18.066 ± 0.584	r'	(30)
5067.494	> 17.835	r'	(30)
5069.653	> 17.945	r'	(30)
5070.651	> 17.724	r'	(30)
5072.505	18.329 ± 0.493	r'	(30)
5073.504	18.646 ± 0.717	r'	(30)
5075.526	> 18.178	r'	(30)
5077.507	> 18.368	r'	(30)
5078.472	> 18.244	r'	(30)

Table 3—Continued

JD (2,450,000+)	Mag	Filter	Notes[a]
5079.489	18.848 ± 0.755	r'	(30)
	M31N 2009-08e		
5114.306	19.56 ± 0.09	B	(17)
5129.835	20.12 ± 0.1	B	(15)
5092.543	19.09 ± 0.08	V	(17)
5095.981	19.32 ± 0.06	V	(13)
5114.308	19.7 ± 0.12	V	(17)
5129.824	20.15 ± 0.1	V	(15)
5055.923	> 20.3	R	(8)
5063.605	> 20.1	R	(22)
5073.441	17.9 ± 0.1	R	(1)
5074.366	18.0 ± 0.1	R	(1)
5075.384	18.1 ± 0.15	R	(1)
5076.478	17.9 ± 0.1	R	(1)
5080.413	18.1 ± 0.1	R	(1)
5081.393	18.7 ± 0.15	R	(1)
5083.357	18.4 ± 0.2	R	(1)
5084.267	18.2 ± 0.2	R	(1)
5094.451	18.2 ± 0.15	R	(3)
5095.968	18.39 ± 0.04	R	(13)
5114.304	18.9 ± 0.11	R	(17)
5114.486	18.6 ± 0.15	R	(3)
5124.491	18.4 ± 0.15	R	(3)
5129.829	19.11 ± 0.08	R	(15)
5135.632	19.1 ± 0.15	R	(12)
5140.546	18.6 ± 0.25	R	(1)
5141.359	19.0 ± 0.25	R	(1)
5148.536	18.9 ± 0.2	R	(1)
5157.316	18.8 ± 0.3	R	(24)
5162.281	19.3 ± 0.25	R	(5)
5173.177	19.7 ± 0.3	R	(1)
5181.226	> 19.8	R	(1)
5184.717	19.9 ± 0.2	R	(19)
5199.299	20.0 ± 0.15	R	(12)
5227.345	20.7 ± 0.25	R	(12)
5228.383	20.6 ± 0.25	R	(12)
	M31N 2009-09a		
5092.506	19.02 ± 0.05	V	(17)

Table 3—Continued

JD (2,450,000+)	Mag	Filter	Notes[a]
5080.413	17.5 ± 0.15	R	(1)
5081.393	17.9 ± 0.1	R	(1)
5083.357	18.1 ± 0.15	R	(1)
5092.506	18.21 ± 0.03	R	(17)
5095.993	18.18 ± 0.04	R	(13)
5148.578	18.0 ± 0.3	R	(1)
5162.513	19.0 ± 0.25	R	(5)
5173.203	19.3 ± 0.2	R	(1)
5226.321	19.7 ± 0.15	R	(12)
5227.306	19.7 ± 0.15	R	(12)
5228.284	19.8 ± 0.15	R	(12)
	M31N 2009-10a		
5114.341	18.59 ± 0.10	B	(17)
5117.718	18.344 ± 0.114	B	(30)
5117.501	18.403 ± 0.029	B	(30)
5118.647	18.705 ± 0.034	B	(30)
5119.495	18.919 ± 0.030	B	(30)
5120.389	19.119 ± 0.033	B	(30)
5127.496	19.888 ± 0.048	B	(30)
5128.375	19.867 ± 0.041	B	(30)
5129.515	20.258 ± 0.057	B	(30)
5130.468	20.522 ± 0.054	B	(30)
5131.408	20.997 ± 0.137	B	(30)
5132.359	> 21.495	B	(30)
5114.361	18.33 ± 0.09	V	(17)
5117.721	18.574 ± 0.094	V	(30)
5117.505	18.367 ± 0.020	V	(30)
5118.650	18.710 ± 0.024	V	(30)
5119.498	18.950 ± 0.023	V	(30)
5120.392	19.113 ± 0.025	V	(30)
5127.499	19.776 ± 0.032	V	(30)
5128.378	19.922 ± 0.035	V	(30)
5129.518	20.252 ± 0.041	V	(30)
5130.472	20.743 ± 0.169	V	(30)
5131.412	> 19.771	V	(30)
5114.340	17.81 ± 0.07	R	(17)
5162.549	> 19.9	R	(5)
	M31N 2009-10b		
5117.487	16.260 ± 0.049	B	(30)

Table 3—Continued

JD (2,450,000+)	Mag	Filter	Notes[a]
5117.711	15.759 ± 0.042	B	(30)
5118.603	15.521 ± 0.042	B	(30)
5119.488	15.316 ± 0.042	B	(30)
5120.370	15.242 ± 0.042	B	(30)
5124.457	16.98 ± 0.04	B	(18)
5127.489	18.338 ± 0.066	B	(30)
5128.368	18.481 ± 0.044	B	(30)
5129.500	18.659 ± 0.077	B	(30)
5130.475	18.827 ± 0.044	B	(30)
5131.393	18.892 ± 0.110	B	(30)
5132.352	19.223 ± 0.053	B	(30)
5134.341	19.108 ± 0.053	B	(30)
5135.354	19.444 ± 0.049	B	(30)
5136.461	19.286 ± 0.065	B	(30)
5137.400	19.649 ± 0.065	B	(30)
5138.449	> 19.033	B	(30)
5139.652	19.411 ± 0.157	B	(30)
5140.529	20.002 ± 0.056	B	(30)
5142.515	19.853 ± 0.172	B	(30)
5143.620	> 19.917	B	(30)
5146.507	> 19.702	B	(30)
5117.714	15.662 ± 0.013	V	(30)
5117.490	16.085 ± 0.012	V	(30)
5118.606	15.424 ± 0.012	V	(30)
5119.491	15.141 ± 0.012	V	(30)
5120.374	15.003 ± 0.011	V	(30)
5124.458	16.46 ± 0.03	V	(18)
5127.493	18.004 ± 0.045	V	(30)
5128.371	18.187 ± 0.016	V	(30)
5129.503	18.489 ± 0.058	V	(30)
5129.824	18.60 ± 0.03	V	(15)
5130.479	18.399 ± 0.020	V	(30)
5131.397	18.903 ± 0.110	V	(30)
5132.355	18.998 ± 0.065	V	(30)
5134.345	19.101 ± 0.025	V	(30)
5135.357	19.275 ± 0.027	V	(30)
5136.465	18.963 ± 0.128	V	(30)
5137.403	18.520 ± 0.173	V	(30)
5138.452	19.170 ± 0.286	V	(30)
5139.656	19.283 ± 0.130	V	(30)
5140.532	19.766 ± 0.044	V	(30)
5142.519	19.628 ± 0.162	V	(30)
5143.623	> 19.170	V	(30)
5144.343	> 18.793	V	(30)

Table 3—Continued

JD (2,450,000+)	Mag	Filter	Notes[a]
4985.974	> 20.2	R	(9)
4988.527	> 20.0	R	(1)
5105.262	> 19.9	R	(3)
5114.486	18.9 ± 0.15	R	(3)
5124.460	15.76 ± 0.04	R	(18)
5124.491	15.78 ± 0.04	R	(26)
5129.829	17.40 ± 0.03	R	(15)
5129.835	18.89 ± 0.04	B	(15)
5135.257	17.6 ± 0.2	R	(3)
5135.632	17.92 ± 0.06	R	(12)
5140.546	18.4 ± 0.2	R	(1)
5141.359	18.1 ± 0.2	R	(1)
5148.536	18.3 ± 0.15	R	(1)
5157.316	18.6 ± 0.25	R	(24)
5162.281	18.8 ± 0.2	R	(5)
5173.177	19.1 ± 0.25	R	(1)
5181.226	19.1 ± 0.2	R	(1)
5199.299	19.73 ± 0.1	R	(12)
5227.345	20.0 ± 0.15	R	(12)
5228.383	20.0 ± 0.15	R	(12)
	M31N 2009-10c		
5114.306	18.06 ± 0.04	B	(17)
5117.725	17.155 ± 0.023	B	(30)
5117.494	17.048 ± 0.017	B	(30)
5118.654	17.283 ± 0.024	B	(30)
5119.471	16.771 ± 0.019	B	(30)
5120.382	17.155 ± 0.017	B	(30)
5127.511	16.427 ± 0.011	B	(30)
5128.361	16.632 ± 0.037	B	(30)
5129.507	15.977 ± 0.030	B	(30)
5130.461	16.311 ± 0.028	B	(30)
5131.401	16.609 ± 0.013	B	(30)
5132.366	16.116 ± 0.013	B	(30)
5134.356	17.118 ± 0.016	B	(30)
5135.340	16.604 ± 0.011	B	(30)
5136.476	16.958 ± 0.016	B	(30)
5137.340	16.935 ± 0.061	B	(30)
5138.469	17.301 ± 0.037	B	(30)
5139.574	17.429 ± 0.020	B	(30)
5140.627	17.629 ± 0.025	B	(30)
5142.540	17.662 ± 0.110	B	(30)
5143.613	18.082 ± 0.207	B	(30)

Table 3—Continued

JD (2,450,000+)	Mag	Filter	Notes[a]
5144.325	> 16.980	B	(30)
5145.520	> 17.737	B	(30)
5146.619	> 18.901	B	(30)
5147.498	18.559 ± 0.049	B	(30)
5114.308	17.69 ± 0.07	V	(17)
5117.728	17.452 ± 0.030	V	(30)
5117.497	17.207 ± 0.056	V	(30)
5118.657	17.437 ± 0.090	V	(30)
5119.475	17.124 ± 0.039	V	(30)
5120.385	17.336 ± 0.020	V	(30)
5127.515	16.513 ± 0.062	V	(30)
5128.364	17.116 ± 0.017	V	(30)
5129.511	16.413 ± 0.037	V	(30)
5130.464	16.985 ± 0.015	V	(30)
5131.404	17.026 ± 0.083	V	(30)
5132.369	16.673 ± 0.013	V	(30)
5134.359	17.380 ± 0.085	V	(30)
5135.343	16.998 ± 0.016	V	(30)
5136.479	17.425 ± 0.025	V	(30)
5137.343	17.537 ± 0.026	V	(30)
5138.472	> 17.347	V	(30)
5139.578	17.931 ± 0.038	V	(30)
5140.630	18.082 ± 0.042	V	(30)
5142.543	18.013 ± 0.148	V	(30)
5143.616	> 17.542	V	(30)
5144.328	> 17.223	V	(30)
5114.304	17.50 ± 0.08	R	(17)
5114.486	17.7 ± 0.3	R	(3)
5124.491	16.4 ± 0.15	R	(3)
5135.257	16.7 ± 0.3	R	(3)
5135.632	17.03 ± 0.1	R	(12)
5140.546	17.4 ± 0.25	R	(1)
5141.359	17.6 ± 0.2	R	(1)
	M31N 2009-11a		
5142.606	18.504 ± 0.078	B	(30)
5142.522	18.411 ± 0.073	B	(30)
5143.606	18.858 ± 0.132	B	(30)
5144.311	18.533 ± 0.180	B	(30)
5145.513	19.017 ± 0.038	B	(30)
5146.498	19.211 ± 0.211	B	(30)
5147.477	19.119 ± 0.057	B	(30)

Table 3—Continued

JD (2,450,000+)	Mag	Filter	Notes[a]
5149.358	19.325 ± 0.025	B	(30)
5150.410	19.610 ± 0.086	B	(30)
5151.559	19.356 ± 0.159	B	(30)
5154.592	19.705 ± 0.043	B	(30)
5155.334	19.532 ± 0.098	B	(30)
5156.309	19.550 ± 0.184	B	(30)
5157.572	19.840 ± 0.184	B	(30)
5159.438	19.810 ± 0.110	B	(30)
5161.539	20.012 ± 0.239	B	(30)
5164.398	21.234 ± 0.317	B	(30)
5168.433	> 20.525	B	(30)
5169.522	> 20.686	B	(30)
5142.609	18.146 ± 0.049	V	(30)
5143.609	18.206 ± 0.088	V	(30)
5144.315	18.801 ± 0.165	V	(30)
5145.516	18.639 ± 0.216	V	(30)
5146.501	18.686 ± 0.169	V	(30)
5147.480	18.835 ± 0.050	V	(30)
5149.361	19.187 ± 0.023	V	(30)
5150.413	19.482 ± 0.025	V	(30)
5151.563	19.392 ± 0.119	V	(30)
5154.595	19.310 ± 0.141	V	(30)
5155.338	19.563 ± 0.030	V	(30)
5156.312	19.557 ± 0.130	V	(30)
5157.575	19.885 ± 0.055	V	(30)
5159.441	19.896 ± 0.086	V	(30)
5161.542	20.160 ± 0.063	V	(30)
5164.401	20.249 ± 0.059	V	(30)
5168.436	> 19.597	V	(30)
5169.525	19.910 ± 0.134	V	(30)
5140.463	17.6 ± 0.1	R	(1)
5141.221	17.74 ± 0.05	R	(5)
5148.564	18.4 ± 0.25	R	(1)
5162.534	19.4 ± 0.3	R	(5)
5160.803	19.71 ± 0.08	r'	(10)
5209.656	21.5 ± 0.15	r'	(16)
5160.806	20.35 ± 0.07	g'	(10)
M31N 2009-11b (recurrent nova)			
5154.412	19.994 ± 0.119	B	(30)
5156.323	19.511 ± 0.120	B	(30)

Table 3—Continued

JD (2,450,000+)	Mag	Filter	Notes[a]
5159.406	19.859 ± 0.043	B	(30)
5162.503	20.347 ± 0.123	B	(30)
5168.480	> 19.123	B	(30)
5169.340	> 19.175	B	(30)
5170.551	19.519 ± 0.098	B	(30)
5171.365	19.439 ± 0.037	B	(30)
5172.330	19.659 ± 0.036	B	(30)
5154.415	20.079 ± 0.139	V	(30)
5156.326	19.299 ± 0.033	V	(30)
5159.409	19.972 ± 0.040	V	(30)
5162.507	20.339 ± 0.055	V	(30)
5168.483	> 18.741	V	(30)
5169.343	19.372 ± 0.145	V	(30)
5170.554	19.482 ± 0.039	V	(30)
5171.368	19.490 ± 0.086	V	(30)
5172.333	19.564 ± 0.032	V	(30)
5148.536	18.9 ± 0.15	R	(1)
5135.632	18.6 ± 0.1	R	(12)
5162.281	19.3 ± 0.25	R	(5)
5162.513	19.6 ± 0.3	R	(5)
5173.177	19.3 ± 0.2	R	(1)
5173.203	19.2 ± 0.2	R	(1)
5181.226	19.7 ± 0.25	R	(1)
5199.299	20.05 ± 0.1	R	(12)
5227.306	20.0 ± 0.15	R	(12)
5228.284	20.0 ± 0.15	R	(12)
5209.616	20.9 ± 0.15	g'	(16)
5207.591	21.2 ± 0.1	g'	(16)
5207.599	20.66 ± 0.1	r'	(16)
5209.621	20.6 ± 0.1	r'	(16)
	M31N 2009-11c		
5145.323	19.144 ± 0.029	B	(30)
5146.516	18.614 ± 0.023	B	(30)
5147.487	18.203 ± 0.018	B	(30)
5148.383	17.453 ± 0.016	B	(30)
5149.503	18.981 ± 0.022	B	(30)
5150.403	18.864 ± 0.022	B	(30)
5154.422	18.636 ± 0.019	B	(30)
5156.337	18.650 ± 0.021	B	(30)

Table 3—Continued

JD (2,450,000+)	Mag	Filter	Notes[a]
5161.546	18.883 ± 0.027	B	(30)
5162.535	18.775 ± 0.026	B	(30)
5168.457	19.075 ± 0.256	B	(30)
5169.333	> 18.858	B	(30)
5170.584	19.676 ± 0.056	B	(30)
5171.373	19.393 ± 0.027	B	(30)
5172.363	19.375 ± 0.028	B	(30)
5173.509	19.635 ± 0.042	B	(30)
5145.326	18.409 ± 0.043	V	(30)
5146.519	17.879 ± 0.040	V	(30)
5147.490	17.497 ± 0.039	V	(30)
5148.386	16.770 ± 0.039	V	(30)
5149.506	18.122 ± 0.040	V	(30)
5150.406	18.178 ± 0.040	V	(30)
5154.425	17.959 ± 0.040	V	(30)
5156.340	18.172 ± 0.040	V	(30)
5161.549	18.710 ± 0.044	V	(30)
5162.538	18.292 ± 0.042	V	(30)
5168.461	18.196 ± 0.138	V	(30)
5169.336	18.742 ± 0.280	V	(30)
5170.587	19.065 ± 0.053	V	(30)
5171.375	18.870 ± 0.044	V	(30)
5172.366	19.070 ± 0.044	V	(30)
5173.512	19.392 ± 0.062	V	(30)
5135.632	> 21.4	R	(12)
5140.463	> 20.3	R	(1)
5141.359	19.9 ± 0.3	R	(1)
5148.536	17.03 ± 0.1	R	(1)
5154.424	17.8 ± 0.15	R	(7)
5157.316	17.9 ± 0.1	R	(24)
5158.542	17.9 ± 0.1	R	(1)
5161.164	18.4 ± 0.15	R	(7)
5162.281	18.1 ± 0.15	R	(5)
5162.513	18.2 ± 0.15	R	(5)
5168.173	18.3 ± 0.1	R	(7)
5169.202	18.6 ± 0.2	R	(1)
5173.177	18.6 ± 0.15	R	(1)
5173.192	18.7 ± 0.15	R	(1)
5173.203	18.5 ± 0.15	R	(1)
5181.226	18.9 ± 0.15	R	(1)
5184.717	19.22 ± 0.1	R	(19)
5227.306	> 22.0	R	(12)

Table 3—Continued

JD (2,450,000+)	Mag	Filter	Notes[a]
5156.756	18.86 ± 0.08	g'	(10)
5156.759	18.32 ± 0.05	r'	(10)
5209.631	> 21.1	r'	(16)
	M31N 2009-11d		
5156.330	17.278 ± 0.016	B	(30)
5157.579	18.659 ± 0.102	B	(30)
5159.445	18.123 ± 0.019	B	(30)
5161.532	18.554 ± 0.023	B	(30)
5168.464	> 19.753	B	(30)
5169.515	19.699 ± 0.040	B	(30)
5170.529	20.139 ± 0.063	B	(30)
5171.358	20.038 ± 0.035	B	(30)
5172.556	19.787 ± 0.112	B	(30)
5173.365	19.997 ± 0.032	B	(30)
5176.376	> 19.722	B	(30)
5156.333	17.050 ± 0.012	V	(30)
5157.582	18.568 ± 0.101	V	(30)
5159.448	18.047 ± 0.014	V	(30)
5161.535	18.288 ± 0.075	V	(30)
5168.468	> 19.415	V	(30)
5169.518	20.034 ± 0.139	V	(30)
5170.532	20.696 ± 0.077	V	(30)
5171.361	19.912 ± 0.098	V	(30)
5172.559	20.501 ± 0.055	V	(30)
5173.368	20.375 ± 0.035	V	(30)
5176.378	20.523 ± 0.077	V	(30)
5157.299	17.26 ± 0.10	R	(24)
5158.560	17.3 ± 0.2	R	(1)
5162.525	17.6 ± 0.15	R	(5)
5168.505	18.1 ± 0.2	R	(7)
5173.192	18.7 ± 0.15	R	(1)
5227.379	> 21.5	R	(12)
5156.787	16.53 ± 0.10	g'	(10)
5207.619	21.3 ± 0.1	g'	(16)
5156.785	16.43 ± 0.08	r'	(10)
5207.626	21.3 ± 0.1	r'	(16)
	M31N 2009-11e		

Table 3—Continued

JD (2,450,000+)	Mag	Filter	Notes[a]
5161.575	18.122 ± 0.074	B	(30)
5162.524	17.445 ± 0.041	B	(30)
5168.445	17.496 ± 0.018	B	(30)
5169.326	17.279 ± 0.079	B	(30)
5170.572	17.110 ± 0.014	B	(30)
5171.379	16.869 ± 0.011	B	(30)
5172.355	16.982 ± 0.011	B	(30)
5173.411	18.485 ± 0.064	B	(30)
5176.408	18.423 ± 0.033	B	(30)
5161.578	18.254 ± 0.066	V	(30)
5162.528	17.786 ± 0.014	V	(30)
5168.448	17.810 ± 0.061	V	(30)
5169.329	17.590 ± 0.104	V	(30)
5170.575	17.418 ± 0.038	V	(30)
5171.382	17.073 ± 0.010	V	(30)
5173.415	19.005 ± 0.094	V	(30)
5176.412	19.185 ± 0.269	V	(30)
5148.536	> 20.6	R	(1)
5157.316	17.8 ± 0.15	R	(24)
5158.542	17.0 ± 0.1	R	(1)
5161.164	17.7 ± 0.1	R	(7)
5162.281	17.4 ± 0.1	R	(5)
5162.513	17.5 ± 0.1	R	(5)
5168.173	17.5 ± 0.1	R	(7)
5169.202	17.2 ± 0.2	R	(1)
5173.177	18.1 ± 0.1	R	(1)
5173.203	18.1 ± 0.1	R	(1)
5181.226	18.5 ± 0.15	R	(1)
5184.717	18.96 ± 0.09	R	(19)
5186.730	18.8 ± 0.25	R	(20)
5199.299	19.09 ± 0.08	R	(12)
5227.345	19.92 ± 0.10	R	(12)
5228.383	19.40 ± 0.10	R	(12)
5157.691	17.80 ± 0.09	g'	(10)
5158.715	17.29 ± 0.10	g'	(10)
5207.591	19.10 ± 0.09	g'	(16)
5210.592	19.65 ± 0.10	g'	(16)
5157.688	17.80 ± 0.04	r'	(10)
5158.713	17.33 ± 0.03	r'	(10)
5207.599	18.91 ± 0.08	r'	(16)

Table 3—Continued

JD (2,450,000+)	Mag	Filter	Notes[a]
5210.598	19.45 ± 0.09	r'	(16)

[a]Observers: (1) K. Hornoch, Ondřejov 0.65-m; (2) K. Hornoch, Lelekovice 0.35-m; (3) P. Kušnirák, Ondřejov 0.65-m; (4) M. Wolf, Ondřejov 0.65-m; (5) K. Hornoch & M. Wolf, Ondřejov 0.65-m; (6) M. Wolf i& P. Zasche, Ondřejov 0.65-m; (7) K. Hornoch & P. Zasche, Ondřejov 0.65-m; (8) P. Zasche, San Pedro Mártir 0.84-m; (9) O. Pejcha, MDM 1.3-m; (10) O. Pejcha, MDM 2.4-m; (11) K. Hornoch & P. Šedinová, Ondřejov 0.65-m; (12) P. Kubánek, J. Gorosabel i& M. Jelínek, Calar Alto 1.23-m; (13) P. Kubánek, MDM 2.4-m; (14) P. Garnavich & A. Karska, MGIO 1.83-m VATT; (15) P. Garnavich, K. Thorne & K. Morhig, MGIO 1.83-m VATT; (16) J. Prieto & R. Khan, MDM 2.4-m; (17) A. Valeev & O. Sholukhova, SAO 6-m; (18) V. L. Afanasiev & S. N. Dodonov, SAO 6-m; (19) T. Farnham & B. Mueller, KPNO 2.1-m; (20) N. Samarasinha & B. Mueller, KPNO 2.1-m; (21) M. Burleigh & S. Casewell, La Palma 2.5-m INT; (22) A. Galád, AGO Modra 0.60-m; (23) P. Cagaš, Zlín 0.26-m; (24) K. Hornoch & P. Kušnirák, Ondřejov 0.65-m; (25) P. Kušnirák & T. Henych, Ondřejov 0.65-m; (26) P. Kušnirák & Z. Bardon, Ondřejov 0.65-m; (27) K. Hornoch & M. Tukinská, Ondřejov 0.65-m; (28) P. Zasche & Ondřejov, 0.65-m; (29) Darnley et al. 2004; La Palma 2.5-m INT; (30) La Palma 2.0-m LT; (31) Mt. Haleakala 2.0-m FTN; (32) P. Kušnirák, L. Šarounová & M. Wolf, Ondřejov 0.65-m; (33) P. Garnavich, MGIO 1.83-m VATT; (34) P. Garnavich & B. Tucker, MGIO 1.83-m VATT; (35) P. Garnavich & C. Kennedy, MGIO 1.83-m VATT; (36) P. Garnavich & J. Gallagher, MGIO 1.83-m VATT; (37) P. Garnavich, KPNO 3.5-m WIYN; (38) D. Mackey, La Palma 2.5-m INT.

Table 4. Full Spectroscopic Sample of M31 Novae

Nova	$\Delta\alpha\ cos\delta$ (′)	$\Delta\delta$ (′)	a (′)	Discovery mag (Filter)	Type	References[a]
M31N 1981-09a	−4.76	−2.89	5.67	16.4(H)	Fe II	1
M31N 1981-09b	−0.65	2.10	2.96	14.9(H)	Fe II	1
M31N 1981-09c	0.78	2.87	3.43	15.0(H)	Fe II	1
M31N 1981-09d	4.11	−2.16	8.07	15.8(H)	Fe II	1
M31N 1986-08a	−4.35	−1.64	4.98	16.3(H)	Fe II	2
M31N 1987-09a	7.80	2.13	10.57	19.4(B)	Fe II	2
M31N 1987-10a	−0.33	1.75	2.28	18.4(B)	Fe II	2
M31N 1989-08a	6.47	−0.29	10.36	17.9(B)	He/N	2
M31N 1989-08b	−1.01	0.00	1.10	19.3(B)	Fe II	2
M31N 1989-08c	−5.22	−4.41	6.84	17.9(B)	Fe II	2
M31N 1989-09a	2.15	4.05	5.06	15.5(H)	Fe II	2
M31N 1989-10a	0.36	3.10	3.91	17.6(B)	Fe II	2
M31N 1990-10b	−1.53	−4.32	5.44	17.6(B)	Fe II	3
M31N 1992-11b	3.07	−1.49	5.04	17.2(V)	Fe II	3
M31N 1993-06a	0.91	1.31	1.64	15.8(R)	Fe II:	3
M31N 1993-08a	0.14	−1.70	1.64	15.8(R)	He/N:	3
M31N 1993-10g	0.63	1.87	2.17	16.7(H)	Fe II	3
M31N 1993-11c	1.08	1.32	1.73	15.8(H)	Fe II:	3
M31N 1998-09d	0.43	−1.33	1.78	16.5(B)	Fe II	3
M31N 1999-06a	0.97	−1.05	1.89	17.8(R)	Fe II	3
M31N 1999-08f	−0.61	3.04	4.44	17.0(w)	Fe II:	3
M31N 1999-10a	1.00	0.39	1.10	17.5(w)	Fe II:	3
M31N 2001-10a	3.56	−3.96	10.81	17.0(R)	Fe II	3
M31N 2001-12a	−0.55	0.26	0.68	15.5(R)	Fe II	3
M31N 2002-01b	−1.97	2.25	4.60	16.8(R)	He/N:	3
M31N 2002-08a	−2.53	−9.93	14.01	17.1(R)	Fe II:	3
M31N 2004-08b	7.98	0.54	12.60	17.3(R)	Fe II	3
M31N 2004-09a	−0.77	−1.44	1.72	17.5(R)	Fe II	3
M31N 2004-11a	−0.29	2.32	3.03	16.5(R)	Fe II	3
M31N 2004-11b	4.34	1.93	4.97	16.6(R)	He/N:	3
M31N 2005-01a	−3.00	0.46	3.98	15.0(R)	Fe II	3
M31N 2005-06d	26.35	17.61	44.21	15.7(w)	He/N	4
M31N 2005-07a	1.21	4.52	5.85	17.4(R)	FeII:	3
M31N 2005-09a	1.48	3.84	4.76	16.7(R)	Fe II	4
M31N 2005-09b	−44.77	−56.00	71.73	16.5(w)	Fe II[b]	4
M31N 2005-09c	−43.70	−48.34	66.76	16.0(w)	Fe II	5
M31N 2006-06a	5.16	−2.40	11.09	17.5(R)	Fe II	4
M31N 2006-09c	−0.37	−7.39	11.61	16.8(w)	Fe II	3
M31N 2006-10a	−11.50	−4.36	17.31	18.7(R)	Fe II	3
M31N 2006-10b	−37.25	−24.81	63.14	16.4(w)	Hy	3
M31N 2006-11a	2.35	−9.84	20.46	17.3(w)	Fe II	3
M31N 2006-12a	−4.38	−2.39	5.11	17.8(R)	Fe II	3
M31N 2006-12b	−6.26	−8.41	10.88	18.0(R)	Fe II	3
M31N 2007-02a	−19.95	−31.22	40.21	16.3(w)	Fe II	3
M31N 2007-02b	−12.04	−1.57	21.34	16.7(R)	Fe II:	3,6

Table 4—Continued

Nova	$\Delta\alpha\ cos\delta$ (′)	$\Delta\delta$ (′)	a (′)	Discovery mag (Filter)	Type	References[a]
M31N 2007-06b	−2.12	−15.71	26.20	16.8(w)	He/N	3,7
M31N 2007-07b	0.29	1.92	2.26	17.7(R)	Fe II	8
M31N 2007-07c	3.56	−1.26	5.55	15.8(R)	He/N	8,9
M31N 2007-07e	−0.20	1.59	2.00	18.1(R)	Fe II	8
M31N 2007-07f	−45.77	−22.95	81.74	17.4(w)	Fe II	10
M31N 2007-08a	−20.78	−22.25	30.49	17.6(w)	Fe II:	8
M31N 2007-08d	−36.91	−46.74	59.56	18.1(R)	Fe II	3
M31N 2007-10a	2.19	−12.78	27.57	16.0(w)	He/Nn	3,11
M31N 2007-10b	8.48	1.09	12.91	17.8(w)	He/Nn	12
M31N 2007-11b	12.94	−12.52	59.72	18.6(R)	He/Nn	3,13,14
M31N 2007-11c	3.72	−0.24	4.77	17.4(R)	Fe II	14,15
M31N 2007-11d	24.34	21.60	34.03	14.9(w)	Fe II	3,16
M31N 2007-11e	34.06	46.07	57.52	16.4(w)	Fe II	3,17
M31N 2007-12a	14.79	22.57	28.53	17.8(w)	Fe II	3
M31N 2007-12b	6.70	−2.37	14.79	16.1(w)	He/N	3,18
M31N 2007-12c	27.26	4.08	66.22	16.4(w)	Fe II	19
M31N 2007-12d	−9.30	−6.35	11.92	17.2(R)	He/N	3
M31N 2008-05c	5.20	3.12	6.18	17.0(R)	Fe II	20
M31N 2008-06b	−3.11	−1.34	3.56	15.9(R)	He/N	21
M31N 2008-07a	−1.87	2.12	4.34	18.3(R)	Fe II	22
M31N 2008-07b	8.08	−6.08	26.01	19.0(g)	Fe II	23
M31N 2008-08a	0.12	0.98	1.09	16.8(R)	Fe II	24,25
M31N 2008-08b	1.51	0.07	1.69	16.4(R)	He/N	24,25
M31N 2008-08c	−0.72	10.15	18.72	16.8(R)	Fe II	25
M31N 2008-08d	33.62	106.41	109.45	18.1(w)	Fe II	26
M31N 2008-09a	−10.85	−8.26	14.26	18.1(g)	Fe II	3
M31N 2008-09c	1.33	−14.25	30.22	17.6(g)	Fe II	3
M31N 2008-10a	9.51	38.60	65.42	17.1(w)	Fe II	3
M31N 2008-10b	3.40	−1.98	6.19	18.3(R)	Fe II	25,27
M31N 2008-11a	−13.58	−10.11	18.51	16.5(R)	He/N	3
M31N 2008-12b	3.85	1.72	4.43	16.8(w)	Fe II	28
M31N 2009-01a	22.44	7.39	48.17	18.5(w)	Fe II	3
M31N 2009-02a	11.11	20.52	26.38	16.8(w)	Fe II	3
M31N 2009-08a	2.57	1.35	3.00	17.2(H)	Fe II	29
M31N 2009-08b	15.93	32.73	45.52	17.1(w)	Fe II	30
M31N 2009-08d	0.45	−0.52	0.81	17.2(R)	Fe II	31
M31N 2009-08e	−1.54	1.89	3.54	17.8(w)	Fe II	32
M31N 2009-09a	−3.45	−12.13	17.38	17.6(w)	Fe II	33
M31N 2009-10a	27.78	48.61	61.67	17.1(w)	Fe II	34
M31N 2009-10b	−4.43	0.60	6.17	14.7(R)	Fe II	35
M31N 2009-10c	0.26	−0.19	0.37	17.2(H)	Fe II	36
M31N 2009-11a	3.81	24.99	48.41	17.6(R)	Fe II	37
M31N 2009-11b	−0.89	−7.09	10.56	18.4(R)	Fe II	23,38
M31N 2009-11c	4.91	−3.83	12.92	17.0(R)	Fe II	39
M31N 2009-11d	17.37	2.79	35.48	16.4(r)	Fe II	40

Table 4—Continued

Nova	$\Delta\alpha\ cos\delta$ (′)	$\Delta\delta$ (′)	a (′)	Discovery mag (Filter)	Type	References[a]
M31N 2009-11e	−1.70	−3.16	3.86	17.4(R)	Fe II	41

[a]REFERENCES: (1) Ciardullo et al. (1983); (2) Tomaney & Shafter (1992); (3) this work; (4) Pietsch et al. (2005); (5) Hatzidimitriou et al. (2007); (6) Pietsch et al. (2007a); (7) Shafter & Quimby (2007); (8) Barsukova et al. (2007); (9) Rau et al. (2007a); (10) Quimby (2007, private communication); (11) Gal-Yam & Quimby (2007); (12) Rau et al. (2007b); (13) Rau (2007); (14) Barsukova et al. (2007b); (15) Ciroi (2007); (16) Shafter et al. (2009); (17) Di Mille et al. (2007); (18) Bode et al. (2009); (19) Rau & Cenko (2007); (20) Rau et al. (2008) (21) Reig et al. (2008); (22) Barsukova et al. (2008); (23) Kasliwal et al. (2011); (24) Di Mille et al. (2008a); (25) Di Mille et al. (2010); (26) Chornock et al. (2008); (27) Di Mille et al. (2008b); (28) Kasliwal et al. (2008); (29) Valeev et al. (2009); (30) Rodríguez-Gil et al. (2009); (31) Di Mille et al. (2009a); (32) Medvedev et al. (2000); (33) Barsukova et al. (2009a); (34) Fabrika et al. (2009a); (35) Barsukova et al. (2009b); (36) Fabrika et al. (2009b); (37) Hornoch et al. (2009a); (38) Kasliwal (2009); (39) Hornoch et al. (2009b); (40) Hornoch et al. (2009c); (41) Hornoch et al. (2009d)

[b]The line with of 4400 km s^{-1} reported by D. C. Leonard referred to an estimate of the full width at zero intensity, not the FWHM. Analysis of the original spectrum reveals the object to be a classic Fe II nova

Table 5. Balmer Emission-Line Properties

Nova	EW (Å)		FWHM (km s^{-1})	
	Hβ	Hα	Hβ	Hα
M31N 1990-10b	−267	−541	1600	1550
M31N 1992-11b	−250	−1219	1670	1740
M31N 1993-06a	−36	−392	1840	1770
M31N 1993-08a	...	...	...	4350
M31N 1993-10g[a]	−87	−324	1630	1680
M31N 1993-11c[a]	−118	−828	1450	1560
M31N 1998-09d	−92	−323	1720	1840
M31N 1999-06a	−322	−1200	1110	920
M31N 1999-08f	−135	−704	1640	1690
M31N 1999-10a	−230	−565	1780	1930
M31N 2001-10a	−279	−945	1540	1540
M31N 2001-12a	...	−1500	...	1310
M31N 2002-01b	...	−760	...	3430
M31N 2002-08a	−94	−470	1360	1320
M31N 2004-08b	−90	−410	1970	1830
M31N 2004-09a	−54	−250	2000	1880
M31N 2004-11a	−175	−830	1230	1580
M31N 2004-11b	−80	−1020	2500	2620
M31N 2005-01a	−50	−107	1810	1680
M31N 2005-07a	...	−120	...	1100
M31N 2006-09c	−127	−470	1910	1920
M31N 2006-10a	−44	−90	950	810
M31N 2006-10b	−64	−102	3330	3090
	−133	−2130	3030	3562
M31N 2006-11a	−35	−57	1420	1120
M31N 2006-12a	−107	−330	1850	1760
M31N 2006-12b	−86	−226	1230	1020
M31N 2007-02a	−35	−61	1530	1310
M31N 2007-02b	−39	−304	1460	1910
M31N 2007-06b	−51	−168	2940	2870
M31N 2007-08d	−68	−284	1160	1180
M31N 2007-10a	−37	−154	470	500
M31N 2007-11b	−147	−535	1480	1290
M31N 2007-11c	−75	−137	1950	1700
M31N 2007-11d	−11	−16	1630	1550
	−297	−1223	2060	2260
M31N 2007-11e	−137	−306	1750	1600
M31N 2007-11g	−18	−13	340	300
M31N 2007-12a	−159	−309	2050	1850
M31N 2007-12b	−247	−990	4070	4080
M31N 2007-12d	−271	−1210	5220	4980
M31N 2008-08d	−130	−440	1150	1050
	−63	−634	1360	1480
M31N 2008-09a	−113	−262	1540	1460
M31N 2008-09c	−16	−23	1590	1010

Table 5—Continued

Nova	EW (Å)		FWHM (km s^{-1})	
	Hβ	Hα	Hβ	Hα
M31N 2008-10a	−97	−300	1390	1270
M31N 2008-10b	−2.8	−19	660	640
	−24	−95	1220	950
M31N 2008-11a	−188	−636	4510	4350
	−33	−370	1460	3160
M31N 2009-01a	−5	−25	560	550
M31N 2009-02a	−4	−15	1280	1410

[a]Due to ambiguity in the data logs from November 1993, it is possible that the data for these two novae are reversed.

Table 6. Light-Curve Parameters

Nova	Filter	$M_{\max}$	Fade Rate (mag day^{-1})	t_2 (days)
M31N 1999-08f	r'	-7.54 ± 0.11	0.063 ± 0.002	31.7 ± 0.9
M31N 2001-10a	r'	-7.54 ± 0.11	0.040 ± 0.004	50.2 ± 4.9
M31N 2002-08a	R	-7.49 ± 0.20	0.044 ± 0.005	45.8 ± 5.1
M31N 2004-08b	R	-7.24 ± 0.25	0.038 ± 0.002	52.0 ± 3.3
M31N 2004-09a	R	-7.10 ± 0.20	0.056 ± 0.006	35.5 ± 3.7
M31N 2004-11a	R	-8.04 ± 0.25	0.105 ± 0.010	19.1 ± 1.9
M31N 2004-11b	R	-7.94 ± 0.20	0.042 ± 0.002	47.2 ± 2.6
M31N 2005-01a	R	-9.59 ± 0.17	0.105 ± 0.009	19.0 ± 1.6
M31N 2005-07a	R	-7.16 ± 0.25	0.017 ± 0.003	120.9 ± 23.5
M31N 2006-06a	R	-7.04 ± 0.11	0.030 ± 0.006	67.3 ± 13.2
M31N 2006-09c	R	-7.88 ± 0.14	0.087 ± 0.006	23.1 ± 1.6
M31N 2006-10a	B	-7.54 ± 0.11	0.035 ± 0.002	56.7 ± 3.1
...	V	-7.67 ± 0.11	0.035 ± 0.002	57.5 ± 3.1
...	R	-6.64 ± 0.20	0.021 ± 0.005	94.3 ± 20.6
M31N 2006-10b	B	-7.85 ± 0.11	0.287 ± 0.018	7.0 ± 0.4
...	V	-7.98 ± 0.11	0.345 ± 0.018	5.8 ± 0.3
M31N 2006-11a	R	-8.54 ± 0.20	0.070 ± 0.006	28.7 ± 2.6
M31N 2006-12a	R	-7.24 ± 0.25	0.057 ± 0.007	34.9 ± 4.5
M31N 2007-02b	R	-7.88 ± 0.20	0.059 ± 0.006	34.1 ± 3.6
M31N 2007-07e	R	-6.64 ± 0.35	0.044 ± 0.010	45.6 ± 10.5
M31N 2007-08d	R	-6.44 ± 0.11	0.025 ± 0.003	80.5 ± 10.5
M31N 2007-10a	B	-8.25 ± 0.11	0.222 ± 0.013	9.0 ± 0.5
...	V	-8.38 ± 0.11	0.255 ± 0.013	7.9 ± 0.4
...	i'	-6.51 ± 0.13	0.225 ± 0.010	8.9 ± 0.4
M31N 2007-10b	B	-7.60 ± 1.15	0.508 ± 0.067	3.9 ± 0.5
...	V	-8.14 ± 1.56	0.690 ± 0.065	2.9 ± 0.3
...	R	-8.18 ± 1.44	0.639 ± 0.085	3.1 ± 0.4
M31N 2007-11b	B	-5.65 ± 0.11	0.055 ± 0.004	36.3 ± 2.6
...	V	-5.78 ± 0.11	0.044 ± 0.003	45.4 ± 3.5
...	R	-6.36 ± 0.25	0.046 ± 0.012	43.6 ± 11.0
...	i'	-5.45 ± 0.14	0.027 ± 0.006	74.4 ± 16.7
M31N 2007-11c	B	-8.25 ± 0.24	0.138 ± 0.006	14.5 ± 0.6
...	V	-8.20 ± 0.27	0.155 ± 0.007	12.9 ± 0.6
...	i'	-7.33 ± 0.18	0.171 ± 0.013	11.7 ± 0.9
M31N 2007-11d	B	-9.35 ± 0.11	0.143 ± 0.009	14.0 ± 0.9
...	V	-9.48 ± 0.11	0.158 ± 0.009	12.6 ± 0.7
...	r'	-9.64 ± 0.11	0.153 ± 0.009	13.1 ± 0.8
...	i'	-8.72 ± 0.11	0.216 ± 0.011	9.2 ± 0.5
M31N 2007-12a	B	-7.02 ± 0.12	0.078 ± 0.005	25.6 ± 1.6
...	V	-7.06 ± 0.11	0.081 ± 0.004	24.8 ± 1.4
...	i'	-7.19 ± 0.11	0.068 ± 0.004	29.6 ± 2.0
M31N 2007-12b	B	-8.15 ± 0.11	0.497 ± 0.034	4.0 ± 0.3
...	V	-8.28 ± 0.11	0.548 ± 0.033	3.6 ± 0.2
...	R	-8.44 ± 0.11	0.403 ± 0.043	5.0 ± 0.5
M31N 2008-05c	R	-7.54 ± 0.11	0.038 ± 0.002	53.0 ± 2.8
M31N 2008-06b	R	-8.64 ± 0.11	0.083 ± 0.005	24.2 ± 1.5

Table 6—Continued

Nova	Filter	$M_{\max}$	Fade Rate (mag day^{-1})	t_2 (days)
M31N 2008-07a	R	-6.24 ± 0.11	0.005 ± 0.001	410.0 ± 51.3
M31N 2008-07b	R	-6.14 ± 0.20	0.049 ± 0.006	40.9 ± 4.7
M31N 2008-08a	R	-8.04 ± 0.20	0.094 ± 0.011	21.2 ± 2.5
M31N 2008-10a	B	-7.15 ± 0.11	0.053 ± 0.003	37.7 ± 2.2
...	V	-7.28 ± 0.11	0.052 ± 0.003	38.3 ± 2.2
...	r'	-7.44 ± 0.11	0.030 ± 0.003	67.5 ± 6.7
M31N 2008-10b	B	-7.08 ± 0.12	0.020 ± 0.003	98.4 ± 14.9
...	V	-6.88 ± 0.12	0.017 ± 0.003	117.3 ± 21.5
...	R	-6.56 ± 0.25	0.032 ± 0.015	63.3 ± 30.2
...	r'	-6.71 ± 0.11	0.027 ± 0.003	73.2 ± 8.1
M31N 2008-11a	B	-7.75 ± 0.11	0.522 ± 0.029	3.8 ± 0.2
...	V	-7.88 ± 0.11	0.457 ± 0.024	4.4 ± 0.2
...	R	-8.04 ± 0.11	0.378 ± 0.044	5.3 ± 0.6
...	r'	-8.04 ± 0.11	0.253 ± 0.013	7.9 ± 0.4
...	i'	-6.13 ± 0.13	0.120 ± 0.006	16.6 ± 0.8
...	z'	-6.61 ± 0.12	0.237 ± 0.017	8.4 ± 0.6
M31N 2008-12b	B	-7.48 ± 0.11	0.055 ± 0.006	36.7 ± 4.1
...	V	-7.61 ± 0.11	0.065 ± 0.006	30.7 ± 2.9
...	r'	-7.74 ± 0.11	0.073 ± 0.006	27.6 ± 2.2
...	i'	-7.00 ± 0.15	0.081 ± 0.012	24.7 ± 3.6
...	z'	-7.73 ± 0.12	0.044 ± 0.011	45.0 ± 10.9
M31N 2009-08a	B	-7.05 ± 0.11	0.006 ± 0.001	351.1 ± 84.5
...	V	-7.18 ± 0.11	0.011 ± 0.001	190.0 ± 24.5
...	R	-7.34 ± 0.11	0.014 ± 0.001	142.3 ± 9.0
...	r'	-7.34 ± 0.11	0.014 ± 0.001	142.3 ± 13.1
M31N 2009-08b	B	-7.15 ± 0.11	0.111 ± 0.005	18.0 ± 0.8
...	V	-7.28 ± 0.11	0.112 ± 0.005	17.8 ± 0.8
...	r'	-7.44 ± 0.11	0.086 ± 0.004	23.1 ± 1.2
...	i'	-6.47 ± 0.12	0.074 ± 0.006	26.9 ± 2.2
M31N 2009-08d	B	-7.23 ± 0.24	0.072 ± 0.017	27.9 ± 6.5
...	V	-7.18 ± 0.11	0.063 ± 0.008	31.7 ± 3.9
...	R	-7.34 ± 0.20	0.055 ± 0.008	36.2 ± 5.2
...	r'	-7.34 ± 0.11	0.077 ± 0.019	25.9 ± 6.5
M31N 2009-08e	R	-6.74 ± 0.11	0.016 ± 0.001	121.3 ± 8.0
M31N 2009-09a	R	-7.04 ± 0.25	0.012 ± 0.001	163.7 ± 15.4
M31N 2009-10a	B	-7.15 ± 0.11	0.123 ± 0.007	16.2 ± 0.9
...	V	-7.28 ± 0.11	0.132 ± 0.006	15.2 ± 0.7
M31N 2009-10b	B	-9.55 ± 0.11	0.250 ± 0.007	8.0 ± 0.2
...	V	-9.68 ± 0.11	0.224 ± 0.005	8.9 ± 0.2
...	R	-9.84 ± 0.11	0.156 ± 0.010	12.8 ± 0.8
M31N 2009-10c	B	-8.75 ± 0.13	0.134 ± 0.008	14.9 ± 0.8
...	V	-8.24 ± 0.14	0.124 ± 0.011	16.1 ± 1.4
...	R	-8.14 ± 0.25	0.065 ± 0.020	30.6 ± 9.4
M31N 2009-11a	B	-6.65 ± 0.11	0.095 ± 0.007	21.1 ± 1.6
...	V	-6.78 ± 0.11	0.092 ± 0.005	21.7 ± 1.2
...	R	-6.94 ± 0.11	0.096 ± 0.009	20.8 ± 1.9

Table 6—Continued

Nova	Filter	$M_{\max}$	Fade Rate (mag day^{-1})	t_2 (days)
M31N 2009-11b	B	-5.85 ± 0.11	0.022 ± 0.004	92.5 ± 16.6
...	V	-5.98 ± 0.11	0.027 ± 0.004	74.8 ± 10.6
...	R	-6.14 ± 0.11	0.023 ± 0.002	88.0 ± 6.6
M31N 2009-11c	B	-7.28 ± 0.11	0.048 ± 0.003	42.0 ± 2.7
...	V	-7.84 ± 0.14	0.062 ± 0.005	32.5 ± 2.4
...	R	-7.57 ± 0.11	0.046 ± 0.004	43.1 ± 3.6
M31N 2009-11d	B	-7.85 ± 0.11	0.178 ± 0.007	11.2 ± 0.4
...	V	-7.98 ± 0.11	0.276 ± 0.025	7.2 ± 0.7
...	R	-8.14 ± 0.11	0.122 ± 0.013	16.3 ± 1.7
M31N 2009-11e	R	-7.56 ± 0.20	0.036 ± 0.002	55.7 ± 3.1